EVOLUTION OF BACTERIAL TYPE VI SECRETION SYSTEM REGULATION AND DEFENSE

A Dissertation
Presented to
The Academic Faculty

By

Siu Lung Ng

In Partial Fulfillment
of the Requirements for the Degree
Doctor of Philosophy in the
School of Biological Sciences
College of Sciences

Georgia Institute of Technology

December 2022

EVOLUTION OF BACTERIAL TYPE VI SECRETION SYSTEM REGULATION AND DEFENSE

Thesis committee:

Dr. Brian Hammer
School of Biological Sciences
Georgia Institute of Technology

Dr. Frank Stewart
School of Biological Sciences
Georgia Institute of Technology

Dr. Marvin Whiteley
School of Biological Sciences
Georgia Institute of Technology

Dr. Peter Yunker
School of Physics
Georgia Institute of Technology

Dr. Willianm Ratcliff
School of Biological Sciences
Georgia Institute of Technology

Date approved: August 18, 2022

To the future Ph.D. students,

Do not let the failure stop you and be comfortable trying new things.

“Feel the fear and do it anyway!” - Susan Jeffers

ACKNOWLEDGMENTS

I would like to first express my sincere appreciation to my advisor Dr. Brian Hammer for his unlimited support, invaluable advice, and patience during difficult times when I was stressing and struggling with experiments and ideas. He was the one encouraging and guiding me to the light when I was running into dead ends. I am truly grateful for being one of his students, and this unforgettable experience has shaped who I am today. Additionally, I would like to thank Dr. Marvin Whiteley, Dr. William Ratcliff, Dr. Frank Stewart, and Dr. Peter Yunker for their time serving as my committee member. Their constructive criticism and ideas always reminds me to think about the same science in different ways.

I also appreciate all the support I received from the past and present Hammer lab members. I would especially like to express gratitude to Dr. Jacob Thomas for training me to be a ”cloning master”, Sophia Kammann for her hard work and contributions to my projects, and Kathryn MacGillivray for letting me to be part of her evolution project. In addition, thanks are also in order to the staffs at VWR stockroom, Verene Lancaster, and Brent Minter and his past and present assistants to keep our building and lab in order.

I would like to offer my next special thanks to the past and present members of the Yunker lab, especially Dr. Gabi Steinbach for her professional microscopy skills. We have been collaborating ever since I joined the Hammer lab. I have learned so much from them, and I have definitely broadened my horizons learning the importance of interdisciplinary studies. Both labs are learning from each other everyday to understand the biophysical processes at work in microbial systems.

During my teaching assistantship, I am grateful to all of the professors who mentored me, specifically Dr. Chrissy Spencer and Dr. Shana Kerr for sharing their valuable knowledge about teaching, Dr. Aakanksha Angra for allowing me to be part of her publication, and Alison Onstine and Angie Lessard for their effort in keeping the teaching lab running smoothly.

Last but not least, my appreciation also goes out to my parents for letting me go to a foreign country alone and allowing me to pursue my dream of being a scientist, my spouse for always being next to me and being patient during my stressful and grumpy days, and my fur babies for their emotional support.

TABLE OF CONTENTS

LIST OF TABLES

LIST OF FIGURES

LIST OF ACRONYMS

gfp green fluorescent protein

5' RACE 5' rapid amplification of cDNA ends

5' UTR 5' untranslated region

A adenine

ACD actin cross-linking domain

AI autoinducer

Aux auxiliary

C cytosine

c-di-GMP 3',5'-cyclic diguanylic acid

CBP chitin binding protein

CDI contact-dependent growth inhibition

ChIP chromatin immunoprecipitation

Cm chloramphenicol

CRE *cis*-regulatory element

Cryo-EM cryo-electron microscopy

CTX Cholera toxin

D. discoideum *Dictyostelium discoideum*

E. coli *Escherichia coli*

EMSA electrophoretic mobility shift assay

G guanine

GI gastrointestinal

GlcNAc N-acetylglucosamine

HCD high cell density

Hcp hemolysin coregulated protein

HGT horizontal gene transfer

IGR intergenic region

LB lysogeny broth

LCD low cell density

MIC minimum inhibitory concentration

NAP Nucleoid associated proteins

nt nucleotide

OD_{600} optical density

P. aeruginosa *Pseudomonas aeruginosa*

PAAR proline-alanine-alanine-arginine

Qrr4 quorum regulatory small RNAs

QS quorum sensing

RBS ribosome binding site

RFU relative fluorescence units

RLU relative luminescence units

RNAP RNA polymerase

ROS reactive oxygen species

S. typhimurium *Salmonella typhimurium*

SNP single-nucleotide polymorphism

Spec spectinomycin

T thymine

T6 type VI secretion system

TF transcription factor

Tn-seq transposon sequencing

TSS transcriptional start site

V. cholerae *Vibrio cholerae*

V. fischeri *Vibrio fischeri*

WT widetype

SUMMARY

Bacteria in nature live in communities with other organisms where resources and space are typically lacking. To compete, bacteria have evolved strategies to increase fitness by eliminating unwanted competitors with secreted goods such as traditional, diffusible antibiotics. A more recently described mechanism of antagonism is a contact-dependent ”nanoharpoon”, the type VI secretion system (T6), which kills neighboring ”target” cells by directly injecting lethal toxins.

The broadly distributed T6 weapon plays an important role in competition and the pathogenicity of many Gram-negative bacteria including *Vibrio cholerae*, with prior studies demonstrating a role for the *V. cholerae* T6 in host colonization and infection. The majority of our understanding of this apparatus in *V. cholerae* is based on studies with isolates that contribute to disease. The current regulatory model of T6 control describes a requirement of one of the two transcription factors: QstR, which is induced by external chemical cues, or TfoY, which is activated by intracellular signals. By contrast, our knowledge of the T6 of *V. cholerae* strains from non-human sources is more limited. So too, the structure of the T6 apparatus, the toxic effector proteins delivered by it, and their corresponding immunity proteins have garnered much attention. Yet we know little about how microbes may protect themselves against T6 attack.

In my dissertation, I describe two major contributions to the field. First, I determined that QstR and TfoY are either dispensable or only play a minor role in *V. cholerae* strains isolated from nonhuman sources, which instead display constitutive T6 activity in laboratory conditions. To begin to determine the mechanism responsible for regulatory differences between human and nonhuman strains, I successfully mapped the promoter region of the major T6 gene cluster and identified a single-nucleotide polymorphism (SNP) in the DNA sequence upstream of the promoter that affects the regulation of T6. Human-derived, QstR-regulated strains encode a guanine (G) at this position, while environmental strains

carry a thymine (T), with varying contributions of TfoY. These results are consistent with a "pathoadaptive" theory that *V. cholerae* dampens the T6 regulation during infection and displays a constitutive T6 activity in natural environments. Second, I participated in the discovery that target cells have two major mechanisms to resist T6 attacks. Using experimental evolution, I help uncover that *Escherichia coli* becomes less susceptible to T6 antagonism following several hundred generations of repeated T6-mediated competition. We identified three genes that contribute to the T6 resistance: *apaH* disruption, a specific *yjeP* missense mutation, and *yejM* mutations that result in C-terminus disruptions. The T6 resistance is greater when *E. coli* carries both the *yjeP* and *yejM* mutations. These mutations however are pleiotropic, reducing growth rate and causing other collateral effects, supporting a hypothesis that evolution of T6 resistance in natural communities is likely constrained by fitness effects. This dissertation provides insight into how T6 aggression and resistance are two facets of an evolutionary arms race: with killer cells evolving strategies for antagonism that provide selective pressure favoring target cells with T6 resistance.

CHAPTER 1
INTRODUCTION

Bacteria are the most abundant forms of life on Earth, present on our planet for over 3 billion years [1]. Over this time, microbes have adapted to live in diverse environments, as free-living cells and also as members of dense polymicrobial biofilms. Surface-attached life is the norm, present on both abiotic and biotic surfaces in industrial, natural, and host settings [2–4]. To adapt the changes in the environment, free-living and attached bacteria alter gene expression by continuously sensing and responding to molecular signals (e.g. self-produced quorum sensing autoinducers) and cues (e.g. nutrients) in their external surroundings [5–8]. Within biofilms, bacterial cells are spatially structured by extracellular polymeric substances and largely influenced by their interactions with kin that are genetically similar and non-kin that are genetically distinct [9]. In these dense communities, cooperative interactions are rare and generally occur in low species diversity and low nutrient environments. The most common interactions are negative [9].

To compete, bacteria have evolved diverse antagonistic mechanisms to minimize competitors [10]. For example, *Pseudomonas aeruginosa* secretes multiple diffusible compounds such as pyocyanin, exotoxin A, and ExoU that aids in competing against other microbes and human cells during infections [11–13]. Soil bacteria like *Streptomyces* are well-documented for producing many antibiotics, such as streptomycin, kanamycin, tetracycline that are important for competition and for maintaining symbiosis with plants by eliminating the pathogens [14, 15]. More recently, another antagonistic system, the type VI secretion system (T6), was first identified in *Vibrio cholerae* [16]. The *V. cholerae* T6 is the focus on my thesis.

In aquatic environments, *V. cholerae* cells live in planktonic suspension but often attache with other bacteria to surfaces composed of chitinous materials (zooplankton molts

and crab shells) in a biofilm (Figure 1.1) [7, 8]. In addition, the gastrointestinal (GI) tract of some marine organisms (fish and oysters) are also the natural reservoirs for *V. cholerae* to colonize [17–21]. Following ingestion of contaminated food or water, *V. cholerae* can also infect humans, survive passage through the stomach and enter the intestine where it causes the fatal cholera diarrhea (Figure 1.1) [20–22]. In the GI tract, *V. cholerae* can colonize the small intestine, reproduce to high cell density (HCD), and produce the Cholera toxin (CTX) that causes fatal diarrhea, which disperses the *V. cholerae* cells back into the environments (Figure 1.1) [20–22]. Because of this dynamic lifestyle, *V. cholerae* has become a model organism to study diverse bacterial behaviors like biofilm formation, quorum sensing (QS), horizontal gene transfer (HGT), and pathogenesis [5, 23–25]. The T6 is a virulence factor of *V. cholerae* that requires physical contacts between "killer" and "target" cells, providing a more direct competitive strategy [26, 27]. The goal of this dissertation is to gain a deeper understanding of how killer bacteria genetically control antagonistic behaviors and how target cells evolve to protect themselves from being targeted.

1.1 Type VI secretion systems in bacteria

1.1.1 Type VI secretion system structure and mechanism

Bacterial protein secretion systems are complex nano-machines that assemble at the cell membranes of Gram negative bacteria for delivering proteins to the extracellular space [29]. These systems play an important ecological role for bacteria to interact with the environment, other microbes, and hosts, including humans where the secreted products can contribute to disease [29]. The T6 was first described in *V. cholerae* and showed antagonistic activity to both eukaryotic and bacterial cells [16, 30–32]. This contact-dependent macromolecular structure has a bacteriophage tail-like injection apparatus that physically punctures cells to deliver a diverse set of toxic effector proteins [33–35]. Genomics analysis predicts approximately 25% of Gram-negative bacteria encode a functional T6s [36, 37]. Subsequent studies demonstrated the diverse ecological roles of T6s in different bacterial

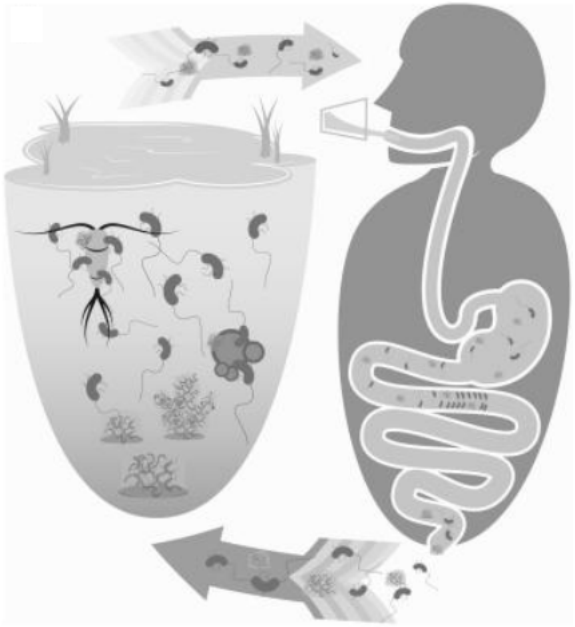

Figure 1.1: **Reservoir, transmission, and dissemination of *V. cholerae***. *V. cholerae* lives in aquatic environments as free-living cells or attached cells in biofilms adhering to chitinous surfaces. Through ingestion, *V. cholerae* colonizes the human gut and causes diarrheal disease that disseminates *V. cholerae* cells back to the natural environment. Image credit: [28].

species [38–40].

The assembly of a T6 in a "killer" cell initiates at the cell membranes with the mounting of a membrane complex (VasD, VasF, and VasK) that spans the the inner membrane, periplasmic space, and outer membrane [41, 42]. A baseplate composed of HsiF, VasA, VasB, VasE, and VasJ then attaches to the membrane complex via protein-protein interactions (Figure 1.2A) [41, 42]. A tube assembles under the baseplate that is composed of ATP-dependent contractile outer sheath proteins VipA/B and an inner tube composed of hemolysin coregulated proteins (Hcps) Figure 1.2A) [41, 42]. The VipA/B outer sheath forms a hollow tube with a helical structure that surrounds the inner tube assembled with stackable Hcps that form tubular hexameric rings with a 80 Å diameter Figure 1.2A) [41–43]. At the distal end of the Hcp inner tube, VgrG proteins assemble into the trimeric spike of the T6 Figure 1.2A) [41, 42]. The spike is loaded with the toxic effector proteins that are delivered by puncturing the target cells (Figure 1.2A) [41, 42]. To aid in the loading of

effectors to the VgrG spike, some bacteria, including *V. cholerae*, encode proline-alanine-alanine-arginine (PAAR) proteins that interact with the VgrG spike [41, 42]. Imaging of the T6 tubular structure with cryo-electron microscopy (Cryo-EM) in various bacterial species indicates the T6 can extend across the width of the cell (Figure 1.2B) [43]. The tubular assemble process terminates upon contacting the opposite side of the cell, as visualized by Cryo-EM [33, 44, 45].

When the T6 fires, the VipA/B outer sheath contracts, which in turn provides energy to rotate and eject the Hcp inner tube along with the VgrG-effector spike, delivering the toxic effectors into the target cells Figure 1.2A) [43]. After a firing event, an AAA+ AT-Pase ClpV disassembles and recycles the VipA/VipB outer sheath inside in killer cell (Figure 1.2A) [46, 47]. In the case of puncturing a sibling cells with a T6, the recipient cell can recycle and reuse the foreign proteins from the ”donor” into its own T6 assembly [48]. The T6 is structurally and functionally similar to a bacteriophage tail [49]. The VipA/B, Hcp, and VgrG proteins are predicted to be homologous to the T4 phage tail sheath, tail tube, and gp5-gp27 cell-puncturing complex, respectively [49]. The similarity between the two systems raises questions of whether they are analogous structures that have arisen by convergent evolution.

1.1.2 Type VI secretion system gene clusters in *Vibrio cholerae*

The T6 was first identified in human-derived *V. cholerae* strain V52 by screening transposon mutants that were deficient for killing the eukaryotic predator *Dictyostelium discoideum*. Genomics analysis identified the transposon insertions primarily in one large gene cluster, the T6 major cluster [16]. Subsequent studies further identified three additional auxiliary (Aux) clusters common in the human-derived strains, including the reference strain C6706 and V52 [27, 51, 52]. The major T6 gene cluster consists of 18 genes (VCA0107-0124), which encode most of the essential structural proteins including the baseplate component VasK (Figure 1.3) [16, 51]. The major cluster also encodes a

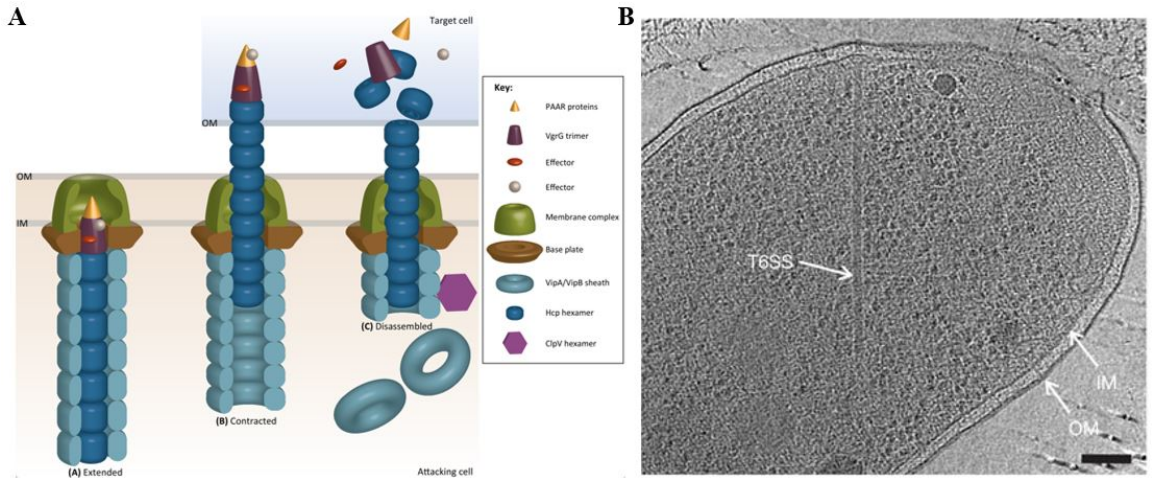

Figure 1.2: **The T6 apparatus of *V. cholerae***. (A) Scheme of T6 contraction event depicts extended VipA/VipB outer sheath contracting to eject the inner Hcp tube, the spike, and the effectors into the target cells. Image credit: Avatar et al., 2016. (B) Cryo-EM image of an extended T6 apparatus in *V. cholerae*. Scale bar: 100 nm. OM, outer membrane; IM, inner membrane. Image credit: [33, 50].

sigma-54 dependent transcription factor (TF) VasH that promotes the transcription of the smaller Aux gene clusters (Figure 1.3) [16, 27, 51, 52]. The number of T6 Aux clusters varies from strain to strain with genome sequencing revealing as few as two and as many as seven clusters [51, 53]. Aux clusters generally encode additional Hcp and VgrG proteins, with the exception of Aux 3, which lacks these two genes (Figure 1.3) [51]. At the end of each locus are the genes for the toxic effector adjacent to a cognate immunity protein that prevents self-intoxication (Figure 1.3) [41, 51]. This conserved gene sequence organization has been used to identify novel effector/immunity pairs in many bacteria encoding T6s, including *V. cholerae*.

1.2 Regulation of Type VI secretion

Bacteria use protein secretion systems like the T6 to deliver diverse cargo to the extracellular space or into target cells, through secretion or injection respectively [29]. Secretion systems are crucial for bacteria to communicate and to interact with their surrounding environments [29]. To control these complex systems, bacteria sense and response to environ-

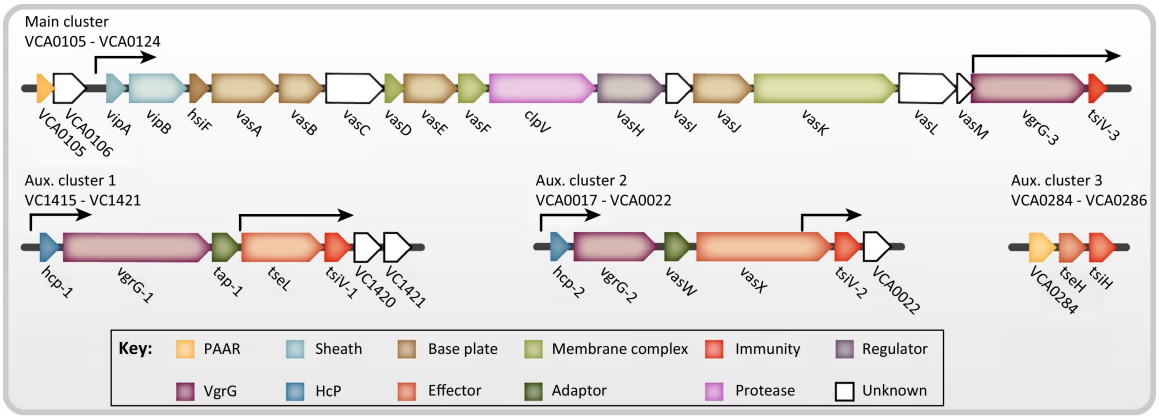

Figure 1.3: ***V. cholerae* T6 gene clusters.** All sequenced *V. cholerae* have a major T6 gene cluster, and Aux clusters 1 and 2. Some human-derived strains also carry the Aux 3 cluster. Effectors and immunity proteins are encoded at the end of each cluster. Image credit: [50].

mental signals and cues that regulate the expression of the secretion system genes [29]. For example, Enteroaggregative *Escherichia coli* encodes two T6s [54]. The initiation of transcription of T6-1 is repressed by the ferric uptake regulator Fur at high iron levels [54, 55] while the T6-2 is positively regulated by the aggregation regulator AggR, which also regulates other virulence factors [54, 56]. This differential regulatory strategy is hypothesized to allow *E. coli* to compete and modulate virulence when infecting the GI track, where iron is a limited nutrient. *P. aeruginosa* has three T6s, which are transcriptionally controlled by the QS regulators LasR and MvfR [42]. At HCD in the presence of QS regulators, the *P. aeruginosa* T6-1 is negatively regulated whereas the T6-2 and -3 are positively regulated [42, 57]. Although all of the T6 in *P. aeruginosa* plays a role in pathogenicity, the T6-1 is likely triggered in patients with long term cystic fibrosis, where Δ*lasR* mutants accumulate [57, 58]. In *V. cholerae*, the T6 in most human-derived strains are also tightly regulated through signal transduction cascades [41, 59]. By contrast, the T6 of many environmental strains is constitutively expressed, by mechanism still unclear [53, 59–63]. The complex regulation of T6 in bacteria vary between genus, species, and between strains. This ”fine tuning” by evolutionary processes enables activation under specific conditions. The regulation of T6 in environmental *V. cholerae* strains, has received minimal attention, and is the

focus of chapter 2.

1.2.1 The type VI secretion system of *Vibrio cholerae* isolates derived from humans

The signal transduction system controlling T6 in *V. cholerae* has been studied extensively in the human-derived strains [41], including the pandemic strain C6706 isolated from a patient during the 1991 pandemic in Peru [64]. In C6706, transcription of the major T6 gene cluster is activated by the presence of chitin, nucleoside starvation, and QS (Figure 1.4A) [65–67]. In addition to the T6, components of these regulatory pathways also control natural competence, biofilm production, and virulence factors [25, 68].

Chitin is a polymer of N-acetylglucosamine (GlcNAc) and the second most abundant polysaccharide in nature [69, 70]. It is commonly found in aquatic environments, comprising the exoskeletons of crustaceans [69, 70]. Many marine bacteria, including *V. cholerae*, secretes chitinases to break down chitin into small and soluble GlcNAc oligomers, which can be used as a carbon source [7, 69, 70]. Additionally, the GlcNAc oligomers are an important environmental cue that alter gene expression in marine bacteria [71, 72]. In *V. cholerae*, the GlcNAc oligomers bind to a periplasmic chitin binding protein (CBP), which derepresses a membrane histidine kinase ChiS (Figure 1.4A) [71]. ChiS in turn activates a membrane-bound TF TfoS that promotes the transcription of a regulatory small RNA TfoR (Figure 1.4A) [73, 74]. In combination with the RNA chaperone Hfq, TfoR unfolds the 5' untranslated region (5' UTR) of *tfoX* gene and allows translation of TfoX, which then enhances the expression of multiple chitinase genes to accelerate the degradation of chitin (Figure 1.4A) [66, 73–76]. TfoX also positively regulates downstream transcription factors and numerous natural competence genes to promote uptake of foreign DNA (Figure 1.4A) [66, 75].

Extracellular nucleosides are valuable resources for nucleotide synthesis or serve as carbon and nitrogen sources [78]. Nucleoside uptake and usage in *V. cholerae* are negatively regulated by a global transcription repressor CytR (Figure 1.4A) [79]. This repres-

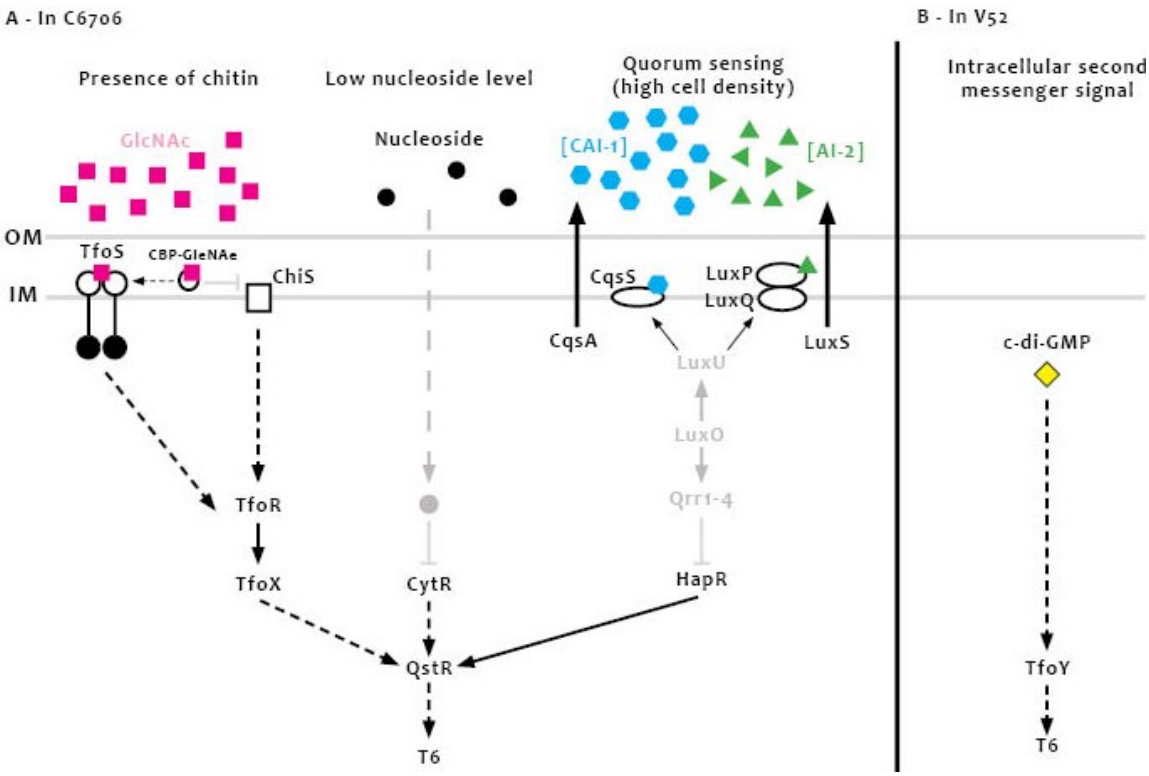

Figure 1.4: **Regulation of T6 in human-derived *V. cholerae* either requires extracellular signaling via QstR or intracellular signals via TfoY**. Under the conditions shown, (A) pandemic strain C6706 senses and responds to the level of chitin, nucleoside, and autoinducers (AIs) in the environment to activate the transcription of T6 via QstR. (B) Non-pandemic V52 controls the T6 via TfoY, which is modulated by c-di-GMP. Dashed lines - regulatory connection unknown; solid lines - direct regulatory connection known. Image is modified from [77].

sion mechanism documented in *E. coli* is conserved in *V. cholerae* [80]. To repress, CytR forms a complex with two cAMP-CRP dimers that bind to the target promoters to prevent initiation of transcription [80]. In addition to nucleoside metabolism, CytR downregulates biofilm formation [81] and also indirectly upregulates natural competence [66] presumably by repressing a putative repressor (Figure 1.4A).

QS is a bacterial communication system that enables changes in gene expression in a cell density dependent manner [5]. In QS systems, the level of secreted signaling molecules known as AIs serve as a proxy for cell density [5]. Most *V. cholerae* strains are capable of quorum sensing and release AIs that accumulate as cells reach HCD (Figure 1.4A). The

two major AIs in *V. cholerae* are 1) CAI-1, which is genus-specific for evaluating the *Vibrio* abundance [82, 83], and 2) AI-2, which is also produced by other bacterial species for measuring the total abundance (Figure 1.4A) [82, 84]. At low cell density (LCD) in the absence of AIs, a phosphorylation cascade is triggered by the membrane-bound AI receptors CqsS and LuxPQ, which act as kinases to phosphorylate the phosphotransfer protein LuxU (Figure 1.4A) [85]. Phospho-LuxU further phosphorylates and activates the response regulator LuxO (Figure 1.4A) [85]. Phospho-LuxO upregulates the transcription of four small regulatory RNAs (Qrr1-4) that work with Hfq to repress the translation of a QS master regulator HapR by destabilizing its mRNA transcript (Figure 1.4A) [85]. At HCD, CqsS and LuxPQ, bounded by their corresponding AIs, behave as phosphatases that remove phosphate from LuxU, which inactivates LuxO (Figure 1.4A) [85]. The deactivation of LuxO halts the transcription of Qrr1-4 and promotes HapR translation (Figure 1.4A) [85]. Although HapR was initially identified as a positive regulator of the haemagglutinin protease [86], it was later found to control many other behaviors in *V. cholerae* such as repressing cholera toxin and biofilm production [85, 87–89]. Using standard genetic methods, *V. cholerae* can be artificially locked at LCD by deleting *luxO* (Δ*luxO*) or locked at HCD by deleting *hapR* (Δ*hapR*).

When conditions permit accumulation of TfoX, CytR, and HapR in the cell, the downstream TF QstR is expressed (Figure 1.4A) [66, 88]. Although the mechanisms by which TfoX and CytR activate QstR are still unclear, direct binding of HapR to the *qstR* promoter was observed by electrophoretic mobility shift assay (EMSA) leading to transcriptional activation of *qstR* [88]. In addition to its role in up-regulating natural competence, QstR is also a positive regulator of T6 in C6706 and other human-derived strains (Figure 1.4A) [59, 65]. Reference strain C6706 expressing QstR constitutively from a non-native promoter (*qstR**) bypasses the requirement of external cues to activate T6.

A recent report hypothesized that QstR may directly interact with a *cis*-regulatory element (CRE) in the intergenic region (IGR) upstream of the T6 major cluster [65]. Evidence

supporting the hypothesis is a C-terminal DNA binding helix-turn-helix domain in QstR [88] and preliminary evidence by chromatin immunoprecipitation (ChIP) of association of QstR from *V. cholerae* cell lysates with a DNA fragment containing the IGR upstream of the T6 major cluster (see chapter 2 for more details) [65]. ChIP utilizes a cross-linking reagent to stabilize binding of DNA to proteins, like transcription factors that transiently bind DNA [90]. ChIP results must be interpreted with caution since levels of cross-linking reagent [90] and the cross-linking time [91] can alter the DNA fragments bound and give false positive results with excess cross-linker and false negatives with too little cross-linker. Because ChIP is sensitive to the experimental conditions, EMSA is often used to verify the ChIP results. Attempts using EMSA and purified QstR were unsuccessful [65], suggesting QstR may regulate the T6 of *V. cholerae* in a more complex manner.

V. cholerae nonpandemic V52 causes mild disease and was isolated in Sudan in 1968 [92]. V52 was instrumental in the discovery of T6 because it is capable of killing *D. discoideum* in standard lab conditions (lacking chitin) [16]. This pioneering study suggested that the activation of T6 may not require external cues, and by extension TfoX and QstR [16]. Indeed, a subsequent study identified the T6 in V52 does not require TfoX or QstR but is positively regulated by a TfoX homolog TfoY, which also controls motility (Figure 1.4B) [67, 93].

TfoY levels are transcriptionally and post-transcriptionally modulated by the intracellular second messenger 3',5'-cyclic diguanylic acid (c-di-GMP) (Figure 1.4B) [94]. This molecule is prevalent in bacterial species and involved in regulation of T6, biofilm formation and motility in *V. cholerae* that are important for survival in aquatic and host environments [25]. To modulate the c-di-GMP levels, *V. cholerae* encodes numerous phosphodiesterases to degrade [95, 96] and diguanylate cyclases to synthesize the c-di-GMP [97, 98]. TfoY has complex transcription regulation that is driven by four independent promoters, three of which are c-di-GMP-dependent [94]. Because TfoY contains no domains or motifs, how it regulates gene expression still remains elusive.

1.2.2 The type VI secretion system of *Vibrio cholerae* isolates from environmental sources

Aquatic environments are a natural reservoir for *V. cholerae* to thrive [99]. While *V. cholerae* strains isolated from environmental sources are genetically similar to the human-derived strains [51], there are phenotypic differences, particularly with respect to T6 [59]. Numerous reports describe constitutive T6 activity by environmental strains in lab conditions [53, 59–62]. This behavior is in contrast to the human-derived strains that display little or no T6 activity in lab condition without chitin [59, 61, 62, 65, 67]. The differences in the T6 regulation between human-derived and environmental strains have led to a ”pathoadaptive” hypothesis that suggests pathogens improve their fitness in the human host by acquiring adaptive mutations or traits [100]. This hypothesis posited that in *V. cholerae*, tightly regulated T6 may be beneficial during infection to reduce the chance of triggering the host immune system while constitutive T6 provides more fitness advantages in the natural habitats to constantly prevent competitors [101].

1.3 Diversity of type VI secretion system toxic effectors

1.3.1 Human-derived *Vibrio cholerae* strains have an identical set of Type VI effectors

When a T6 harpoon punctures a target, multiple toxic effectors are delivered into the periplasm and cytoplasm of the cell. Effectors may be coded by separate genes or as a domain of dual-purpose proteins [41]. In *V. cholerae*, the number of antibacterial effectors are generally identical to the number of T6 gene clusters it carries (Figure 1.5) [51]. For most human-derived strains, including C6706 and V52, the effectors are predicted to code for proteins with identical activities (Figure 1.5) [51].

VgrG3 is an dual-purpose effector encoded in the T6 major gene cluster. It contains an N-terminus that folds into the T6 spike, similar to the T4 tail spike, and a C-terminal domain with peptidoglycan degradation activity [102, 103]. Expression of the VgrG3 C-terminus in the *E. coli* periplasm leads to lytic activity and cell death [102]. The Aux 1

cluster encodes TseL that has a lipase domain. While there is no direct measure of the lipase activity, a catalytic residue within the lipase domain was identified based on the conserved sequences [31, 103]. A change in a residue within this domain (D425A) eliminates TseL toxicity [103]. TseL directly interacts with the VgrG spike via a Tap-1 linker protein, and both proteins are delivered together into the target cells [31, 103–105]. Human *V. cholerae* isolates also encode another lipase/pore-forming effector in the Aux 2 cluster, VasX, which shows homology to colicins [106]. VasX displays activity against both bacterial and eukaryotic cells [27, 106]. VasX activity requires delivery to the periplasm via the VgrG spike, where it interacts with the inner membrane of the target cells [27, 106, 107]. VasX also induces killing of *D. discoideum*. [27]. It is hypothesized that an N-terminal pleckstrin homology domain of VasX binds to and disrupts the phospholipids of eukaryotic cell membranes, specifically the phosphatidic acid and phosphatidylinositol phosphates that are important for eukaryotic cell-cell signaling [27]. Lastly, TseH is encoded in the Aux 3 cluster found in many, but not all, human-derived *V. cholerae* isolates [51]. TseH carries a hydrolase domain and has minimal effects on *E. coli* [108]. Although the mechanism of action is still poorly understood, it is hypothesized that TseH degrades the peptidoglycan in the periplasm [108]. Since most bacteria use a T6 to deliver multiple effectors, like *V. cholerae*, the T6 can be viewed as a multi-drug delivery system.

Besides these anti-bacterial effectors, the VgrG1 protein in most human-derived strains has an additional C-terminal actin cross-linking domain (ACD) similar to a related RtxA toxin that is absent in the environmental strains, supporting a hypothesis that human-derived strains represent a distinct clade from the environmental *V. cholerae* [109]. Like RtxA, the VgrG1-ACD shows activity against eukaryotic cells [53, 110]. *In vitro*, the expression of VgrG1-ACD causes cell rounding and covalently cross-linking actin in *D. discoideum* and macrophages [110]. *In vivo*, the presence of the ACD leads an intestinal inflammation in infant mice and plays an important role during *V. cholerae* colonization [111]. In a zebrafish model of colonization, the ACD is responsible for the induction of

dramatic peristalsis that is sufficient to eliminate resident gut bacteria [112]. These results imply the anti-eukaryotic activity of VgrG1 likely serves an important role during human infection.

1.3.2 Environmental *Vibrio cholerae* isolates have diverse Type VI effectors

Similar to the human-derived strains, environmental *V. cholerae* also have an Aux 1 and 2 cluster, but their Aux 1 and 2 effectors appear to have different predicted activities based on protein sequence (Figure 1.5) [51]. For example, the Aux 1 effector in most environmental strains has a hydrolase domain instead of a lipase in the human-derived strains (Figure 1.5). Four different Aux 2 effectors (e.g. NTPase, transferase, LysM, and unknown function) are encoded in different environmental strains (Figure 1.5) [51]. Unlike human-derived strains, most environmental *V. cholerae* also lack the Aux 3 cluster. Several carry extra Aux clusters (Aux 4, 5, and 6) increasing the diversity of effectors deliverable by the T6 (Figure 1.5) [51, 53, 113]. Most of these effectors have a predicted domain but have not been experimentally tested [51]. Recently, researchers started exploring new features of the novel Aux clusters and effectors with whole genome sequencing data [51]. For example, TpeV is a new membrane permeabilizing effector encoded in the Aux 4 [113]. TpeV kills *E. coli* by disrupting membrane potential, resulting in cytotoxicity [113]. TleV is encoded in Aux 5 and is predicted to be a lipase [51]. It has been shown that TleV has the strongest effect when delivered to the periplasm and moderate effect in the cytoplasm, but the mechanisms of action is unclear [51]. Lastly, Aux 6 encodes a putative unnamed effector/immunity pair that shows killing activity against *E. coli* [53]. While it is not clear why the environmental *V. cholerae* carries different set of T6 effectors, the current model suggests the selection of effectors are largely dependent on the environmental factors like species of competitors or hosts [51, 59].

While human-derived strains have a set of highly conserved effectors, environmental strains are more diversified (Figure 1.5) [51]. Similar to the regulation of T6, this observa-

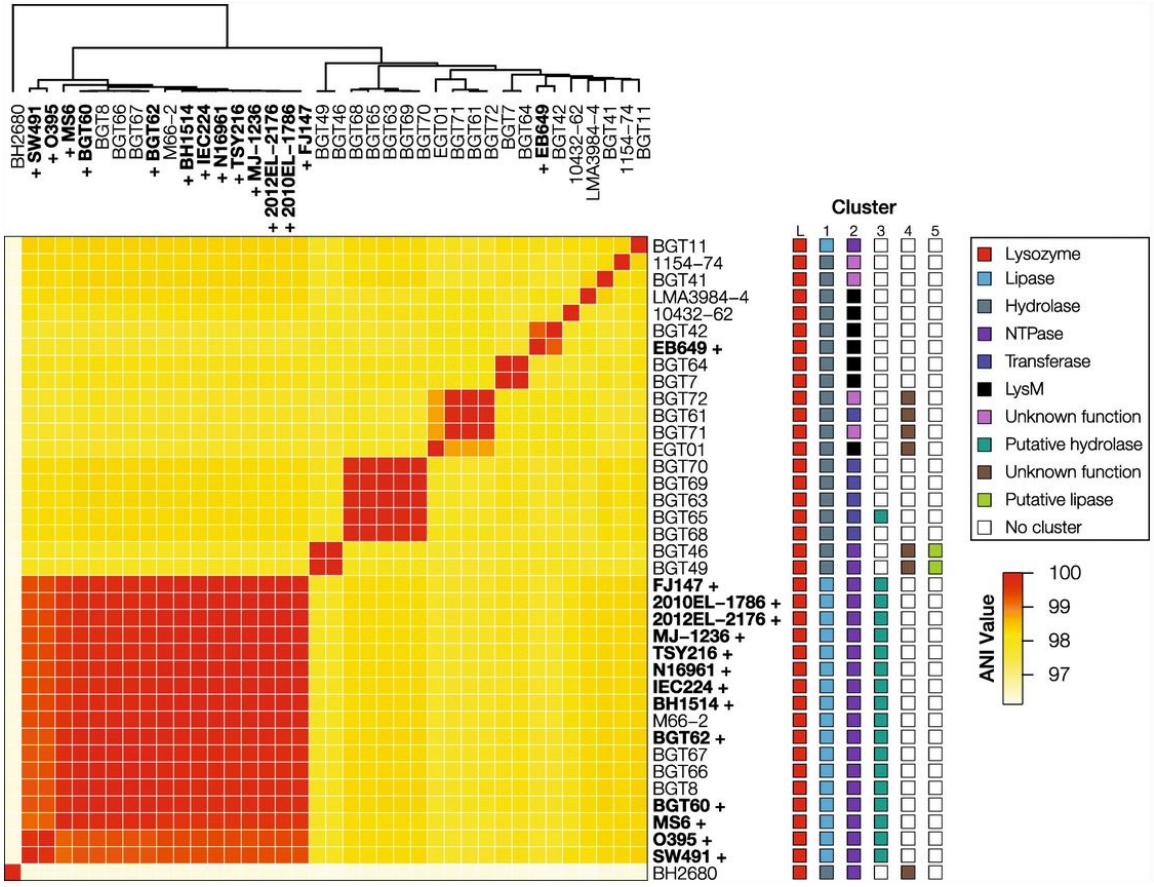

Figure 1.5: **Diversity of T6 gene cluster in *V. cholerae***. Average nucleotide identity analysis was conducted with sequenced human-derived and environmental *V. cholerae* strains. Up to five T6 gene clusters and ten predicted features of the effectors were identified. The human-derived strains are in bold, and the environmental strains are in plain text. Image credit: [51].

tion is also consistent to the pathoadaptive hypothesis that the effectors in human-derived strains are selected for infections [100]. However, environmental strains are collected from diverse locations, range from marine organisms to sewer water [59]. Their T6 effectors have been selected based on their living environments, and the selection can happen via HGT because *V. cholerae* is naturally competence. In fact, effector swapping has been observed *in vitro* when growing in conditions that simulate the natural settings [114].

1.4 Type VI secretion system protective mechanisms

To successfully compete in polymicrobial communities, bacteria have evolved not only mechanisms of antagonism but also processes to defend themselves. This attack-defend relationship is commonly seen with diffusible antibiotics, in which susceptible cells develop antibiotic resistance [115]. Since the discovery of T6, there has been an emphasis of T6 regulation, apparatus structure, and effector activities with less attention to protection mechanisms. For example, *P. aeruginosa* can survive a T6 attack from *V. cholerae* by counterattacking with its own T6 system, also known as "Tit-for-Tat" [34]. Recently, new studies have begun to investigate other processes that allow target cells to survive attack by T6. In these studies *E. coli* is a common model target cell.

1.4.1 Immunity proteins

In a dense biofilms, bacteria with active T6 pierce non-sibling target cells as well as sibling cells. To maintaining the fitness advantage without self-intoxication, T6 killers produce intracellular immunity proteins to neutralize cognate effectors [116]. While each immunity gene is located adjacent to their cognate effector gene, each is driven by an independent promoter [106, 116]. The effector genes are controlled by the the inducible T6 gene cluster's promoter, which also drives immunity gene expression [106]. This dual-expression profiles provide constant protection to sibling cells.

In *V. cholerae*, there are six effector/immunity pairs identified: VgrG3/TsiV3, TseL/TsiV1, VasX/TsiV2, TseH/TsiH, TpeV/TpiV, and TleV/TliV [31, 32, 51, 108, 113]. While most of immunity proteins are poorly understood, TsiV3 is an exception. TsiV3 was crystallized and analysed in an interaction kinetics study [117]. In the presence of VgrG3, TsiV3 forms a dimer and binds to the active site of VgrG3 [117]. This results in a distortion of the effector's confirmation which prevents VgrG3 from interacting with peptidoglycan [117]. This neutralization mechanism provides an insight into how other immunity proteins likely

inhibit their cognate effector activities.

The T6 plays an important role in shaping the gut microbiome [118, 119]. This antagonistic interaction in the gut is mainly described in *Bacteroidetes* species, one of the dominant symbiotic phyla in the human gut [120, 121]. By genomics comparison, some T6-deficient *Bacteroidetes* harbor "orphaned" immunity gene clusters without encoding cognate effectors [120, 121]. These immunity genes are acquired from diverse T6 killers in the gut (e.g. *Burkholderiales*) via recombinase-associated HGT events and protect the cells from T6-mediated killing [120, 121]. Similar observations have been made in *V. cholerae* [122].

1.4.2 Physical separation

Diffusible antibiotics are widely used to target bacteria in environments like clinical and agricultural settings [123, 124]. Over time, bacteria develop mechanisms like biofilm production to become more resistance against antibiotics [125]. The complex extracellular polymeric matrix of biofilms limits the diffusion of molecules and acts as a physical barrier between cells and the external environments [126, 127]. Interestingly, the biofilms also stop T6 attacks from the outside but allow the biofilm producing cells to attack with their T6 [128]. Within the biofilm, T6-mediated combats result in dead cells at the interface of killer and target cells [129]. The accumulation of the dead cell debris can also form a barrier that physically separates the competing strains and prevents target cell killing [129]. The combination of T6 killing and dead cell debris promotes phase separation that plays an important role in organizing polymicrobial communities [130, 131]. In this manner, the T6 serves a role in both kin discrimination and competition. In *V. cholerae*, the T6 can eliminate non-kin cells, preventing cheaters and invaders that are susceptible to T6 killing in the population [132, 133]. This aggression behavior promotes phase separation in a bacterial community, facilitating coexistence and resulting in a spacial organization that is hypothesized to promote cooperative interactions [131]. Understand the interactions

outside and within the biofilm are crucial in assessing how bacteria sense and response to antagonistic mechanisms.

1.4.3 Stress responses

During respiration in aerobic organisms, including *E. coli*, reactive oxygen species (ROS) (e.g. superoxide O_2^- and hydrogen peroxide H_2O_2) are generated as a by-product [134]. ROS are highly reactive and cause oxidative damage to the building blocks of the cell, including DNA mutations and protein oxidation which changes structure and leads to malfunction [134, 135]. In *E. coli*, the level of ROS is controlled by OxyR and SoxR/SoxS systems that help against H_2O_2 and O_2^-, respectively [136]. Interestingly, *soxS* is highly expressed when *E. coli* is attacked by *V. cholerae* T6, and *E. coli* without the SoxR/SoxS but not OxyR system is even more susceptible [137]. This suggests T6 attack increases ROS production in target cells, with stress response systems playing a role in protection against T6 attack [137].

As previously described, most T6 toxins target the cell membrane, which acts as the first line of defense. Disruption of the cell membrane by T6 attack induces envelop stress response [137, 138]. In *E. coli*, T6 attack with the *V. cholerae* peptidoglycan-degrading effector TseH induces two envelop stress responses, the Rcs and Bae systems [137, 138]. A gene knockout of either Rcs or Bae regulator (Δ*rcsB* or Δ*baeR*) leads to decrease in survival [137, 138]. RcsB regulates genes responsible for osmotic stress, supporting the model that T6 effectors alter membrane function by the peptidoglycan degradation [138]. In addition, RcsB also induces the production of colanic acid to promote capsule formation and form mucoid colonies [138, 139]. These exopolysaccharides act as a physical barrier to prevent further T6 attacks. The mechanisms of Bae system to increase T6 resistance remains unclear, yet overexpression of periplasmic chaperon Spy, a component of the BaeR regulon, improves *E. coli* recovery against TseH [137, 138].

1.4.4 Environmental inputs

Bacteria alter gene expression and behaviors depending on environmental conditions. *E. coli* has been recently reported by the Hammer lab to show an increase in T6 resistance when grown on media supplemented with glucose [140]. Although the mechanism of resistance is currently not known, the CRP, a global transcription factor that is negatively regulated by the presence of glucose, is involved [140]. Deletion of CRP recapitulates the increase in T6 resistance observed when growing *E. coli* on a glucose medium [140]. Hence, the current model suggested in high glucose condition, CRP is inactive in *E. coli* and directly or indirectly represses putative genes resulting in protection from T6 attacks [140].

1.4.5 Dissertation outline

In this dissertation, my work in Chapter 2 highlights the discovery of a new T6 regulatory mechanism, with results recently published on *mBio* [61]. Combining phenotypic, genetic, and genomic analysis, I discovered a *cis*-acting single-nucleotide polymorphism (SNP) in *V. cholerae* that converts T6 expression between an inducible and constitutive state. This SNP is highly conserved within human-derived strains and environmental strains, consistent with the pathoadaptive hypothesis. In Chapter 3, I describe new results submitted for publication describing mutations that lead to increase in T6 resistance in *E. coli*. We describe how these mutations come with trade-off such as growth defects. Finally, in Chapter 4 I summarize my dissertation and discuss how the contribution of my work addresses the knowledge gaps in the field and improves our understanding of the evolution of gene regulation and antagonistic interaction in bacteria.

CHAPTER 2

EVOLUTION OF A *CIS*-ACTING SNP THAT CONTROLS TYPE VI SECRETION IN *VIBRIO CHOLERAE*

Reproduced in part with permission from Siu Lung Ng, Sophia A Kammann, Gabi Steinbach, Tobias Hoffmann, Peter J Yunker, Brian K Hammer. Evolution of a *cis*-acting SNP that controls Type VI secretion in *Vibrio cholerae*. *mBio*. 2022. e00422-22.[141]

2.1 Abstract

Mutations in regulatory mechanisms that control gene expression contribute to phenotypic diversity and thus facilitate the adaptation of microbes and other organisms to new niches. Comparative genomics can be used to infer rewiring of regulatory architecture based on large effect mutations like loss or acquisition of transcription factors (TFs) but may be insufficient to identify small changes in noncoding, intergenic DNA sequence of regulatory elements that drive phenotypic divergence. In human-derived *Vibrio cholerae*, the response to distinct chemical cues triggers production of multiple TFs that can regulate the type VI secretion system (T6), a broadly distributed weapon for interbacterial competition. However, to date, the signaling network remains poorly understood because no regulatory element has been identified for the major T6 locus. Here we identify a conserved *cis*-acting single-nucleotide polymorphism (SNP) controlling T6 transcription and activity. Sequence alignment of the T6 regulatory region from diverse *V. cholerae* strains revealed conservation of the SNP that we rewired to interconvert *V. cholerae* T6 activity between chitin-inducible and constitutive states. This study supports a model of pathogen evolution through a noncoding *cis*-regulatory mutation and preexisting, active TFs that confers a different fitness advantage to tightly regulated strains inside a human host and unfettered strains adapted to environmental niches.

2.2 Importance

Organisms sense external cues with regulatory circuits that trigger the production of TFs, which bind specific DNA sequences at promoters (*cis*-regulatory elements (CREs)) to activate target genes. Mutations of TFs or their regulatory elements create phenotypic diversity, allowing exploitation of new niches. Waterborne pathogen *V. cholerae* encodes the T6 "nanoweapon" to kill competitor cells when activated. Despite identification of several TFs, no regulatory element has been identified in the promoter of the major T6 locus, to date. Combining phenotypic, genetic, and genomic analysis of diverse *V. cholerae* strains, we discovered a SNP in the T6 promoter that switches its killing activity between a constitutive state beneficial outside hosts and an inducible state for constraint in a host. Our results support a role for noncoding DNA in adaptation of this pathogen.

2.3 Introduction

A central role in the dynamic, temporal control of gene expression is played by TFs, diffusible "*trans*" products that bind to molecular switches within DNA sequences termed CREs. In eukaryotes, where horizontal gene transfer (HGT) is rare, mutations in CREs that alter TF binding sites are major contributors to phenotypic diversity [142–144]. In bacteria, pervasive HGT can alter entire regulatory circuits that allow adaptation to new niches, as prominently demonstrated in *Vibrio fischeri*, where host range is altered by the presence or absence of a histidine kinase RscS, which regulates biofilm and colonization genes via indirect mechanisms [145, 146]. By contrast, specific mutations at CREs in noncoding DNA are more difficult to identify and receive less attention as drivers of phenotypic divergence and evolutionary adaptation [147]. Thus, elucidation of how microbes adapt to new niches, a process of fundamental importance in bacterial pathogenesis, requires coupling of genome-wide computational methods with experimental approaches to map the *cis*- and *trans*-regulatory interactions across and within species.

To understand how mutations play a role in microbial adaptation, pathogenic viruses and bacteria with lifestyles that exploit niches within and outside a human host are of great interest. Following ingestion, pandemic strains of the bacterium *V. cholerae* can colonize the human gastrointestinal tract and secrete the cholera toxin that leads to the often fatal diarrhea responsible for seven pandemics to date [92, 148, 149]. Conversely, *V. cholerae* isolated from nonhuman niches lack the horizontally acquired prophage that carries the cholera toxin, and cause mild illness [7]. By contrast, all sequenced *V. cholerae* encode a T6, a broadly distributed "nano-harpoon" weapon that injects toxic effector proteins into neighboring bacterial cells, leading to cell envelope damage and cell lysis [30, 51]. Due to its broad distribution among bacteria including those of the human gut, there is intense interest in understanding the T6 interactions between our microbiota and foreign pathogens, and whether they can be manipulated to influence health [150].

V. cholerae obtained from humans carry a limited arsenal of effectors and a T6 believed to be tailored for *in vivo* success [51, 60, 101, 122, 151–153], while strains from nonhuman niches encode a more diverse effector repertoire [51, 53, 60, 113]. To date, however, adaptive evolution mechanisms of T6 regulation in *V. cholerae* derived from nonhuman sources have largely been overlooked. Since the discovery of T6, studies of human-derived strains identify two primary TFs for T6 activation [41, 50, 65, 67, 154]. T6 control in pandemic strains (e.g., C6706 and A1552) requires QstR, which is positively regulated by multiple external cues, including chitin that triggers TfoX production, and quorum-sensing autoinducers that control the well-studied LuxO/HapR regulatory circuit [66, 71, 88, 155]. QstR also contains a C-terminal DNA binding domain postulated to interact with a presumptive CRE of the major T6 gene cluster, yet how QstR-DNA interaction affects T6 transcription remains unclear [65, 88]. On the other hand, T6 regulation in nonpandemic strain V52, which causes mild disease, requires TfoY. Expression of *tfoY* is modulatable by the intracellular second messenger 3',5'-cyclic diguanylic acid (c-di-GMP) [67, 154]. At low c-di-GMP levels, *tfoY* expression is posttranscriptionally regulated by a *cis*-acting

riboswitch located upstream of the gene. At high c-di-GMP levels *tfoY* is regulated by transcription factor VpsR, which binds the second messenger [94]. Despite significant progress over the past decade in uncovering the signaling systems that modulate QstR and TfoY, the mechanisms by which these two regulatory proteins control gene expression remain unclear. Similarly, direct regulators of T6 transcription, still remain elusive, with only one putative T6 CRE described [65]. Elucidation of the differences in intraspecies T6 regulatory mechanisms between diverse *V. cholerae* isolates will provide insights into how pathogens emerge from nonpathogenic progenitors.

To understand the regulatory differences in *V. cholerae* strains, we examine several environmental isolates that exhibit T6-mediated killing [59]. Despite encoding functional signaling circuity and TFs, we find that QstR is dispensable for killing and that TfoY plays only a minor role for killing in the strains tested. Thus, existing regulatory models fail to explain the T6 control in *V. cholerae* from human and nonhuman sources. Genomic analysis identifies one conserved noncoding SNP that we show interconverts *V. cholerae* T6 activity between chitin-inducible and constitutive states, which are QstR-dependent and TfoY-independent, respectively. We demonstrate that noncoding SNPs can rewire CREs, which may aid in adaptation of bacteria to different niches, including the human host.

2.4 Results and discussion

2.4.1 Constitutive, *in vitro* T6 activity requires neither QstR nor TfoY in many environmental *V. cholerae* isolates

In pandemic C6706, high cell density (HCD) and chitin are required for induction of *qstR* which leads to activation of T6 genes. In the absence of chitin, C6706 with *qstR* expressed from a heterologous promoter (defined here as *qstR**) reduces survival of *E. coli* "target" cells in coculture by over 4-orders of magnitude (˜10,000), compared with widetype (WT) C6706, a T6 strain with a mutation in an essential structural gene ($\Delta vasK$), and a strain with a $\Delta qstR$ mutation (Figure 2.1A) [66]. Deletion of *tfoY* does not reduce the

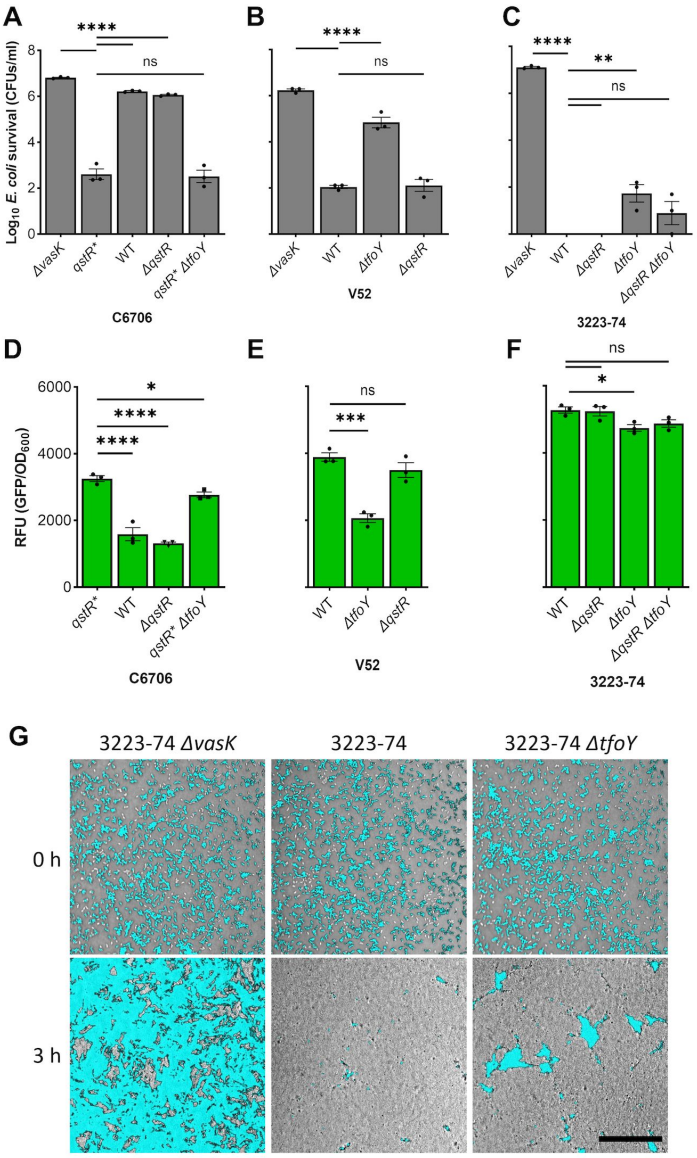

Figure 2.1: ***V. cholerae* 3223-74 T6 activity is QstR- and TfoY-independent.** (A to C) *V. cholerae* strains with the indicated genotypes were cocultured with chloramphenicol (Cm) resistant *Escherichia coli* followed by determination of *E. coli* survival by counting of CFU on lysogeny broth (LB) agar with Cm. A *V. cholerae* Δ*vasK* mutant defective in T6 assembly served as a T6- negative control. (D to F) Relative Fluorescence Units are from reporters with green fluorescent protein (*gfp*) fused to the intergenic region 5' of *vipA* derived from the strains shown. The mean value ± S.E. from cocultures (A to C) and monocultures (D to F) are derived from three independent biological replicates. A one-way ANOVA with Dunnett post hoc test was conducted to determine the significance: ns denotes not significant, ****, $P \leq 0.0001$; ***, $P \leq 0.001$; **, $P \leq 0.01$; *, $P \leq 0.05$. (G) *E. coli* cells expressing constitutive *gfp* were competed against 3223-74, with the same frame imaged at 0 h and 3 h by confocal microscopy. In the images, *gfp* signal from the *E. coli* is overlaid on top of bright-light images of the coculture. Scale bar = 50 μm.

killing activity of the T6+ *qstR** strain, but eliminates the robust killing in the nonpandemic strain V52 (serogroup O37), which requires TfoY but not QstR (Figure 2.1B) [67].

To determine whether QstR or TfoY participates in control of the T6 in nonhuman derived strains, we examined 3223-74, a genetically amenable, T6-proficient environmental strain [59]. Like V52, 3223-74 does not require QstR to efficiently kill *E. coli* in conditions without chitin, but surprisingly, also does not require TfoY. Isogenic strains carrying the Δ*tfoY* and Δ*qstR* Δ*tfoY* mutations retain >99.99% killing activity, with only modest *E. coli* survival (Figure 2.1C). Gene fusions of the 5' intergenic region (IGR) of the major TFs cluster of each strain fused to *gfp* confirm that transcriptional differences account for the killing observed, with maximal gfp expression mirroring activity (i.e., low *E. coli* survival with high *gfp* expression, and vice versa) (Figure 2.1D to F). To confirm that expression of the major T6 loci is not influenced by transcriptional read-through from a regulatory element upstream of the IGR, a T7 terminator [156] was inserted directly after the stop codon of *vca0106* in *V. cholerae* with activated T6 (Figure A.1). We observed no differences in T6 killing, demonstrating that the IGR is sufficient for control of the major T6 locus. Confocal microscopy reinforces the negligible role of TfoY on killing by 3223-74, with a Δ*tfoY* mutation having little effect on killing WT (Figure 2.1G). Transcription of plasmid-borne reporters is significantly higher in *V. cholerae* than in *E. coli* (Figure A.2), supporting a hypothesis that an additional *V. cholerae*-specific regulator of the T6 may remain to be identified.

To probe each strain's T6-related regulatory circuitry, we measured canonical behaviors under the control of HapR, QstR, and TfoY; quorum sensing (QS) controlled bioluminescence, natural transformation, and motility, respectively [86, 94, 157]. As expected, each TF is intact in C6706; but like several *V. cholerae* strains, V52 lacks a functional *hapR* gene that prevents QS and natural transformation [26, 158]. Nonetheless, V52 encodes a functional *tfoY* that controls motility (Figure 2.2A and B) [67]. Interestingly, the regulatory circuity of *V. cholerae* 3223-74 is intact, like C6706, confirming that it encodes functional

TFs (Figure 2.2C), which are nonetheless expendable for T6-mediated killing. Nucleoid associated proteinss (NAPs) that bind DNA both specifically and nonspecifically [159] may contribute to T6 transcription. NAPs participate in regulation of many promoters in numerous bacteria including *Vibrios* [160], yet NAP regulation and expression levels may differ in C6706 and 3223-74 [161]. It is also possible that T6 regulation is complex and involves more than one TF specific to *V. cholerae*.

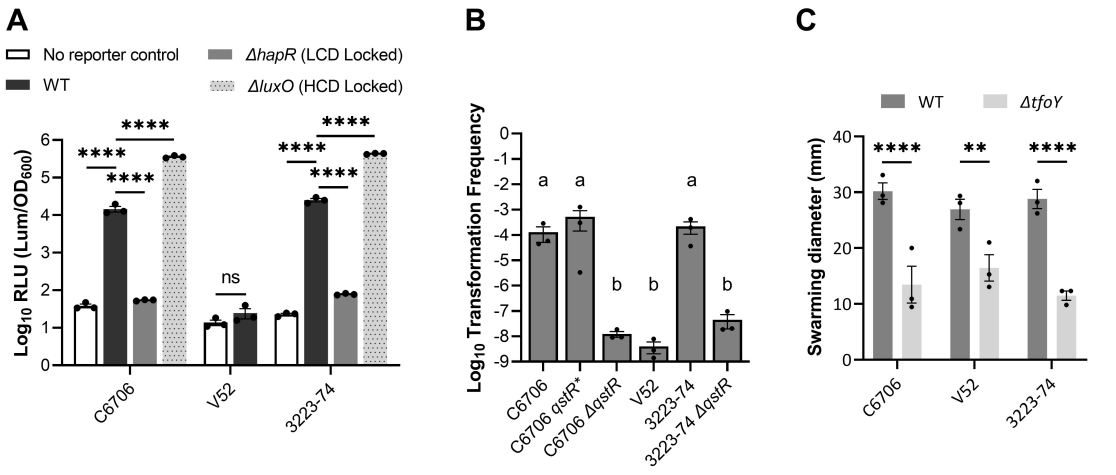

Figure 2.2: ***V. cholerae* 3223-74 encodes functional HapR, QstR, and TfoY.** (A) *V. cholerae* strains with and without a QS-dependent lux reporter cosmid (pBB1) were grown in liquid LB with relative luminescence units per optical density (OD_{600}) measured at HCD (OD_{600} = 0.6-0.8). Statistical analyses were conducted with one-way ANOVA with Tukey post hoc test (C6706 and 3223-74) and one-tailed Student's t test (V52). The Δ*hapR* mutant is defective at QS and effectively "locked" at low cell density (LCD), while the Δ*luxO* mutant that constitutively produces HapR is effectively "locked" at HCD. (B) *V. cholerae* strains with the indicated genotypes were grown in ASW with crab shell and exogenous spectinomycin (Spec)-marked genomic DNA. Transformation frequency = $Spec^R$ CFU mL^{-1}/total CFU mL^{-1}. Statistical analyses were conducted with one-way ANOVA with Tukey post hoc test. Letters "a" and "b" identify statistically significance ($P \leq 0.05$) of transformation frequency between *V. cholerae* strains. (C) *V. cholerae* strains were inoculated on 0.3% LB agar and grew overnight. Statistical analyses were conducted with one-tailed Student's t test. Colony diameters were physically measured from the furthest edges. All data shown are the mean ± S.E. from 3 independent biological replicates. ns: not significant, ****, $P \leq 0.0001$; **, $P \leq 0.01$.

2.4.2 A SNP in the T6 intergenic region confers QstR-dependency

Human and environmental isolates of *V. cholerae* we have characterized prior [59] share $\geq$97% average nucleotide identity with many chromosomal differences [51]. Yet, inspection of the T6 IGRs of C6706, V52, and 3223-74 revealed only 17 SNPs and three multinucleotide polymorphisms (Figure 2.3A), which we hypothesized could contribute to the differences in T6 transcription and killing activity observed. To address this, we replaced the T6 IGR of C6706 on the chromosome with that from V52 and 3223-74 and measured killing activity. While C6706 carrying the *qstR** allele, but not WT, adeptly kills *E. coli*, both IGR replacements increase the killing efficiency of WT C6706 by 5- to 6-orders of magnitude (Figure 2.3B), mimicking the robust killing observed by WT V52 and 3223-74 (Figure 2.1B and C). Deletion of *tfoY* but not *qstR* in C6706 with V52's IGR increases *E. coli* survival (˜2-logs), as observed with V52, but does not alter *E. coli* survival with 3223-74's IGR (Figure 2.3B; Figure A.3). Chromosomal transcriptional *gfp* reporters with identical mutations were elevated relative to WT C6706 in each IGR replacement strain (Figure 2.3C), consistent with the enhanced killing detected. How TfoY controls gene expression is currently unknown and beyond the scope here. However, we speculate that slight differences detected in survival but not T6 transcription when *tfoY* is deleted from C6706 carrying the IGR of V52 may result from indirect effects of TfoY, or a factor(s) specific to V52 and absence in C6706. These results support a hypothesis that a novel CRE lies within the IGR 5' of the T6 locus, despite a lack of any known direct TF-DNA interactions at this locus identified to date.

To begin mapping the T6 IGR region and SNP locations, we experimentally determined the transcriptional start site (+1) by 5' rapid amplification of cDNA ends (5' RACE) (section 2.5). The +1 of transcription resides 320 nucleotides (nts) 5' of the ATG of the first T6 gene (*vipA, vca0107*), and adjacent to a putative promoter with 8/12 identical nucleotides compared with the consensus sigma70-dependent promoter (Figure 2.3A). The +1 is consistent with paired-end RNA-seq results we have reported prior [66]. Because the majority

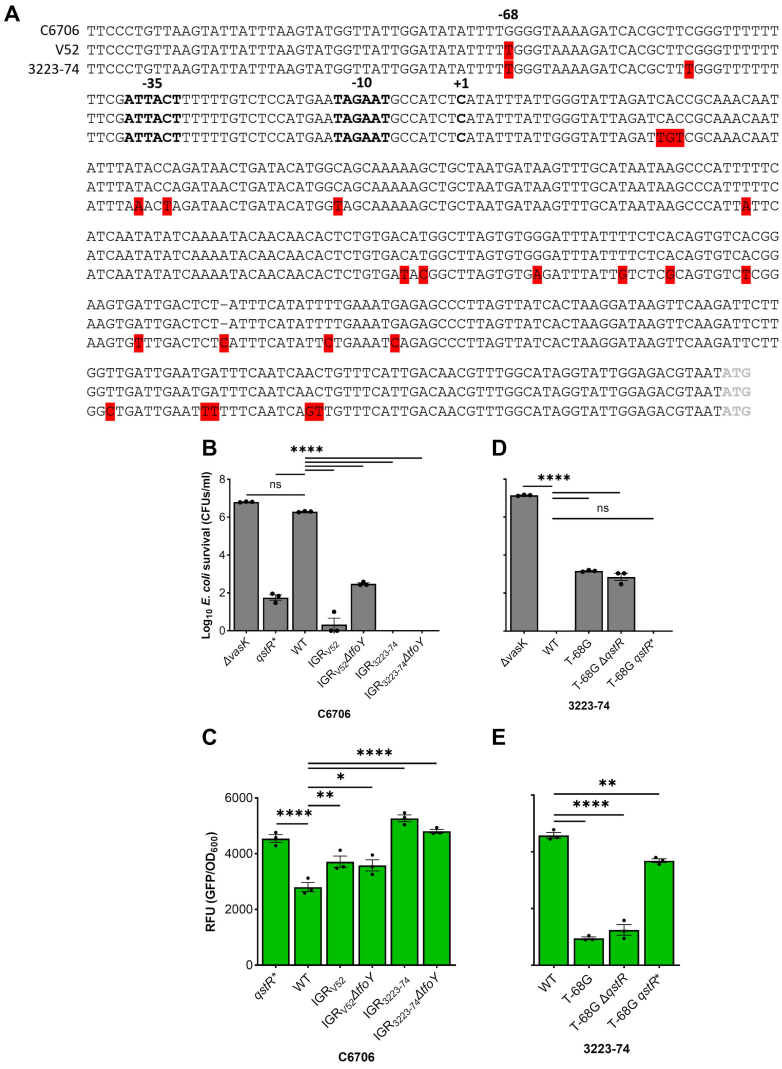

Figure 2.3: **G-68T mutation abolishes QstR dependence in C6706 and T-68G confers QstR dependence to 3223-74.** (A) Alignment of the IGR upstream of *vipA* was conducted using MUSCLE. SNPs and MNPs are highlighted in red, one gap indicated with a "-," the putative promoter and the transcriptional start site (TSS; +1) in bold, and the start codon of *vipA* in gray. (B) the C6706 5' IGR of *vipA* was replaced with the IGR from either V52 or 3223-74. (D) A T-68G mutation in the 5' IGR of *vipA* was introduced into 3223-74 with different *qstR* alleles. Competition assays were conducted by coculturing *V. cholerae* killers and Cm^R *E. coli* target followed by determination of *E. coli* survival by counting of CFU on LB agar with Cm. The *V. cholerae* Δ*vasK* mutant unable to assemble a functional T6 served as a T6- negative control. (C, E) Shown are fluorescence levels of transcriptional reporters with *gfp* fused to corresponding IGRs of *vipA* expressed in either C6706 (C) or 3223-74 (E). Shown are mean values ± S.E. from three independent biological replicates of cocultures (B and D) and monocultures (C and E). A one-way ANOVA with Dunnett post hoc test was conducted to determine the significance. ns, not significant; ****, $P \leq 0.0001$; **, $P \leq 0.01$; *, $P \leq 0.05$.

of 5' untranslated regions (5' UTRs) in *V. cholerae* are 20 to 40 nt, with few exceeding 300 nt [162], we speculate that the 320 nt 5' UTR of the major T6 gene cluster may be posttranscriptionally regulated, beyond the sRNA interactions already described near the ribosome binding site (RBS) [163]. Alignment of the IGRs of C6706 and V52 reveals a single SNP at -68, with a guanine (G) in C6706 at that position and a thymine (T) in V52 (Figure 2.3A).

The replacement of the C6706 IGR with V52 was effectively a G-68T mutation (Figure 2.3B and C), thus we further tested whether G was necessary for QstR activation by replacing the T with a G at position -68 (T-68G) in the 3223-74 WT, *qstR**, and Δ*qstR* backgrounds. The T-68G mutation significantly increases *E. coli* survival and decreases T6 transcription in WT 3223-74 and the Δ*qstR* derivative, with killing restored in the strain with the *qstR** allele (Figure 2.3D and E). Thus, a G at position -68 confers inducible, QstR-control, while a T results in constitutive killing *in vitro*, consistent with results recently reported during manuscript revision [62]. Based on these results we predicted this SNP is a result of adaptive evolution to control T6 activity in different environments.

2.4.3 The SNP at -68 is evolutionarily conserved

To determine whether the SNP at -68 is prevalent in *V. cholerae*, we aligned the T6 IGR sequences of diverse strains that we have characterized prior for T6 killing activity (Figure 2.4A) [59]. Consistent with prior studies [51, 60, 122, 152], our phylogenetic analysis (section 2.5) of the T6 IGRs places human strains in a distinct clade, with the exception of two O1 strains isolated nearly a century ago (NCTC8457 and MAK757), and two non-O1 strains (MZO-2 O14 and V52 O37; Figure A.4). All 23 environmental isolates carry the T-68 SNP and displays constitutive T6 activity, with one exception that is chitin-inducible (1496-86) (Figure 2.4A; Figure A.4). By contrast, the 18 human-derived isolates tested carry either G or T at the -68 position (Figure 2.4A; Figure A.4). The 13 chitin-inducible human isolates carry a G; five show constitutive activity and carry a T, like

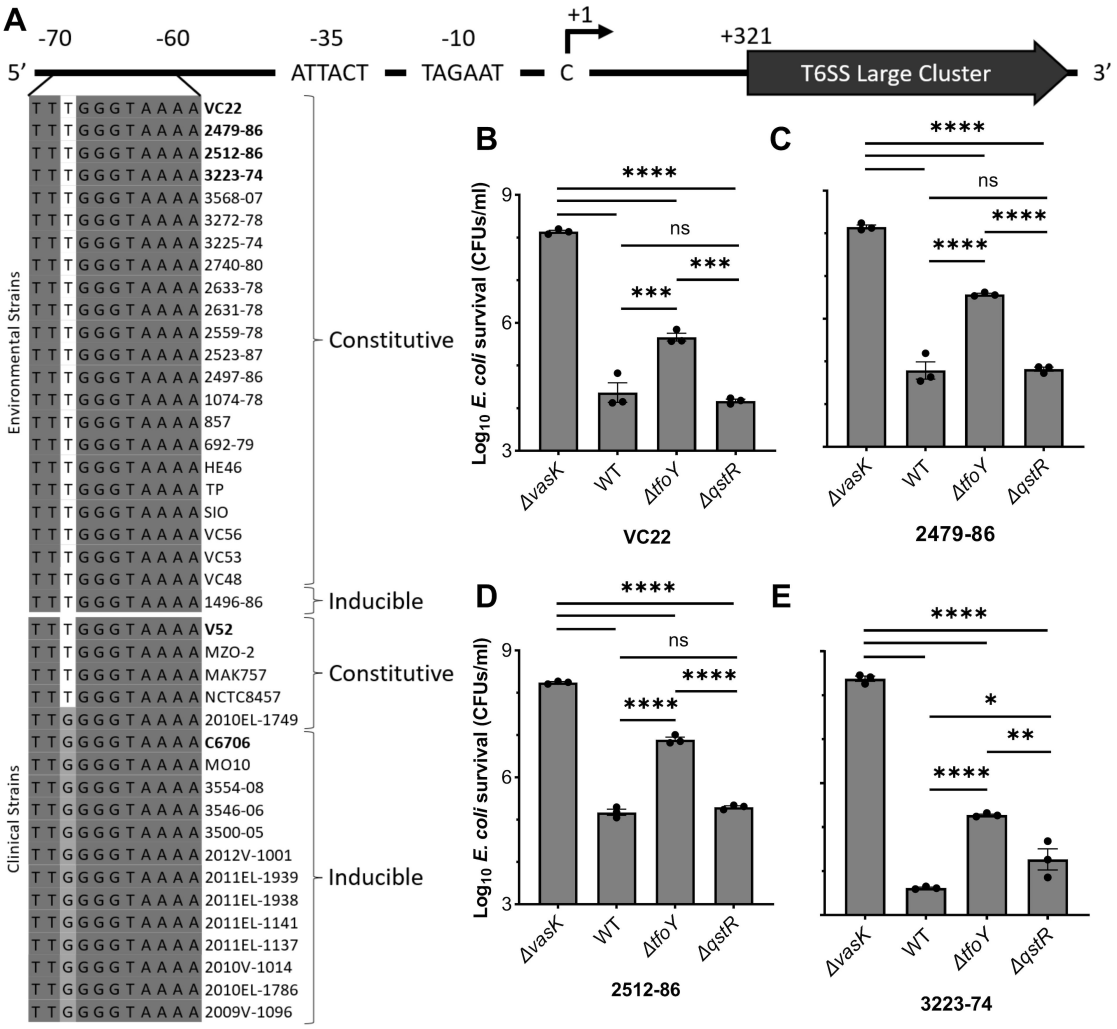

Figure 2.4: **Environmental *V. cholerae* isolates encode a T at position -68 while human, chitin-induced isolates encode a G.** (A) A SNP at position -68 in the IGR of the major T6 cluster controls killing activity. Conserved nucleotides are in dark gray and the SNP of interest is highlighted in white/gray. T6 control was categorized as described [59]. (B to E) Survival of *E. coli* following competition assays with WT *V. cholerae* strains and mutants was determined by CFU counts. The *V. cholerae* Δ*vasK* mutant served as a T6- negative control. Data shown are mean values ± S.E. of three independent biological replicates. A one-way ANOVA with Tukey post hoc test was conducted to determine the significance. ns, not significant; ****, $P \leq 0.0001$; ***, $P \leq 0.001$; **, $P \leq 0.01$; *, $P \leq 0.05$.

environmental strains, with one exception that is constitutive yet carries the G (2010EL-1749) (Figure 2.4A; Figure A.4). Neither adenine (A) nor cytosine (C) are observed at -68 in any stains tested, although both pyrimidine nucleotides (T and C) confer constitutive killing at -68, and both purines (G and A) behave similarly (Figure A.5). The focal SNP location is distal from the promoter, but inconsistent with AT-rich "UP-elements" that reside immediately upstream of the promoter at -38 to -59 and interact directly with the alpha subunit of RNAP [164]. We propose the SNP is more likely a component of a CRE for a TF to be determined. Indeed, transversion mutations have greater effects of TF binding than transitions, as noted here (Figure A.5) likely due to changes in shape of the DNA backbone or DNA-amino acid contacts [165, 166].

We examined regulation of three additional genetically manipulatable environmental strains (VC22, 2479-89, and 2512-86) that exhibit T6 killing [59]. Like 3223-74, QstR is expendable in each strain (Figure 2.4B to E) while TfoY contributes to some extent in activating T6, with varying *E. coli* recovery observed in each derivative carrying the Δ*tfoY* mutation (Figure 2.4B to E). Taken together, our findings reveal that the constitutive T6 killing activity of environmental *V. cholerae* is driven by a T at position -68, which obviates the QstR requirement, and permits modest TfoY regulation.

Bacterial adaptation to unexploited niches can be the result of horizontal gene transfer events [146] as well as mutations in protein coding and promoter regions [167, 168]. Here we describe an intergenic noncoding SNP that coordinates adaptation by altering T6 control between two states-one that is inducible and the other that displays constitutive activity. While the T6 was first described in *V. cholerae* in 2006, the knowledge of its regulation remains largely restricted to human isolates, and the identity of a TF that directly controls the major T6 cluster remains elusive to this date [41, 50]. We speculate that the focal SNP we identified at position -68 is a component of a CRE that contributes to pathoadaptation (Figure 2.3A), a result of adaptive evolution, which allows *V. cholerae* to carefully control the T6 expression in specific environments. Our results are consistent with the hypothesis

that constitutive T6 is beneficial in aquatic environments outside a human host [63], with varying degrees of TfoY contribution, which may act directly or indirectly at the transcriptional or posttranscriptional level (Figure 2.3A; Figure 2.4B to E; Figure A.6). During human infection where selection promotes dampened T6, *V. cholerae* with a T-to-G mutation (inducible T6) are favored. In fact, T6-deficient human isolates (e.g., O395) have been reported to have less competitive fitness in human intestinal colonization and infection [32, 153]. Although low level, basal expression of T6 contributes to pathogenesis of C6706 [169], overexpression of T6 may be deleterious *in vivo*. Indeed, we have reported prior that *V. cholerae* with constitutive T6 induces violent peristaltic contractions in a fish host [112], which may disrupt the interaction between *V. cholerae* and the gut microflora.

There remains a pressing public health need to understand the emergence of pathogens from environmental reservoirs [170]. Efforts such as microbial genome wide association studies [171] to identify genetic variants in genomes that are associated with phenotypes like virulence and antibiotic sensitivity will be bolstered by knowledge of the ecological and evolutionary processes that promote pathogen-host association. Defining the plasticity of the regulatory circuity controlling the T6 weapon will provide insights into the role of polymorphisms in the evolution of this and other pathogens.

2.5 Materials and methods

2.5.1 Bacterial growth conditions and plasmid constructions

All *V. cholerae* and *E. coli* (Table A.1) strains were grown aerobically at 37°C overnight in LB with constant shaking or statically on LB agar. Ampicillin (100 μg/mL), kanamycin (50 μg/mL), Cm (10 μg/mL), Spec (100 μg/mL), streptomycin (5 mg/mL), sucrose (20% weight/volume), and diaminopimelic acid (50 μg/mL) were supplemented where appropriate.

Plasmids (Table A.2) used were constructed with DNA restriction nucleases (Promega, WI, USA), Gibson Assembly mix (New England Biolabs, MA, USA), and PCR amplifi-

cation (Qiagen, Hilden, Germany) by PCR with Q5 polymerase (New England Biolabs, MA, USA), and primers (Table A.3) generated by Eton Bioscience Inc. (NC, USA) or Eurofins Genomics (KY, USA). All reagents were used according to the manufacturer's instructions. Plasmids were confirmed by PCR and Sanger sequencing by Eton Bioscience Inc. (NC, USA).

2.5.2 *V. cholerae* mutant construction

All genetically engineered strains of *V. cholerae* were constructed with established allelic exchange methods using vector pKAS32 [172] and pRE118 (Addgene - Plasmid #43830). All insertions, deletions, and mutations were confirmed by PCR and Sanger sequencing conducted by Eton Bioscience Inc. (NC, USA). Primers used are in Table A.3.

2.5.3 Fluorescence microscopy

Variants of *V. cholerae* strain 3223-74 and an *E. coli* MG1655 strain with *gfp* introduced into the chromosome were separately back-diluted 1:100 and incubated at 37°C for 3 h. *V. cholerae* and *E. coli* were normalized to OD_{600} = 1 and mixed in a 1:5 ratio. A 2 μL aliquot of a mixed culture was inoculated on LB agar and allowed to dry. Cells were imaged before and after a 3 h of incubation at 37°C and 96% to 100% humidity using an Eclipse Ti-E Nikon (NY, USA) inverted microscope with a Perfect Focus System and camera previously described [51]. The images were processed with ImageJ [157].

2.5.4 Motility assay

Overnight cultures of *V. cholerae* were diluted to OD_{600} = 0.1, and 1 μL inoculated onto predried LB plates with 0.3% agar. Cells were incubated at 37°C statically overnight, with motility determined by measuring the swarming diameter.

2.5.5 Transformation assay

Chitin-induced transformation frequency was measured as described with defined artificial seawater (450 mM NaCl, 10 mM KCl, 9 mM CaCl2, 30 mM MgCl2·6H2O, and 16 mM MgSO4·7H2O; pH 7.8) [173]. Bacteria were incubated with extracellular DNA in triplicate wells containing crab shell tabs, and transformation frequency calculated as Spec^R CFU mL^{-1}/total CFU mL^{-1}.

2.5.6 Quorum sensing dependent luciferase assay

A previously described, pBB1 cosmid was used as a QS-dependent lux reporter in *V. cholerae* [174]. Overnight cultures of the *V. cholerae* strains were diluted to OD_{600} = 0.001 in liquid LB in microtiter plates and incubated at 37°C with shaking. The OD_{600} and luminescence were measured each hour with a BioTek (VT, USA) Synergy H1 microplate reader to calculate relative luminescence units (RLU) as luminescence/OD_{600}. *V. cholerae* without the cosmid served as a negative control (no reporter control). Data were collected when OD_{600} = 0.6 to 0.8. LB medium was used to blank the microplate reader for OD_{600} and luminescence readings.

2.5.7 GFP Transcriptional reporter quantification

Overnight cultures of *V. cholerae* or *E. coli* were diluted 1:100 and incubated at 37°C for 3 h. To enhance the translation of *gfp*, the sequence of the native RBS (12 nt sequence) was replaced with the T7 RBS (12 nt sequence) in the primers used to make the fusions. Cm was added to maintain the plasmid-borne versions of reporters that were cloned into plasmid pSLS3. Then, 300 μL aliquots were transferred to black microtiter plates to read the OD_{600} and *gfp* fluorescence (Excitation: 485, Emission: 528) with a BioTek Synergy H1 microplate reader (VT, USA) to calculate relative fluorescence units (RFU) as fluorescence/OD600. LB medium was used as the blank for the OD_{600}. Strain lacking reporters were used to blank the spectrophotometer for *gfp* fluorescence measurements.

2.5.8 T6-mediated killing assay

Overnight cultures of *V. cholerae* or *E. coli* were back-diluted 1:100 and incubated at 37°C for 3 h. *V. cholerae* strains and the Cm^R *E. coli* target were normalized to OD_{600} = 1 and then mixed at a ratio of either 10:1 or 1:5. A 50 μL mixed culture was spotted onto LB agar and dried. After a 3 h of incubation at 37°C, cells were resuspended in 5 mL of LB, and serial dilutions were conducted. Finally, the resuspension was inoculated on a LB agar containing Cm to select for the surviving *E. coli*, which was incubated overnight at 37°C and the *E. coli* colonies were counted and shown as CFU mL^{-1}.

2.5.9 RNA extraction and determination of the +1 of transcription by 5'-RACE

Overnight cultures of *V. cholerae* were back-diluted 1:100 and incubated at 37°C for 3 h before lysing. Three independent cultures of TFs-active *V. cholerae* C6706 *qstR** and 3223-74 WT were harvested by centrifugation at room temperature. RNA isolation, genomic DNA removal, and RNA cleanup were performed as previously described [175]. Genomic DNA contamination was confirmed by conducting PCR with primer pair specific for 16S rRNA loci (rrsA) as previously described (Table A.3) [176]. RNA purity was confirmed by NanoDrop (260/280 $\approx$ 2.0).

5' RACE (Invitrogen, MA, USA) was conducted according to the manufacturer's protocol with slight modifications. Specifically, SuperScript IV reverse transcriptase (Invitrogen, MA, USA) was used to complete the first strand cDNA synthesis. Two *vipA*-specific primers (GT3056 and GT3060) were used to identify the +1 of transcription for the major T6 gene cluster (Table A.3). PCR products were purified with QIAquick PCR purification kit (Qiagen, Hilden, Germany) or Zymoclean gel DNA recovery kit (Zymo Research, CA, USA). Sanger sequencing was conducted by Eton Bioscience Inc. (NC, USA) with the corresponding nesting primer (Table A.3).

2.5.10 Genomic and phylogenetic analysis

Genome sequences of *V. cholerae* strains were collected from NCBI Genome database (Table A.4) [177]. The IGR upstream of major T6 cluster was extracted, aligned, and presented using BLAST+ v2.2.18 [178], MUSCLE v3.8 (https://www.ebi.ac.uk/Tools/msa/muscle/) [179, 180], and ESPript 3.0 (https://espript.ibcp.fr/) [181]. The DNA sequence of the IGR was used for phylogenetic analysis, and the phylogenetic tree was constructed by the Maximum likelihood method using MEGA11 [182, 183].

For 2012V-1001, 2011EL-1939, 2011EL-1938, and 2011EL-1141 that do not have genome sequence available, colony PCR was conducted to amplify the 5' IGR of the major T6 cluster using OneTaq DNA polymerase (New England Biolabs, MA, USA). PCR products were confirmed with gel electrophoresis and Sanger sequencing by Eton Bioscience Inc. (NC, USA) with the identical primer pair (Table A.3).

2.6 Acknowledgments

I thank Dr. Jyl S. Matson for assistance with RNA isolation and Dr. Marvin Whiteley and current and past members of the Hammer Lab for critiques and discussion, specifically, Dr. Samit Watve and Rakin Choudhury for bioinformatic advice and assistance.

CHAPTER 3

TRADE-OFFS CONSTRAIN ADAPTIVE PATHWAYS TO T6 SURVIVAL

Reproduced in part with permission from Kathryn A. MacGillivray, Siu Lung Ng, Sophia Wiesenfeld, Randi L. Guest, Tahrima Jubery, Thomas J. Silhavy, William C. Ratcliff, Brian K Hammer. Trade-offs constrain adaptive pathways to T6 survival.

3.1 Significance

Bacteria are the most abundant organisms on Earth that often live in dense, diverse communities, where they interact with each other. One of the most common interactions is antagonism. While most research has focused on diffusible toxins (e.g., antibiotics), bacteria have also evolved a contact-dependent nano-harpoon, the type VI secretion system (T6), to kill neighboring cells and compete for resources. While the co-evolutionary dynamics of antibiotic exposure is well understood, no prior work has examined how targets of T6 evolve resistance. Here, we use experimental evolution to observe how an *Escherichia coli* target evolves resistance to T6 when it is repeatedly competing with a *Vibrio cholerae* killer. After 30 rounds of competition, we identified mutations in three genes that improve *E. coli* survival but these mutations come at a cost to other key fitness components. Our findings provide new insight into how contact-dependent antagonistic interaction drives evolution in a polymicrobial community.

3.2 Abstract

Many microbial communities are characterized by intense competition for nutrients and space. One way for an organism to gain control of these resources is by eliminating nearby competitors. The T6 is a nano-harpoon used by many bacteria to inject toxins into neigh-

boring cells. While much is understood about mechanisms of T6-mediated toxicity, little is known about the ways that competitors can defend themselves against this attack, especially in the absence of their own T6. Here we use directed evolution to examine the evolution of T6 resistance, subjecting eight replicate populations of *E. coli* to T6 attack by *V. cholerae*. Over 500 generations of competition, the *E. coli* evolved to survive T6 attack an average of 27-fold better than their ancestor. Whole genome sequencing reveals extensive parallel evolution. In fact, we found only two pathways to increased T6 survival: *apaH* was mutated in six of the eight replicate populations, while the other two populations each had mutations in both *yejM* and *yjeP*. Synthetic reconstruction of individual and combined mutations demonstrate that *yejM* and *yjeP* are synergistic, with *yejM* requiring the mutation in *yejP* to provide a benefit. However, the mutations we identified are pleiotropic, reducing cellular growth rates, and increasing susceptibility to antibiotics and elevated pH. These trade-offs underlie the effectiveness of T6 as a bacterial weapon, and help us understand how the T6 shapes the evolution of bacterial interactions.

3.3 Introduction

Bacteria are one of the most common forms of life on Earth and often live in polymicrobial biofilms. Within this complex community, negative bacterial interactions are the norm [9], constantly competing for resources such as nutrients and space. One way for bacteria to gain an advantage over their competitors is by killing. They have developed two major classes of antagonistic mechanisms to eliminate competitors: diffusible and contact-dependent. Diffusible antibacterial molecules have been extensively described in soil bacteria like *Streptomyces*, which produces antibiotics (e.g. streptomycin, kanamycin, and tetracycline) to kill competitors, gain resources for their own population, and maintain symbiosis with associated plants [184]. *Pseudomonas aeruginosa* is also known to secrete lethal toxins like pyocyanin, exotoxin A, and ExoU that aid in competing against other microbes and human cells during infections [11–13]. On the other hand, contact-

dependent antagonisms are less diverse and understudied in the social interaction aspects. The T6 discovered in 2006, for example, is a contact-dependent "nano-harpoon" similar to a contractile spear that kills neighboring cells by injecting them with a set of toxic proteins [16]. The T6 is estimated to be found in 25% of all Gram-negative bacterial species [36, 37], and targets diverse cell types, including eukaryotes like macrophages and largely Gram-negative bacteria like *E. coli*, in both an environmental and host context [16, 30].

While the regulation, genetics and functional mechanics of the T6 have been well studied [41], we know relatively little about how targeted cells respond, defend, and survive T6 attack. Similar to antibiotic resistance, one strategy is to neutralize the toxins. Bacteria wielding a T6 that carries anti-microbial toxins do not intoxicate themselves or their sibling cells because a conjugate immunity protein is encoded in the same gene cluster as each toxin [31, 106, 116]. However, cells lacking immunity proteins are vulnerable to the toxins. In some cases, bacteria can acquire a library of orphan immunity proteins via horizontal gene transfer and mobile genetic elements, enabling them to survive toxins expressed by unrelated cells [60, 114, 122, 185]. *P. aeruginosa*, a model organism for T6 research, is able to use cues from the environment to fight back against a T6-wielding aggressor in two ways. In a "tit-for-tat" mechanism, cells that have been intoxicated by T6 can then assemble their own apparatus and launch a counter-attack in the same direction from which the first attack came [34]. *P. aeruginosa* is additionally able to induce T6 attack in response to kin cell lysis, via a mechanism called "danger sensing" [186]. Physical processes can also offer protection. Extracellular polysaccharide can protect cells from T6 attack, as does the accumulation of cellular material from lysed cells and physical separation, which are both consequences of T6 antagonism [128, 129, 131, 187]. External signaling can play a role in this protection, with recent reports that the presence of glucose enhances survival of *E. coli* cells to T6 attack, mediated through cyclic AMP and its cognate target, the CRP regulator [140]. Other regulators that coordinate stress response systems, such as Rcs and BaeSR may also play an important role, as deletions of these genes reduces survival from attack

[138, 188]. Transposon sequencing (Tn-seq) [189] offers one approach to identify genes that affect T6 resistance, uncovering mutations that either increase or decrease survival [190]. However, this technique has a limited range of mutations it can uncover, identifying only single null mutations contributing to a phenotype, but not deleterious mutations in essential genes, functional point mutations, or epistatic relations between multiple genes. Mutagenic screens also do not take pleiotropic side-effects of mutations into account. For example, mutations that increase T6 survival but come at a steep cost to cellular growth rates would be detected in such a screen, but might not be expected to arise under conditions where reproductive fitness is important.

Experimental evolution [191] circumvents many of these issues, allowing interrogation of the whole genome in a high-throughput, unbiased manner. By including periods of growth between rounds of T6 attack, this approach allows selection to include key pleiotropic fitness effects. Clonal interference among beneficial mutations means that only a small fraction of possible beneficial mutations will arise to high frequency in any given experiment [192], typically favoring those that are most adaptive. Rather than reporting all possible routes to surviving T6 attack, experimental evolution thus provides insight into genetic mechanisms that provide the largest fitness advantage over hundreds of generations of growth and periodic T6 assault.

In this paper, we explore how *E. coli* evolves resistance to T6 attack by *V. cholerae*. After 500 generations of growth, punctuated by 30 rounds of attack by the T6, we identified two main mutational pathways, each of which convergently evolved in multiple populations, that enabled dramatically improved survival by *E. coli* during T6 attack. Similar to other types of antibiotic resistance [193], we find that there was a strong trade-off between increased T6 survival and reduced fitness during growth, which may help explain the continued efficacy of T6 antibiotics in natural populations despite billions of generations of T6 exposure.

3.4 Results

3.4.1 Experimental evolution of T6 resistance

We report the development of an experimental evolution platform with two model organisms, to identify mechanisms by which bacteria can become resistant to T6 attack Figure 3.1A). We experimentally evolved eight replicate populations of *E. coli* MG1655, exposing them to daily attack by a *V. cholerae* C6706 strain variant that constitutively expresses the building blocks of the apparatus and its four T6 effectors, two that act in the periplasm to degrade the peptidoglycan cell wall (VgrG3 and TseH) and two that disrupt membranes (TseL and VasX) (see Materials and Methods) [31, 41, 102, 106, 108]. Delivery of inactive *V. cholerae* T6 effectors induces stress, but not decreased viability in *E. coli* [188]. The two species were co-cultured on agar plates in 1:10 ratio (target to killer) to ensure direct contact between cells, which is necessary for T6 attack. Between rounds of competition, *E. coli* populations were grown for 16 generations in lysogeny broth (LB) medium overnight. We also evolved four control populations, competing the same ancestral *E. coli* against a T6-deficient *V. cholerae* $\Delta vasK$ strain. We reasoned that mutations arising in these four control populations would account for adaptation in our environment, including growth, dilution, and co-culture with *V. cholerae* on solid media, but not from injury from T6. After 30 rounds of selection, evolved strains were an average of 27-fold more resistant to *V. cholerae*'s T6 attack, and the control populations had on average 3.9% higher survival, a negligible difference ($F_{11,71} = 15.8$, $p \leq 0.0001$, ANOVA with replicate nested in treatment. Fold survival was log-transformed prior to analysis to homogenize variances, and treatment effect was assessed with pre-planned contrast, $F_{1,60} = 234$, $p \leq 0.0001$; Figure 3.1B).

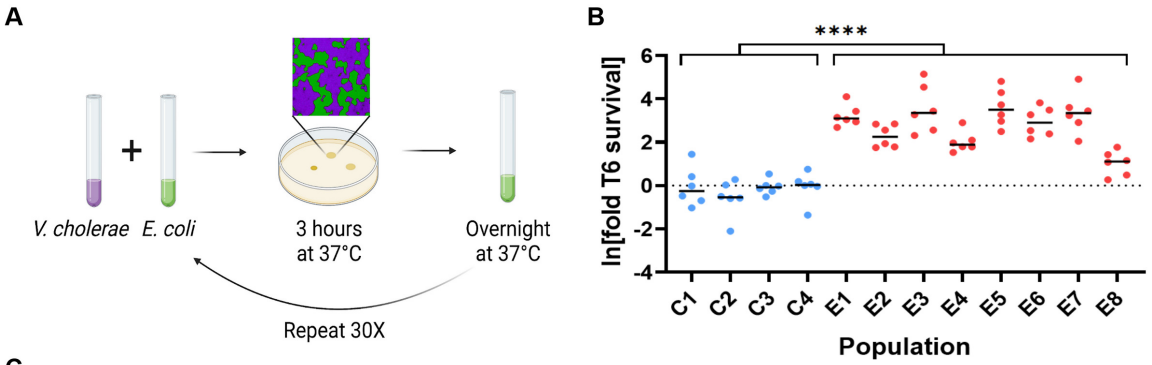

C

Gene	E1	E2	E3	E4	E5	E6	E7	E8
apaH **(280 AA; 840 nt)**	Δ1bp (121)	Δ13bp (602-614)		Δ1bp (359)		D37N	Δ4bp (125-128)	W249X
yejM **(586 AA; 1758 nt)**			$(8bp)_{2->3}$*		I427N			
yjeP **(1107 AA; 3321 nt)**			I724T		I724T	Q201L		

Figure 3.1: Experimental evolution of resistance to *V. cholerae*'s T6. (A) Experimental design. We experimentally evolved eight replicate populations of *E. coli*. Each round of selection included 16 generations of growth in liquid media, followed by co-culture with T6-expressing *V. cholerae* on solid media, where initially the vast majority of *E. coli* were killed. *V. cholerae* were removed via antibiotics, and the surviving *E. coli* resumed growth in liquid media. (B) Over 30 rounds of selection, *E. coli* in the T6 treatment evolved a 27-fold increase in T6 survival, while controls competed against a T6- *V. cholerae* did not evolve a significant increase in T6 resistance. **** denotes a difference in survival with $p \leq 0.0001$, determined via ANOVA and a pre-planned contrast. (C) Convergent evolution of genes affording T6 survival. Three genes were mutated in all eight independently evolving populations: *apaH* arose in six, while mutations in *yejM* and *yjeP* arose in the other two populations. For deletions (Δ), numbers in parentheses refer to the nt position of the deletion. (8bp)2->3* refers to an 8 nt repeat that expanded from 2 repeats to 3 repeats long, resulting in a frameshift mutation. W249X refers to a premature stop codon at position 249, resulting in a protein product truncated near the C terminus. (AA = amino acids; nt = nucleotides).

3.4.2 Identifying and characterizing key mutations

We identified mutations arising in our experiment by sequencing a single genotype from each population after 30 rounds of selection. With an average of 2.75 (standard deviation 1.09) mutations per genome in the experimental populations, we chose to focus on mutations that occurred in more than one replicate population, as convergent evolution strongly suggests these mutations are adaptive (Figure 3.1C, Figure B.1). Six of the eight isolates had mutations in *apaH*. Four of which are frameshift mutations, suggesting they resulted in loss-of-function (Figure 3.1C). This gene is responsible for the "de-capping" of mRNAs in a bacterial cell [194]. Little is known about the global regulatory effect of loss of *apaH*, but it is hypothesized that a null mutation leads to RNA stabilization. Notably, the isolate from population E8 only gained a 3-fold increase in survival relative to its ancestor; which was significantly lower than five of the seven other replicate experimental populations (Fold survival was log-transformed prior to analysis to homogenize variances, pairwise differences between each replicate population assessed via ANOVA and Tukey's HSD with overall significance at $\alpha = 0.05$; Figure 3.1B). The mutation in *apaH* found in this isolate creates a premature stop codon near the end of the gene (amino acid 249 out of 280) that likely retains partial function of *apaH*, resulting in a more modest survival advantage.

Two of the eight isolates did not have a mutation in *apaH*. Instead, these two populations each had missense or frameshift mutations in both *yjeP* (also known as *mscM*) and *yejM*, suggesting an interaction between these two genes (Figure 3.1C). *yjeP* encodes a mechanosensitive channel that protects cells from osmotic shock [195]. The gene *yejM* (also known as *pbgA* and *lapC*) encodes a metalloprotein that regulates bacterial lipopolysaccharides biosynthesis [196, 197]. Deletion of *yejM* is lethal in *E. coli*, while C-terminal truncation mutations result in partial function of the gene [198]. Both mutations we found in *yejM* occur near the C-terminus.

To test the function of mutations found in *apaH*, *yjeP*, and *yejM* independent of the role of other mutations that arose in experimental lineages (Figure B.1), we re-engineered

mutations in these genes in the ancestral strain. A clean deletion of *apaH* increases T6 protection by 3-fold, whereas E. coli carrying a single copy of *apaH* expressed from a heterologous constitutive promoter at the Tn7 site are 0.4-fold more susceptible than the ancestor (Fold survival was log-transformed prior to analysis to homogenize variances, comparison of means was accessed with one-sample t-test (μ = 0) and Bonferroni correction with overall significance at α = 0.05, p $\leq$ 0.0001 and p $\leq$ 0.001; Figure 3.2A; see Methods and Materials).

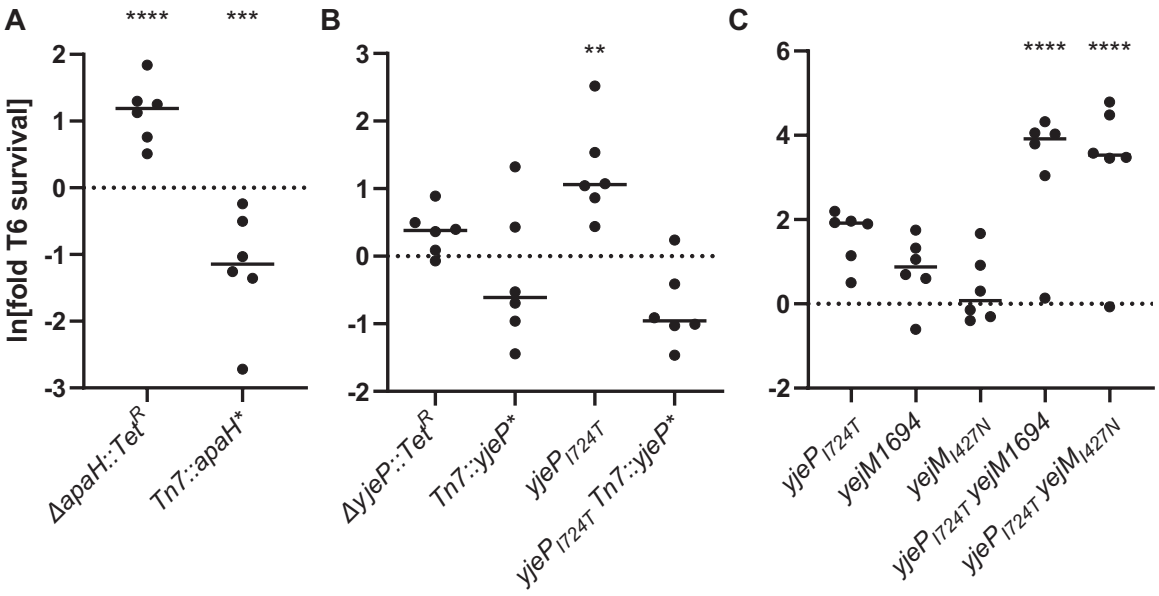

Figure 3.2: While all mutations of interest increase T6 resistance in various degrees, the *yjeP/yejM* double mutants survive significantly better. While (A) deletion of *apaH* did not offer significant increase in T6 protection, (B) *E. coli* with $yjeP_{I724T}$ had a slight increase in T6 resistance that was not observed in the constitutive variants. (C) The combination of $yjeP_{I724T}$ and mutations in the C-terminus of YejM significantly improved the *E. coli* survival by more than 42-fold. Linked markers used to construct the mutants are not indicated in the figure. ****, ***, and ** denote, differences in survival with p $\leq$ 0.0001, p $\leq$ 0.001, and p $\leq$ 0.01 respectively, determined via ANOVA and Dunnett's Multiple Comparison.

3.4.3 $yjeP_{I724T}$ is a gain-of-function mutation that confers T6 resistance

yjeP is one of four paralogs predicted to encode the MscS mechanosensory channel [195]. An identical missense mutation in *yjeP* ($yjeP_{I724T}$) occurred independently in two lineages (Figure 3.1C), suggesting that this amino acid substitution enhances T6 survival

and represents a gain-of-function mutation. In the ancestor genetic background, we introduced a *yjeP* disruption, constitutively expressed *yjeP*, and reconstructed the $yjeP_{I724T}$ mutation. Interestingly, neither the absence of *yjeP* nor its constitutive expression affected T6 survival. However, *E. coli* carrying the $yjeP_{I724T}$ mutation experienced a 4-fold survival benefit (Fold survival was log-transformed prior to analysis to homogenize variances, pairwise differences between each replicate population assessed via ANOVA and Dunnett's test with overall significance at α = 0.05, p $\leq$ 0.01; Figure 3.2B).

Because YjeP is predicted to be a mechanosensitive channel [195], we determined how the $yjeP_{I724T}$ mutant responded to pH and osmotic shock, classic stressors for probing mechanosensor function. A *yjeP* null mutant behaved like widetype (WT). Interestingly, while the $yjeP_{I724T}$ mutant was unaffected by changes in osmolarity, it did exhibit 1.1- to 1.4-fold decreases in maximum growth rate in the exponential phase, which was more pronounced with potassium, suggesting that the YjeP may be an ion channel (optical density (OD_{600}) was log-transformed prior to analysis, and the pH effect was assessed with linear regression comparison of the slopes in the exponential phase with significance at α = 0.05; Figure 3.3). To determine whether YjeP is the only MscS mechanosensitive channel protein that can affect T6 resistance, we also tested one of three YjeP homologs, YbdG [195], because a prior study showed a $yjeP_{I724T}$ gain-of-function mutation also confers sensitivity to osmotic shock [199]. Unlike $yjeP_{I724T}$, the $yjeP_{I724T}$ did not confer T6 resistance, nor did a *ybdG* null (Figure 3.3; Figure B.2). Thus, we conclude that $yjeP_{I724T}$ is a gain-of-function, or co-dominat, mutation in an ion channel that confers T6 resistance.

3.4.4 *E. coli yjeP/yjeM* double mutants are much more resistant to novel T6 toxins

The fact that *yejM* and *yjeP* accrued mutations in parallel in two independent populations suggests there may be an epistatic relationship between these two mutations. To test this hypothesis, we introduced both *yejM* mutations into the ancestral *E. coli* without and with the $yjeP_{I724T}$ mutation. While the $yjeP_{I724T}$ mutation confers a modest benefit (4-fold

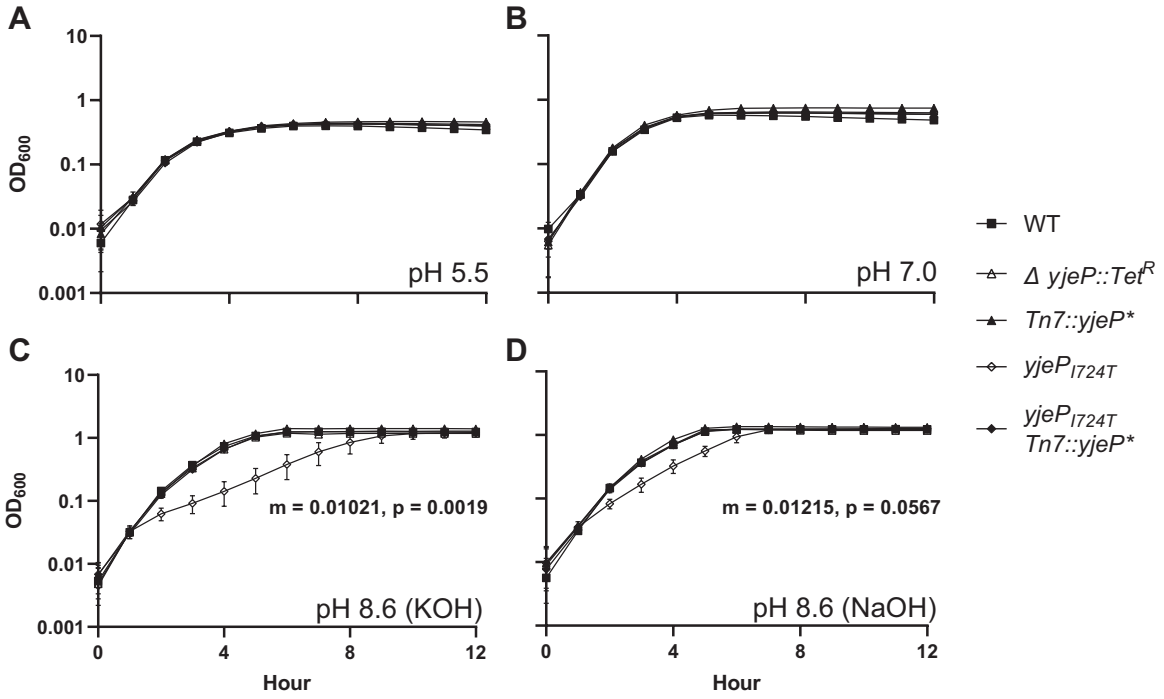

Figure 3.3: *E. coli* $yjeP_{I724T}$ has reduced fitness under basic conditions. (A-B) *E. coli* and its *yjeP* derivatives grow similarly under acidic and neutral pH. (C-D) In basic media, however, the $yjeP_{I724T}$ mutant has a 1.4-fold lower maximum growth rate. Linked markers used to construct the mutants do not affect growth in the tested conditions (Figure B.3). Linear regression comparisons were performed to analyze the statistical differences between slopes. "m" = slope of $yjeP_{I724T}$ mutant in the exponential phase.

increased survival; fold survival was log-transformed prior to analysis to homogenize variances, pairwise differences between each replicate population assessed via ANOVA and Dunnett's test with overall significance at α = 0.05, p $\leq$ 0.01; Figure 3.2B), the presence of either *yejM* mutation by itself has no effect on resistance (Figure 3.2C). However, the $yjeP_{I724T}$ mutation combined with either yejM mutation enables a 40-50-fold increase in survival compared to the ancestor (fold survival was log-transformed prior to analysis to homogenize variances, pairwise differences between each replicate population assessed via ANOVA and Dunnett's multiple comparison with overall significance at α = 0.05, p $\leq$ 0.0001; Figure 3.2C). In other words, mutation in *yejM* increases resistance only in strains that also have the *yjeP* point mutation.

We next examined whether the mutations that arose in our experiment provide general

resistance to T6 attack, or are specific to the toxins employed by the *V. cholerae* C6706 strain, used in this evolution screen, which codes three auxiliary T6 effectors in addition to the large cluster. We therefore competed each mutant *E. coli* strain against an environmental isolate of *V. cholerae* killer, BGT41 (also known as VC22), which encodes a constitutive T6 with effectors predicted to have different enzymatic activities compared to the ones in C6706 and were not encountered by *E. coli* during experimental evolution [51, 59]. This environmental isolate is a superior killer of *E. coli*, relative to C6706 [59], necessitating that we perform our killing assays at a 1:4 killer:target ratio, rather than the 10:1 ratio used with C6706. Evolved strains with $yjeP_{I724T}$ and *yjeP/yejM* double mutations survived 4,000-fold better than the *E. coli* ancestor, but *apaH* did not measurably increase survival (Fold survival was log-transformed prior to analysis to homogenize variances, pairwise differences between each replicate population assessed via ANOVA and Dunnett's multiple comparison with overall significance at α = 0.05, p $\leq$ 0.0001; Figure 3.4). In addition, unlike with C6706 killer (Figure 3.2C), the *yejM* mutations did not further increase the survival of the $yjeP_{I724T}$ mutant (Figure 3.4). This suggests that I724T in *yjeP* may provide broad spectrum resistance to T6 while protection conferred by mutations in the YejM C-terminus and in *apaH* may depend on the specific effector employed.

3.4.5 Experimental evolution reveals trade-offs between T6 resistance and growth rate

So far we have shown that *E. coli* readily evolves resistance to T6 attack, one of the most common mechanisms of antimicrobial warfare. Why, after billions of years of evolution, are bacteria still so poorly defended against T6? Evolutionary theory predicts that trade-offs between antibiotic resistance and other fitness-dependent traits can maintain susceptibility [200]. To test this hypothesis, we examined the effect of each mutation on cellular growth rate by competing them against the ancestral genotype of *E. coli*, under the conditions that mirrored our selection experiment. Mutations in *apaH*, *yejM*, and *yjeP* decreased fitness during growth (Figure 3.5). In fact, there was an overall negative correlation between T6

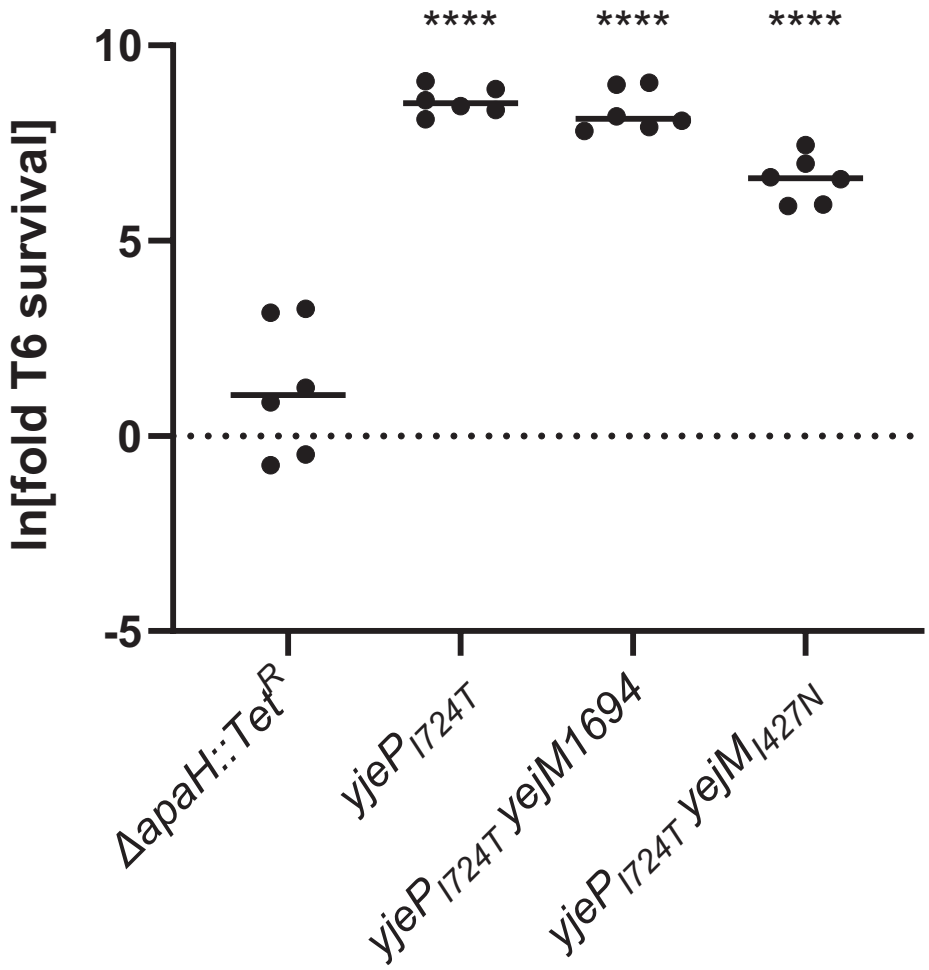

Figure 3.4: The *yjeP* and the *yjeP/yejM* mutants provide general resistance to T6 attack. When competed against *V. cholerae* with a set of toxins not encountered during experimental evolution, *E. coli* mutants with $yjeP_{I724T}$ had an increase of ¿250-fold in T6 resistance whereas deletion of *apaH* did not provide protection against novel T6 effectors. Linked markers used to construct the mutants are not indicated in the figure. **** denotes a difference in survival with $p \leq 0.0001$, determined via ANOVA and Dunnett's Multiple Comparison.

survival and growth rate for the strains generated in this study ($\log_{10}$(survival) = -2.988 $\log_{10}$(growth) - 0.2698, R^2 = 0.65; this regression excludes the *crp* and *rlmE* mutants, which never arose during experimental evolution; Figure 3.5A).

Our evolution experiment consisted of 16 generations of exponential growth in LB media, followed by T6 killing. We thus calculated a fitness isocline across the phase space of this trade-off (dashed line in Figure 3.4A), along which a mutant would have equal fitness to the ancestor across one round of growth and killing, with the equation y = 1/x (in $\log_{10}$ space). For example, along this line, a 100-fold increase in T6 survival is exactly canceled out by a 100-fold decrease in overnight growth. Mutations that lie above this line should be more fit than our ancestral strain, while mutations below the line should be maladaptive. Perhaps unsurprisingly, given the strong selection on both growth and T6 survival, all mutations we identified are adaptive.

We also measured growth and survival rates for two disruptive mutations that did not arise in our experimentally evolved populations - *crp* and *rlmE* ((Figure 3.5A), Figure B.4). We have previously shown that deletion of *crp*, a global transcriptional repressor, results in increased survival to the T6 in *E. coli*, but also greatly reduces growth rate [140, 201, 202]. While this mutation does fall above the fitness isocline, it did not appear in our evolution experiment (Figure 3.5). Because all of our mutations of interest result in decreased growth rate, we also sought to test whether decreased growth rate was sufficient to increase T6 resistance. For example, slower growth could prevent microcolonies of the two strains from physical contact on the plate during the course of the co-culture competition. We constructed an *E. coli* strain with a *rlmE* deletion, which grows 0.14% as much as the ancestor during one round of growth (t-test p = $8.75*10^{-5}$). This strain results in much smaller colonies when growing on plates, but has only a 10-fold increase in survival when challenged with T6 attack (Figure B.4). The *rlmE* mutant is below the fitness isocline in Figure 3.4A, as the modest increase in survival is not commensurate with the huge growth defect of this mutant if slower growth always led to higher T6 resistance. This shows

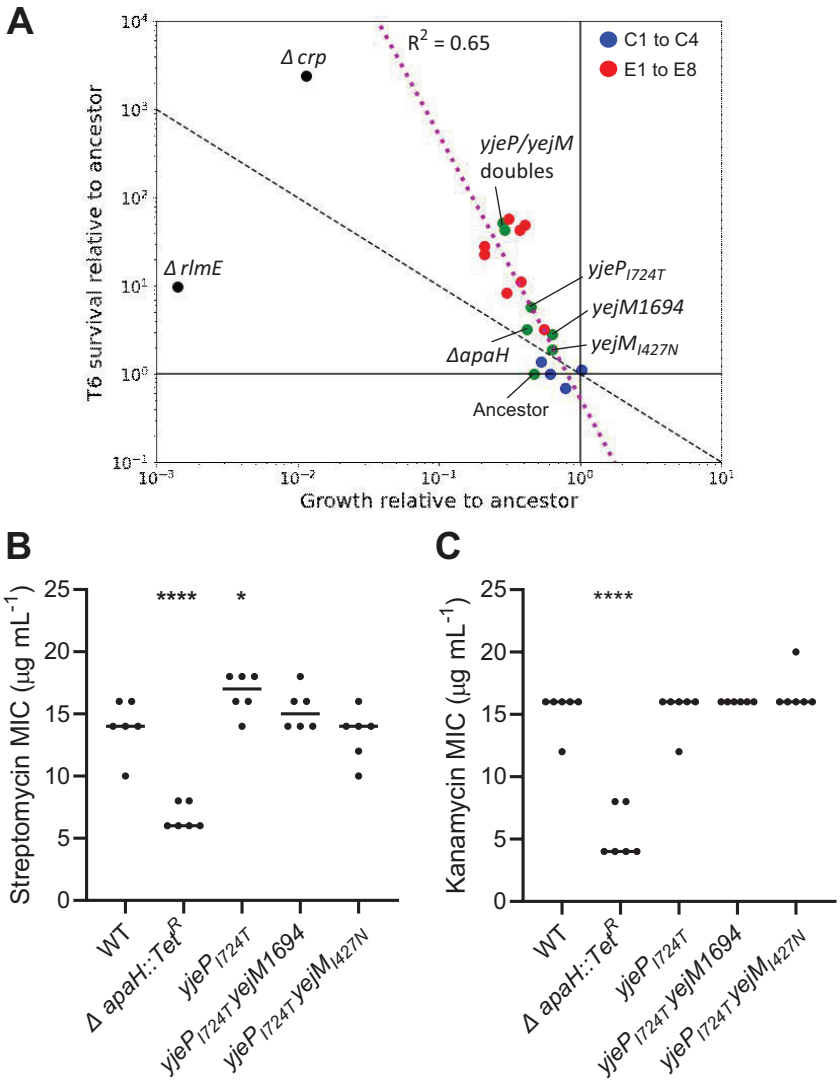

Figure 3.5: Trade-offs between T6 resistance and fitness during growth. (A) Mutations conferring a larger T6 survival advantage also resulted in a greater reduction to reproductive fitness. Plotted are the change in frequency of each mutant across one 16 generation growth assay, and one T6 attack, following the protocols from our evolution experiment. The dashed line represents a fitness isocline, y = 1/x, where fitness across one round of selection is equal to that of the ancestor. In other words, the isocline represents where increased fitness during T6 survival is exactly outweighed by decreased fitness in the growth phase. The pink dashed line represents correlation between survival benefit and growth cost; $\log_{10}$(survival) = -2.988 $\log_{10}$(growth) - 0.2698, R^2=0.65. Green: reconstructed mutations; Red: Evolved isolates; Blue: evolution controls. (B,C) Disruption of *apaH* results in decreased minimum inhibitory concentration (MIC) for streptomycin (B) and kanamycin (C). The point mutation $yjeP_{I724T}$ does not affect susceptibility to these antibiotics. Linked markers used to construct the mutants are not indicated in the figure. **** and * denote differences in survival with $p \leq 0.0001$ and $p \leq 0.05$, determined via ANOVA and Dunnett's Multiple Comparison.

that slower growth is a side-effect of mutations that increase T6 resistance, not a cause of increased resistance.

Another trade-off we tested is susceptibility to aminoglycoside antibiotics. The apaH disruption strain has a significantly lower MIC than the ancestor when grown in streptomycin and kanamycin (pairwise differences between each replicate population assessed via ANOVA and Dunnett's test with overall significance at α = 0.05, p $\leq$ 0.0001 and p $\leq$ 0.05; Figure 3.5B,C), meaning that they are more susceptible to these antibiotics. This is consistent with previous work on apaH [203]. However, strains containing the yjeP point mutation did not show increased susceptibility.

3.5 Discussion

Here we present the use of experimental evolution as an unbiased, forward genetics technique to identify the first *de novo* mutations that promote increased survival to T6 attack. Populations of *E. coli* were subject to alternating selection for rapid growth followed by attack by *V. cholerae*'s T6 (Figure 3.1A). All replicate populations evolving increased T6 resistance (seven of the eight populations) utilized one of two pathways: either a loss-of-function mutation in *apaH*; or a gain-of-function mutation I724T in *yjeP* combined with a partial loss-of-function in *yejM*, with both mutations necessary to provide a large survival advantage (Figure 3.1B-C). For a $yjeP_{I724T}$ mutant, the protection appears to be broad-spectrum, increasing resistance to novel effector proteins by more than 3,000-fold (Figure 3.4). Interestingly, the *yjeP/yejM* double mutants are also comparatively resistant to T6 when competing against *V. cholerae* BGT41 (Figure 3.4), suggesting $yjeP_{I724T}$ provides a broader protection while the additional yejM mutations are specific to C6706 T6 effectors (Figure 3.2C). While the mechanism is beyond the scope of this study, we hypothesize $yejM_{I427N}$ is a less severe mutation and still encodes a partially functional YejM periplasmic domain, whereas an insertion of 8 bp (*yejM1694*) is a frameshift mutation, resulting in a complete disruption of the C-terminus. In contrast, mutations in apaH were specific to

the T6 effectors they were evolved against, showing no efficacy against a different strain of *V. cholerae* with novel T6 effectors (Figure 3.2A, Figure 3.4).

Of the two primary mutational pathways we focused on in this study, it is interesting that the less beneficial path to T6 resistance, loss of function in *apaH*, evolved more times than the far more beneficial combination of $yjeP_{I724T}$ and a partial loss-of-function of *yejM* (Figure 3.4). This is likely because it is easier to gain beneficial mutations in the *apaH* pathway: any loss of function mutation in the gene gives the phenotype [204] whereas the *yejM/yejP* pathway requires not only mutations in two gene targets, but for *yjeP* to be a missense mutation at a particular position. Additionally, given the difference in T6 resistance between evolved isolates with an *apaH* mutation (Figure 3.1B,C) and the constructed apaH mutant (Figure 3.2A), we hypothesize that other mutations acquired by the evolved populations may contribute to T6 survival.

Over 500 generations of experimental evolution in 8 replicate populations, we found just two paths to increased T6 resistance. While prior work has shown that many genes that can affect T6 survival [138, 190, 205–207] implying that adaptation might be idiosyncratic among independent populations, our results suggest that adaptive pathways to T6 resistance are remarkably constrained. One possibility is that our populations are mutationally limited. This is unlikely, as we can expect 9.2 x 10^5 mutations to arise within each growth cycle (based on 1010 cells being produced per cycle, a per base mutation rate of 0.2 x 10^{-10} [208] and a genome size of 4.6 MB), or 2.8 x 10^7 mutations in each population over the course of the experiment. Alternatively, there may be relatively few routes to increased T6 survival in which the benefits of the mutation, integrated across the culture cycle to include pleiotropic costs, are great enough to drive the clonal lineage to high frequency.

The evolution of resistance to diffusible antibiotics has been extensively studied [209]. While the details depend on taxon and environment [210, 211], antibiotic resistance often comes with trade-offs to other fitness components [210–213]. This is especially true for mutations in essential genes that are the target of antibiotics, such as genes encoding

ribosomal proteins [214]. However, compensatory evolution often reduces initially severe costs of resistance, either via the fixation of epistatic mutations elsewhere in the genome, or by replacing initially costly resistance mutations with lower-cost alternatives [214–217]. In contrast to diffusible antibiotics, the eco-evolutionary dynamics of contact-mediated killing remains largely unexplored, and it is unclear if or when similar compensatory adaptation would occur if we continued our experiment.

Trade-offs over antibiotic resistance can maintain the long-term efficacy of these antimicrobial agents, and may play a key role in maintaining diversity within microbial communities [200, 213, 218]. The fitness of bacteria can be thought of as a function of two processes: (1) how much the bacteria die, and (2) how much the bacteria grow and reproduce, otherwise known as "birth-death" processes [219]. The trade-offs we observed in our evolved strains are a direct illustration of the importance of birth-death processes – an increase in fitness through dying less to T6 attack is partially offset by a decrease in fitness through growing less. These trade-offs enable the proliferation and widespread evolutionary success of bacterial weapons like T6, because if defending populations could easily evolve resistance "for free", the weapon would not be effective and would not be maintained in the genome.

In contrast to diffusible antibiotics, the T6 may present a greater challenge for resistance evolution. The T6 typically delivers more than one effector simultaneously, often targeting different components of the intoxicated cell [220]. Multidrug treatment is a widely-used strategy in medicine to slow the rate of resistance evolution [221]. This is because the probability a susceptible cell will simultaneously gain mutations allowing them to survive multiple antibiotics is far lower than the probability of gaining resistance to any single antibiotic. Under such conditions, general mechanisms of antibiotic resistance may be favored. However, general mechanisms of resistance are expected to come with larger fitness costs compared to toxin-specific resistance, because a genetic change that neutralizes multiple different antibiotic targets would likely have off-target regulatory effects. Further, the

genetic loci encoding T6 effectors can act as mobile genetic elements, allowing a lineage to rapidly rotate their T6 arsenal via horizontal gene transfer [114, 122, 185]. Co-evolution between T6 killers and target cells may thus be expected to induce Red Queen dynamics, in which there is selection on both parties for novel effectors and resistance mechanisms. Importantly, under a Red Queen regime [222–224], T6 should retain its overall efficacy as an anti-microbial mechanism, even if their targets are constantly evolving resistance.

It has only recently become apparent how important social interactions are to microbial ecology and evolution [225, 226]. Antagonistic interactions appear to be more common than cooperation or commensalism [9], at least for species that are capable of being cultured. The Type VI secretion system - a ballistic harpoon containing multiple types of toxins capable of quickly killing susceptible cells, represents the cutting-edge of microbial weaponry. In this paper, we show that *E. coli* can indeed evolve substantial genetic resistance to T6 assault, but doing so entails inexorable trade-offs with reproductive fitness. We also found that one convergently evolving solution appeared to provide effector-specific protection, while the other appeared to be more general. So far, relatively little effort has gone into understanding the mechanisms (both genetic and behavioral) through which microbes can evolve to resist dying from T6- a crucial gap in our knowledge that limits our ability to understand the ecology and evolution of this widespread microbial weapon. Further work will be required to determine if trade-offs between T6 survival and reproduction are found in other taxonomic pairs, and whether such trade-offs can be mitigated over longer evolutionary timescales via compensatory mutation.

3.6 Methods and Materials

3.6.1 Bacterial strains and media

Bacterial strains and media Bacterial strains were grown aerobically at 37 °C overnight in LB (1% w/v tryptone (Teknova, CA, USA), 0.5% w/v yeast extract (Hardy Diagnostics, CA, USA), 1% w/v NaCl (VWR Life Sciences, PA, USA) or liquid basal medium

(100 mM Tricine (Thermo Scientific, MA, USA), 10 mM K_2HPO_4 (Fisher Scientific, NH, USA), 0.5% w/v tryptone, 0.25% w/v yeast extract, 0.5% w/v glucose (VWR, PA, USA), and pH 5.5 with HCl (Fisher Scientific, NH, USA) or pH 8.6 with KOH (Fisher Scientific, NH, USA) or NaOH (Fisher Scientific, NH, USA)) with constant shaking or on LB agar (1.5% w/v agar; Genesee Scientific and Hardy Diagnostics, CA, USA). Ampicillin (GoldBio, MO, USA and VWR Life Sciences, PA, USA), spectinomycin (Sigma-Aldrich, MO, USA and Enzo Life Sciences, NY, USA), streptomycin (VWR Life Sciences, PA, USA), kanamycin (GoldBio, MO, USA and VWR Life Sciences, PA, USA), chloramphenicol (Sigma-Aldrich, MO, USA and EMD Millipore, MA, USA), tetracycline (Sigma-Aldrich, MO, USA and Fisher BioReagents, PA, USA), arabinose (GoldBio, MO, USA), NaCl (Thermo Scientific, MA, USA), and KCl (Thermo Scientific, MA, USA) were supplemented where appropriate. Specific concentrations will be described below.

3.6.2 Mutant construction

Mutations were introduced into *E. coli* K-12 strain MG1655 Δ*araBAD::cat* by P1vir transduction [227]. Point mutations in *ybdG*, *yejM*, and *yjeP* were transduced into the recipient strain using the genetically linked markers *purE79::Tn10*, *zei-722::Tn10*, and Δ*yjeJ::ampR*, respectively. Transductants were selected for using 10 μg $mL^{-}1$ tetracycline or 25 μg $mL^{-}1$ ampicillin and screened for the presence of the point mutations by DNA sequencing (Azenta Life Sciences, MA, USA). All null mutations were confirmed by PCR.

yjeJ and *rlmE* were deleted and replaced with the Amp^R or Tet^R cassette, respectively, by λ Red recombination as previously described [228]. To generate Δ*yjeJ::ampR*, the Amp^R cassette from pUC19 was amplified by PCR using the primers KOyjeJBla.Fwd and KOyjeJBla.Rev, which contain homology to the 5' and 3' ends of *yjeJ*, respectively. To generate Δ*rlmE::tetA*, the *tetA* gene and promoter were amplified from Tn10 using the primers rrmJTET.Fwd and rrmJTET.Rev. Δ*yjeJ::ampR* or Δ*rlmE::tetA* DNA were transformed into DY378, a strain of *E. coli* K-12 that expresses the λ Red recombination system

from a temperature sensitive promoter. Prior to transformation, the λ Red system was induced by incubating midlog phase DY378 cells at 42 °C for 15 minutes in a shaking water bath. Recombinants were selected for on LB containing 25 µg mL$^{-}1$ ampicillin (for Δ*yjeJ::ampR*) or 10 µg mL$^{-}1$ tetracycline (for Δ*rlmE::tetA*).

To generate the Δ*apaH::tetA*, Δ*ybdG::tetA*, and Δ*yjeP::tetA* null alleles, Δ*apaH::kanR*, Δ*ybdG::kanR*, and Δ*yjeP::kanR* from the Keio library [229] were moved into DY378 by P1vir transduction [227]. The Kan^{R} cassette in each Keio allele was replaced with *tetA* from Tn10 by λ Red recombination [228]. The *tetA* DNA was amplified by PCR using the primers pKD13TetA.Fwd and pKD13TetA.Rev, which contain homology to the 5' and 3' ends of the Kan^{R} cassette, respectively. Recombinants were selected for on LB containing 10 µg mL$^{-}1$ tetracycline and screened for sensitivity to 25 µg mL$^{-}1$ kanamycin.

ybdG$_{I}167T$ was constructed using CRISPR-Cas9 gene editing as previously described [230]. The *ybdG* guide RNA plasmid pCRISPR-ybdG493 was constructed by ligating ybdG493.CRISPR duplexed DNA (Integrated DNA Technologies, IA, USA) into BsaI-digested pCRISPR. 100 ng of pCRISPR-ybdG493 and 10 µM of the editing oligonucleotide ybdGI167T.MAGE (Integrated DNA Technologies, IA, USA) were transformed into MG3686, a derivative of DY378 that constitutively expresses Cas9 from a plasmid. Transformants were selected for on LB containing 25 µg mL$^{-}1$ chloramphenicol and 50 µg mL$^{-}1$ kanamycin. Recombinants containing the *ybdG*$_{I}167T$ mutation were identified by DNA sequencing (Azenta Life Sciences, MA, USA). Two phosphorothioate bonds were added at the 5' and 3' ends of the ybdGI167T.MAGE oligonucleotide to increase stability.

Genes were inserted at the Tn7 attachment site following a similar protocol described previously [231, 232]. WT *apaH* or *yjeP* expressed from the constitutive promoter J23119 ([http://parts.igem.org/Part:BBa_J23119]) were cloned into XhoI and HindIII (New England Biolabs, MA, USA) digested pZS21, resulting in the plasmids pZS21-apaH and pZS21-yjeP. The J23119 promoter, gene, and rrnB1 terminator from pZS21-apaH or pZS21-yjeP were amplified by PCR using the primers pGRG25GA.Fwd and pGRG25GA.Rev. The

Ω streptomycin/spectinomycin resistance cassette from pHP45Ω was amplified using the primers pGRG25SpcGA.Fwd and pGRG25SpcGA.Rev. *apaH* or *yjeP* DNA along with DNA corresponding to the Ω streptomycin/spectinomycin resistance cassette were inserted into PacI and AvrII digested pGRG25-ModularBamA-Kan by Gibson Assembly (New England Biolabs, MA, USA). The resulting plasmids were transformed into MG1655 and transformants were selected for on LB containing 25 μg $mL^{-}1$ spectinomycin and 0.2% (w/v) arabinose. Transformants were screened for integration of apaH or yjeP and the Ω spectinomycin resistance cassette at the Tn7 site by PCR.

V. cholerae was genetically engineered with established allelic exchange methods using vector pKAS32 [172] to overexpress *qstR* with a Ptac promoter to enable a constitutive T6 activity or introduce a clean deletion of *vasK* to prevent T6 from assembling, as described previously [114]. All Insertions, deletions, and mutations were confirmed by PCR and DNA sequencing (Eton Bioscience Inc, NC, USA).

3.6.3 Experimental evolution

Twelve replicate populations of *E. coli* with chloramphenicol (10 μg $mL^{-}1$) were initiated from an overnight culture of MG1655 with chromosomal Cm^R cassette and a plasmid encoding Kan^R cassette. Each round, cultures were washed twice with LB to remove antibiotics, then mixed with an overnight culture of either *V. cholerae* C6706 *qstR** (for the 8 experimental populations) or C6706 *qstR** Δ*vasK* (for the 4 control populations) in a 10:1 killer to target ratio. 50 μL of each mixture was spotted onto an LB agar plate, dried, and incubated at 37 °C for 3 hours. Competition mixtures were then resuspended in 5 mL of ddH2O containing kanamycin (50 μg $mL^{-}1$) and chloramphenicol (10 μg $mL^{-}1$), and put at 4 °C for 30 minutes, conditions which allow for survival of *E. coli* but not *V. cholerae*. Surviving cells were then diluted 10-fold into LB containing kanamycin (50 μg $mL^{-}1$) and chloramphenicol (10 μg $mL^{-}1$) for overnight growth at 37 °C. This procedure was repeated daily for 30 rounds. A sample of each whole population was frozen at -80 °C

every five rounds. At the end of 30 rounds, a clonal isolate from each population was taken for subsequent phenotypic and genomic testing.

3.6.4 Antibiotic MIC determination

Antibiotics were added to wells of a 96-microtiter plate, starting at 1280 μg $mL^{-}1$ for streptomycin and 640 μg $mL^{-}1$ for kanamycin, and serially diluted 2-fold across the plate. Overnight cultures of bacteria were diluted and added to the wells for a final OD_{600} of 0.001. Once a target range was determined to contain the MIC for each antibiotic, a linear range of antibiotic concentrations were prepared and tested in 96-microtiter plate (4 through 36 μg $mL^{-}1$ for kanamycin and 2 through 18 μg $mL^{-}1$ for streptomycin), and bacteria were added at a an OD_{600} of 0.001. Plates were incubated stationary at 37 °C for 24 hours. A well was determined to have growth if the OD_{600} was above 0.2, as measured by a BioTek Synergy H1 microplate reader (VT, USA), and the MIC was determined to be the lowest concentration at which no growth occurred.

3.6.5 T6-mediated competition assay

The OD_{600} of overnight cultures of *V. cholerae* killer and Cm^{R} *E. coli* target were normalized to 1. Killer and target are then mixed in either 10:1 or 1:4 ratio, inoculated onto a pre-dried LB agar, and allowed to dry. After 3 hours of static incubation at 37 °C, cells were resuspended in 5 ml of LB, following with serial dilutions. Finally, the resuspension was inoculated on a LB agar containing chloramphenicol (10 μg mL^{-1}) to select for the surviving *E. coli*, which was incubated overnight at 37 °C and the *E. coli* colonies were counted. Data is presented as the fold increase of the survival rate for a given genotype as compared to the ancestor (measured in the same experiment), as given by: Fold increase = Survival rate of genotype / Survival rate of ancestor, where the survival rate for each strain is calculated by dividing recovered *E. coli* colonies from competition with the T6+ *V. cholerae* strain by the number of colonies recovered from competition with the T6- strain.

3.6.6 Genomic DNA preparation, whole genome sequencing, and genomic analysis

E. coli genomic DNA from each population was isolated using Promega Wizard Genomic DNA Purification Kit (Madison, WI). The DNA quality was analzyed using gel electrophoresis to confirm no degradation and NanoDrop to confirm the purity of the samples (260/280 = 1.8-2.0). Whole genome sequencing was conducted using Illumina sequencing on a NextSeq 2000 platform at Microbial Genome Sequencing Center (PA, USA). Once we received the DNA sequencing results, quality check, filter, base correction, adapter trimming, and merging were conducted using fastp v0.20.0 [233]. Reads were then mapped and compared to the *E. coli* MG1655 reference genome (accession U00096) from NCBI Genome database using Breseq v0.35.1 with bowtie2-stage2 [177, 234, 235]. Other parameters remain default.

3.6.7 Acknowledgments and funding sources

Figure 1A was made using Biorender.com. K.M. is supported by NIH T32 grant T32GM142616. SLN is supported by NSF grant BMAT 2003721.

CHAPTER 4
CONCLUSIONS AND RECOMMENDATIONS

Bacteria adapt to their surroundings on ecological time scales through sensing and responding to external signals and cues, which triggers a variety of signal transduction cascades [236, 237]. Signal sensing results in changes in gene expression and phenotypic behaviors suited to the environment [236]. Over evolutionary timescales bacteria can acquire mutations that are selected upon in the niches they occupy. In *Vibrio cholerae*, populations responsible for pandemic cholera circulate between human and aquatic environments, while other populations occupy non-human habitats as common members of marine habitats [7, 8, 17–21]. These two populations of *V. cholerae* both carry the type VI secretion system (T6), yet they T6 differ in important ways [59]. Pandemic strains encode a common set of effector proteins tailored to the human host, while environmental strains carry a wider array of T6 toxins [16, 41]. These two populations also differ in the manner of T6 regulation, a focus of my thesis. The majority of strains from human sources tightly regulate the T6 via two main transcription factors (TFs), QstR or TfoY [59, 65, 67]. Most strains from environmental sources express the T6 constitutively [59]. Expanding our understanding of the poorly characterized regulatory mechanisms in both populations of *V. cholerae* strains will help determine how pathogens like *V. cholerae*, that occupy multiple niches, adapt antagonistic strategies over time.

The research presented in this dissertation aimed to define regulatory mechanisms responsible for the differences observed in T6 control of *V. cholerae* killers derived from different sources: humans and the environment. This was followed by an investigation of the evolutionary consequences of T6-mediated competition from the target perspective. First, with T6-mediated competition assay and a green fluorescent protein (*gfp*) transcriptional reporter, I confirmed the T6 in environmental *V. cholerae* is constitutively expressed

even in the absence of the known T6 activators QstR and TfoY [61]. I also identified the first *cis*-regulatory elements (CREs) of the T6 major gene cluster of *V. cholerae*, including the +1 transcriptional start site (TSS) and the -10 and -35 of the promoter [61]. More importantly, I found a guanine (G)-to-thymine (T) single-nucleotide polymorphism (SNP) that can convert T6 activity from QstR-dependent to a Qst-independent and constitutive [61]. Secondly, using genomics approaches, I discovered most human isolates of *V. cholerae* with a QstR-dependent T6 carry a G in the 5' intergenic region (IGR) whereas environmental strains with a constitutive T6 have a T, consistent with my findings and a previously proposed "pathoadaptive" model. In the second half of my thesis, using experimental evolution of *Escherichia coli* over 500 generations, I was able to observe emergence of resistance against T6 attacks by *V. cholerae* in a collaboration with my peer, PhD student Katie McGillivray. Resistance was the result of disruption in *apaH*, a missense mutation in *yjeP*, and C-terminal disruptions in *yejM* that I identified by genome resequencing [234].

4.1 Chapter 2 future directions

4.1.1 Determining the environmental *V. cholerae* T6 expression in natural settings

V. cholerae is not the only opportunistic pathogen that lives inside and outside of a human host. Bacteria like *Pseudomonas aeruginosa* also encode T6s and can be found in both natural and clinical settings [238]. Similar to *V. cholerae*, most *Pseudomonas aeruginosa* studies of the T6 are conducted with human-derived reference strains. For example, the regulation of the three T6s in *P. aeruginosa* is very complex and involves controls at both the level of transcription and translation [42]. Specifically in transcription, the T6s are mainly regulated by quorum sensing (QS) and a hybrid sensor kinase-response regulator protein RetS [42, 57, 239, 240]. Both T6 regulatory mechanisms were identified in the reference strain PAO1, with a deletion of *retS* commonly used to activate T6s and serves as a killer [240]. In addition, the PAO1 T6-2 secretes a copper binding effector to scavenge extracellular copper ions. This system is induced in a copper limited environment and plays a

role in bacterial competition and infection [241]. However, it is possible that *P. aeruginosa* strains solely living in a non-human environment, like *V. cholerae*, have a different regulatory network controlling not only T6 but also other virulence factors. In fact, my work showed a single nucleotide change in a non-coding region is sufficient to rewire the T6 regulation, and the G/T SNP is highly correlated to the T6 activity based on our previous study [59]. All of the inducible, human-derived *V. cholerae* strains carry a G whereas the environmental strains with constitutive T6 harbor a T (Figure 2.4). This suggests that the acquisition by *V. cholerae* of a SNP to control T6 activity is likely a result of adaptive evolution [61], with human-derived strains dampening T6 expression to reduce the chance of triggering immunity response, and instead relying on other mechanisms, such as Cholera toxin (CTX) and biofilm formation, during human infection. However, the environmental strains armed with a constitutive T6 may increase their competitiveness to survive in diverse environments with unpredictable competitors. That being said, the T6 activity in natural environments outside of a host or lab conditions have never been experimentally tested.

V. cholerae has a complex lifestyle, thriving in aquatic environments and animal hosts such as seabirds, fish, crustaceans, mollusca, and humans [20, 22, 242–245]. Besides humans, the ecological role and activity of T6 in other environments are poorly understood, and the constitutive T6 killing observed is often conducted in laboratory settings with rich growth media like lysogeny broth (LB) agar [53, 59–63]. To be truly constitutive by definition, the T6 should be actively transcribed irrespective of growth conditions, like housekeeping genes. In Chapter 2, I showed that the T6 promoter was inactive in *E. coli*, implying the promoter is likely not constitutive and requires *V. cholerae*-specific factor(s) (Figure A.2) [61]. Whether what we observed *in vitro* represents the T6 expression in a non-laboratory setting is unclear. It would be interesting to simulate *V. cholerae*'s natural living conditions to understand the native activity and study the role of T6 in other ecosystems. While this is challenging due to the complex lifestyle, there are a few minimal media

that mimic sea water conditions, such as defined artificial sea water, which can be supplemented with chitin [173]. Culturing *V. cholerae* in artificial sea water at lower temperatures would be a great starting point to determine the T6 activity in a more natural setting [173]. To investigate the T6 inside of hosts, murine models (e.g. mice and rabbits) are commonly used for pathogenesis and immunity studies [246, 247]. However, these studies are typically conducted in infant or germfree animals, which lack the complex gut microbiome that plays a critical role in interacting with non-native bacteria and maintaining a host's health. In addition, murine animals like mice are not a natural non-human host of *V. cholerae* [112, 247–249]. Copepods, however, are a well-established host colonized by *V. cholerae* because of its chitinous exoskeleton [245]. While copepods are not the system for studying pathogenesis, use of this model system could aid in understanding how *V. cholerae* uses its T6 in natural reservoirs [245]. Developing methods and growth media mimicking the natural settings are important steps to acquiring ecologically relevant insights into how bacteria behave. It will be interesting to determine in future studies whether the environmental *V. cholerae* strains have constitutive T6 activity in non-laboratory settings and if we can detect secreted T6 components like hemolysin coregulated protein (Hcp) in other settings such as non-human hosts.

4.1.2 Exploring T6 transcriptional regulation in *V. cholerae*

Bacterial transcription is the first step of gene expression and requires binding of RNA polymerase (RNAP) to promoter DNA to initiate the process of transcribing DNA into RNA. By contrast with housekeeping genes that are constitutively produced (well known examples include *recA*, *16S rRNA*, and *malE*) [250], the levels of transcription of most genes are often fine tuned in response to the environmental changes [251]. One common transcription regulatory mechanism relies on TFs, DNA binding proteins that interact with the IGR upstream of a gene, where CREs, like promoters and TF binding sites, are located [252]. Some TFs serve as activators and promote activation of transcription by recruiting

the RNAP or changing the conformation of the DNA to expose the promoter for RNAP to bind while other TFs repress gene expression by interacting directly with the CREs or looping the DNA to prevent activators and RNAP from binding [252]. Thus, changes in the binding site DNA sequence can affect gene expression, and further have an impact in adaptation and pathogenesis [253]. For example, this was documented in a non-biofilm producing strain of *Salmonella enteritidis*, which is enhanced for biofilm production by acquiring a cytosine (C)-to-T transition mutation in the promoter of the biofilm regulator *csgD* [167]. In addition, *Salmonella typhimurium* is capable of becoming a animal pathogen when horizontally acquiring a CRE, a TF binding site, to activate genes responsible for virulence factors [168]. While SNPs in coding regions (e.g., missense, nonsense, or frameshifts) are important because that potentially alters the protein structure, changes in the non-coding regions do not affect the outcome of the proteins and are often overlooked because it is challenging to determine if the SNPs are functional or silent, especially when the promoter of a gene and the +1 of transcription are unknown. While my work identified a CREs and a regulatory SNP [61] that controls the *V. cholerae* T6 large gene cluster, the mechanism of action is still unclear. For example, there is no evidence of protein binding at the SNP. Because the SNP is only effective when it is a transverion mutation, not a transition mutation (Figure A.5), I hypothesize the SNP results in a structural change of the DNA, which either exposes or occludes a TF binding site, resulting in changes in T6 expression. Future studies could use biotinylated 5' IGR DNA with a G or a T, incubated with cell lysate. TFs that bind form a biotinylated DNA-TF complex, which can be isolated with streptavidin that forms a strong bond with biotin [254]. The isolated complex can then be identified by gel shift assay [254]. If there is DNA-TF interactions, the complex would migrate slower than the free DNA control, and the associated protein can be eluted from the DNA and identified with mass spectrometry [254]. Besides T6, similar adaptive SNPs in non-coding regions likely exist in the promoter regions of other genes either acquired by horizontal gene transfer (HGT) or by spontaneous mutation. With bioinformatics and

genomics analysis, bacterial genome wide association study might be used to identify small genetic variants and the associated traits [171]. Tracing changes in regulatory circuits not only helps us to determine how bacteria control their behaviors but also allows us to acquire a better understanding of how bacteria evolve and adapt in response to environmental changes.

Interplay between multiple transcription activators and repressors is commonly observed. *E. coli* for example has 300 transcription factors [255]. The global regulator CRP control 200 operons directly by binding to the promoters, or indirectly by binding to the promoter of another regulatory gene like *rpoS* [256]. Some of which are also TFs (e.g. TfoX in Figure 1.4 [76]) that further control other genes, forming a complex regulatory network. To bind DNA, CRP interacts with cAMP and forms a CRP-cAMP complex required to recruits RNAP [257]. Another TF CytR, when activated, can also bind to DNA between two CRP-cAMP complexes and prevent RNAP from binding, which in turn represses gene expression [66, 258, 259]. With HGT, bacteria can acquire or lose TFs to rewire regulatory networks, resulting in new phenotypes that may benefit cells in other conditions. For example, *Vibrio fischeri* can colonize two different hosts by acquiring a TF gene encoding the histidine kinase RscS that is essential for establishing a symbioses relationship with squid hosts or losing the *rcsS* gene and becoming a fish symbiont [146]. Similarly, it is possible that human-derived *V. cholerae* alters their regulatory circuitry to be more adaptive in the human hosts. It would be interesting to conduct a pan-genome analysis to compare differences in accessory genes present in the human-derived strains but absent in the environmental strains, or vice versa. Several *V. cholerae* pan-genome analyses were conducted, but the focus was strains isolated from animal hosts, including humans [260–262]. Environmental strains in our lab were collected from diverse environments, ranging from animal hosts like oyster and crab to aquatic environments like sea water and storm drains [59]. Our diverse human- and non-human-derived isolate collections could provide a bigger picture and a set of genes that are essential 1) in all conditions, 2) in non-human

hosts, 3) in human host, and 4) outside of the host. The genes of interest could be further analysed with bioinformatic tools and experiments. This has direct implications for understanding the evolution of pathogenic *V. cholerae* and further strengthens the pathoadaptive model.

To add another layer of complexity in transcription regulation, some genes have more than one promoter to initiate transcription, and the promoters can be regulated together or independently. One example is *tfoY* with four promoters (see 4.1.3 Investigating TfoY and QstR regulatory mechanism) [94]. While another research group and I recently identified the identical T6 promoter [61, 62], our prior study used a luciferase reporter fused with a truncated IGR upstream of T6 major cluster, which excludes the promoter I identified, to measure the T6 expression level [66]. Interestingly, reporter expression was still altered in response to the presence or absence of QstR [66]. This truncated IGR may contain an additional promoter to initiate the transcription, or a component that works in conjunction with the CRE I identified. In addition, I observed two products when using 5' rapid amplification of cDNA ends (5' RACE) to identify the +1 of transcription: one dominant bright band but also a faint band, suggesting there may be an alternative +1 (data not shown). Based on these results, I hypothesize a second promoter may exist in the 5' IGR of T6 major cluster. Additional 5' RACE and extracting the shorter product for sequencing could help determine whether there is another T6 promoter, which has never been described in T6. A future study in this regard could provide new insights into how *V. cholerae* fine tunes the T6 expression.

4.1.3 Investigating TfoY and QstR regulatory mechanisms

TfoY was first identified as a TfoX homolog in a comparative genomics study in 2007 [263] and later found to control natural transformation in *V. fischeri* and T6 and motility in *V. cholerae* [67, 93]. Over a decade since the discovery, although regulation of *tfoY* was investigated and it is described as a regulator [67, 94], it is still unclear how TfoY

regulates motility and T6, as it lacks a DNA binding domain and has not been shown to interact with DNA. In chapter 2, I observed small differences in *E. coli* survival but not T6 expression when *tfoY* is deleted from C6706, when the T6 is driven by the promoter from the V52 (Figure 2.3B-C). I hypothesize this may result from indirect effects of TfoY, a regulatory factor specific to V52 and absent in C6706, or post-transcriptional regulation by TfoY like a RNA binding protein. Using transposon mutagenesis in a *tfoY* constitutive background, one could screen for motility mutants to determine if there is a co-factor or downstream regulator needed. Investigating post-transcription regulation without knowing the target mRNA is challenging, especially since TfoY does not have predicted domains or motifs. It may be more practical to first determine the structure of TfoY with bioinformatic tools, such as AlphaFold [264], for protein structure prediction, which could provide new insights to biological functions, such as grooves and pockets that serve as the active sites [265]. Uncovering the downstream regulatory mechanisms of TfoY does not only help to complete the regulatory network in *V. cholerae* but also in other *Vibrios* as TfoY is conserved among the species and also regulates behaviors that are ecologically important [266].

In chapter 2, we observed variable T6 activity when *tfoY* is deleted in different environmental *V. cholerae* (Figure 2.4). I hypothesize this could be due to the differences in levels of TfoY inside the cells. Transcription of *tfoY* is very complex and controlled by four promoters [94]. The first two promoters transcribe an mRNA encoding a riboswitch that represses *tfoY* transcription while the last two promoters require co-factors to induce the transcription [94, 267]. Similar to T6, it is not surprising that there could be strain variation in regulating TfoY expression, resulting in different intracellular levels of TfoY among the environmental strains. Furthermore, TfoY also regulates motility that is important for pathogenesis as well as the transition between natural reservoirs and hosts [67, 266, 268, 269]. Loss of motility in *V. cholerae* in fact reduces virulence and surface attachment [269, 270]. On the other hand, although QstR affects T6 expression when the

environmental strains acquired a G at the 5' IGR of T6 major cluster, deletion of *qstR* does not completely eliminate killing (Figure 2.3D, compare Δ*vasK* to Δ*qstR*) [61]. While this suggests the T-to-G SNP is crucial for QstR direct/indirect activation, this leads to questions of 1) whether there are other TFs that promote the T6 expression in the absence of QstR, and 2) what genes QstR regulates other than the genes associated with natural transformation (Figure 2.2B). Future research of QstR and TfoY is critical to understand the ecological and pathogenic roles of these gene regulators in *V. cholerae* strains. The work I presented also serves as an important reminder that while studying human-derived strains is crucial for understanding the pathogenesis, the observations may not reflect the diversity of strains isolated from other sources.

4.1.4 Exploring potential post-transcriptional regulation of T6 in *V. cholerae*

Gene regulation does not only occur at the initiation of transcription but also post-transcriptionally at the mRNA level. Most bacterial mRNAs include a 5' untranslated region (5' UTR), coding sequence, and 3' UTR. Translation initiates with ribosomes recognizing the ribosome binding site (RBS) sequence in the 5' UTR. This process can be interfered with by RNA binding proteins or regulatory small RNAs, which have diverse mechanisms to inhibit or enhance translation [271, 272]. Indeed the T6 of *P. aeruginosa* is negatively regulated at the post-transcriptional level by RNA binding protein RsmA [42]. This is also observed in *V. cholerae*. *V. cholerae* encodes four well-studied quorum regulatory small RNAs (Qrr4), which repress the translation of HapR (Figure 1.4) [273] as well as the T6 major locus [163]. However, this T6 study was published before QstR was identified as the major regulator of T6 in *V. cholerae* C6706. While the authors observed a complementary sequence in the 5' UTR where the Qrr4 may bind, the fact that they did not report a direct RNA-RNA interaction could suggest the Qrr4 may simply regulate T6 through the HapR/QstR pathway as shown in Figure 1.4.

Translation is also controlled by the sequence of the 5' UTR of an mRNA, which can

form secondary structures that expose or cover the RBS and facilitate or prevent ribosome binding [274]. This mechanism has never been described in controlling T6 expression. With the new results I collected from 5' RACE, I experimentally confirmed the 5' UTR of the T6 major cluster in *V. cholerae*, which is surprisingly long (318 bp) (Figure 2.3). As a comparison, the most abundant length of the 5' UTR found in *E. coli* and *Klebsiella pneumoniae* is 25-35 bp [275]. Since most of the SNPs in the IGR upstream of T6 are located after the TSS (Figure 2.3), it is possible that these interstrain genetic variants play a role in altering the secondary structures, and thus affect the post-transcriptional regulation of T6. To test this hypothesis, it is possible to predict the secondary structure of the 5' UTR with bioinformatics tools, such as UNAFold [276], to identify whether a SNPs potentially alters RNA structure in silico, and then mutate the specific nucleotide to determine if the mutation in turn affects T6 translation and killing. Translation activity can be measured with translational reporters, such as a *gfp* fusion to the T6 structural proteins encoded in the major cluster like *vipA* and *clpV* (Figure 1.3). Similar fusions were documented in studies conducted by other labs [34, 277].

4.2 Chapter 3 future directions

4.2.1 Experimental evolution with T6 killing

T6-mediated killing, like antibiotics, provides a strong selection on competitors in mixed communities, and we hypothesized that target cells can become T6 resistant, similar to resistance observed to traditional diffusible antibiotics. The first T6 resistant bacterium was documented by Basler et al., who observed that *Acinetobacter baylyi* and *V. cholerae* with active T6s cannot kill *P. aeruginosa* [34]. However, *P. aeruginosa* can counterattack with its own T6 [34]. This phenomenon is also known as "Tit-for-Tat" [34]. It is still unclear how *P. aeruginosa* is unaffected by *V. cholerae* T6 toxins. We also observed that *Enterobacter sp.* (ZOR0014) is not susceptible to the *V. cholerae* T6 (data not shown). Subsequent research has uncovered that T6 effectors cause an increase in reactive oxygen

species (ROS) [278], which triggers different stress responses, such as the Rcs and Bae systems, in bacteria, reducing the amount of ROS and indirectly minimizing the damage caused by T6 [137, 138]. These studies raise questions regarding how target cells respond and evolve to become resistant to T6 killing. Our results from the experimental evolution suggest *E. coli* can reduce the T6 susceptibility by acquiring de novo mutations, but that evolutionary trade-off and epistasis likely prevent *E. coli* populations from becoming fully resistance. These trade-offs thus maintain the genetic diversity of a population and prevent dominance of a single strain [200, 218].

Experimental evolution serves as a useful tool to explore evolutionary theories and examine the adaptive processes of bacteria [191]. Similar techniques have been used with other fast-growing organisms including viruses, *Caenorhabditis elegans*, and fruit flies [191]. In experimental evolution, a specific environment is provided to examine how populations adapt and survive over generations. Mutations that emerge over time can then be identified by whole-genome sequencing and comparative genomic analysis. As described in chapter 3, we experimentally evolved *E. coli* to become resistant against *V. cholerae*'s T6. While the evolved *E. coli* gained 27-fold T6 resistance (Figure 3.1B), the associated mutations came with growth trade-offs. Similar phenomenon has been observed in antibiotic resistance studies, where the bacteria often acquire subsequent mutations to compensate for the fitness costs [214]. For example, a prior study showed antibiotic resistant *E. coli* rewire its metabolic networks to circumvent metabolic costs [279]. This implies it is possible that second site mutations may arise in our evolved *E. coli* to circumvent the fitness disadvantage. Future studies extending our experimental evolution may identify such mutations that maintain the T6 resistance while improving growth. However, I predict the evolved *E. coli* may also slowly increase their T6 resistance, which in turn reduces the selection force by T6 attack. It will be important to monitor changes in *E. coli* survival as well as their growth and perhaps adjust the killer-to-target ratio to ensure the selective force is maintained. Furthermore, we can also experimentally evolve the T6 resistant *E. coli* in

the absence of a T6 competitor to determine if the previously evolved mutations are stable; observing whether the T6 resistance mutations are maintained over generations or if the *E. coli* can acquire new mutations to improve growth in order to compensate the decrease in fitness. These proposed experiments allow us to further understand the killer-target dynamic in a contact-dependent manner, which has never been described. Continuing our experimental evolution while maintaining a strong selection with T6 killing will provide insights into the long-term fate of the mutations we identified and the dynamic interactions between subsequent mutations, similar to what we observed with *yjeP* and *yejM*.

The outcome of experimental evolution are sensitive to the experimental conditions, such as the growth media, incubation time, and in this experiment, class of T6 effectors [191]. In chapter 3, we hypothesized becoming fully resistant to T6 is challenging, and one of the reasons is the T6 apparatus is loaded with a cocktail of four toxins targeting different parts of the cell. This is consistent with studies that multi-drug antibiotic treatment can slow down the emergence of drug-resistant *Mycobacterium tuberculosis* during human infection [280]. To investigate if *E. coli* can be fully protected from T6 attack, it will be interesting to conduct a similar experimental evolution with *V. cholerae* killer harboring only one functional T6 effector to minimize the confounding variables from the other effectors. A second and third effector can be added once *E. coli* is no longer susceptible to the first toxin. To determine whether the only routes for resistance to all three T6 toxins are the ones we identified: namely *apaH* or *yejM/yjeP*.

The genes, *apaH*, *yjeP*, and *yejM*, identified in chapter 3 confer T6 in *E. coli*. Each of these genes encoded proteins that serve important cellular functions. ApaH is a decapping enzyme that promotes degradation of RNAs by removing the nucleoside tetraphosphate RNA caps at the 5' end [281]. YjeP is one of the mechanosensitive channels to protect the cells from sudden change in ion concentration [195]. Lastly, YejM regulates biosynthesis of LPS, which is a major component of the outer membrane [196, 198]. It is not surprising that bacteria other than *E. coli* also encode proteins with similar functions. With genomic

analysis, we can determine how conserved these three genes are in the bacterial domain. Similar mutations can be introduced to determine the T6 susceptibility in different bacteria. On the other hand, we can conduct a similar experimental evolution with other target bacteria, such as *Aeromonas veronii* that is susceptible to T6 killing from *V. cholerae* [112], to determine if similar mutations will arise in other bacteria under T6 selection.

4.2.2 Investigating the YjeP membrane channel

Mechanosensitive channels serve as gatekeepers regulating the potential of the cell by sensing the lateral tension in the cytoplasmic membrane, and the tension changes in an osmolarity-dependent manner [282]. This mechanism does not only allow cells to survive through osmotic shocks, but also allow cells to control the amount of cytoplasmic water to maintain the rigidity of cells [282]. YjeP is one of the mechanosensitive ion channels responsible for MscS activity, which stands for "Small Conductance Mechanosensitive Channel" [195]. However, little research has been conducted on YjeP. It is still unclear which ions it is permeable to and its mechanism of action. To understand how the I724T mutation we identified in YjeP improves protection against T6 attack in *E. coli*, understanding the function of this protein is crucial. Transmembrane protein prediction tools [283] comparing widetype (WT) and mutated YjeP can serve as a starting point to determine if the I724T mutation affects the protein structure. High-throughput channel activity assays can be performed in microtiter format to examine an array of growth conditions with common ions, such as hydrogen (pH), potassium, and sodium ions. Before making a connection of I724T mutation and T6 resistance, understanding the mechanism of the natural function of YjeP in *E. coli* is essential. In addition, our previous research identified a new T6 effector (TpeV) that permeabilizes the target cell membranes and disrupts the membrane potential, which was measured using a membrane potential-sensitive dye $DiBAC_4(3)$ [113]. It is possible that we could use $DiBAC_4(3)$ to determine whether the I724T mutation in *yjeP* has any impact on the membrane potential relative to the WT, *yjeP* null, and constitutive *yjeP*. In

chapter 3, we found *E. coli* with $yjeP_{I724T}$ is also more susceptible in a high pH condition (Figure 3.3). One hypothesis is the $yjeP_{I724T}$ mutant no longer maintains the membrane potential in high pH. Additionally, we do not know whether the pH effect is specific to the growth medium. Future experiments using $DiBAC_4(3)$ to survey the membrane potential of the $yjeP_{I724T}$ mutant in various growth media with a range of pH will provide more details into how this mutation affects YjeP channel and which ions YjeP regulates. These results may relate to the T6 resistant mechanism because many T6 effectors target the cell membranes.

4.2.3 Investigating the trade-offs of YejM C-terminus disruption

YejM is an essential protein that plays an important role in outer membrane synthesis [197]. Previous studies showed deletion of *yejM* is lethal [284]. While *E. coli* survives with a YejM C-terminus deletion, cells are more sensitive to high temperature and have a lowered LPS level [198]. In our evolved *E. coli* with *yejM*/*yjeP* double mutations, we observed an increase in sensitivity to vancomycin (data not shown) but not aminoglycoside antibiotics (Figure 3.5B-C). Because vancomycin targets cell wall synthesis [285], this result implies there may be a defect in the outer membrane. Yet, preliminary evidence reports no change in LPS level in the *yejM*/*yjeP* double mutants (data not shown). While these preliminary results need repeating, we hypothesized $yjeP_{I724T}$ mutation rescues *E. coli* from the damaged caused by the YejM C-terminus disruption. Measuring the antibiotic sensitivity and LPS levels in *E. coli* with *yejM* mutation alone will be able to determine if $yjeP_{I724T}$ is a compensation mutation. In addition, it will be interesting to disrupt genes that are related to LPS synthesis in $yjeP_{I724T}$ *E. coli* to determine if the *yjeP* mutation is specific to the YejM C-terminus disruption.

4.2.4 Determining the order of epistatic mutations

Epistasis describes interactions between at least two mutated gene, resulting in phenotypic changes [286]. This phenomenon is well-studied in the evolution of antibiotic resistance because resistant mutations often comes with fitness costs, which are often compensated by secondary mutations [287]. In our experimental evolution, it was surprising to identify two identical *yjeP* mutations and C-terminus disruptions of YejM in two independent evolved population, with enhanced T6 resistance relative to the *apaH* null mutation. We believe this is an example of epistasis. However, we do not know which mutation first arose during the experimental evolution and if the order of mutation acquired matters. Since we have the fossil records of the evolved *E. coli*, it is possible to trace back and sequence the *yejM* and *yjeP* genes to determine how they were acquired, which allows us to investigate the process of epistatsis.

4.3 Other future directions

4.3.1 Additional rolls for T6 in *V. cholerae* other than killing

In other bacterial species, T6 has been shown to play a diverse role other than killing. For example, *Burkholderia pseudomallei* has four T6s [288]. Interestingly, instead of toxic effectors, the T6-2 encodes and delivers a zincophore and a manganeseophore to neighboring cells and provide protections against oxidative stresses, such as ROS [38, 288]. Similar observations documented in *P. aeruginosa* PAO1 as mentioned prior that the T6-2 releases a copper binding effector azurin in copper limited conditions [241]. This effector couples with a copper ion specific transporter at the outer membrane to maintain the intracellular copper ion level, and deletion of the azurin effector reduces the fitness and virulence [241]. *Proteus mirabilis* recognizes and communicates with the neighboring cells by delivering ”self-identity protein” via T6 [40]. With sister cells, swarming motility is upregulated [40]. When encountering non-sister cells, a visible boundary is formed to prevent merging two

populations of cells [40]. Besides T6, one of the type V secretion systems, the contact-dependent growth inhibition (CDI) system, in *Burkholderia thailandensis* was also shown to deliver the CDI to immune sister cells, resulting in gene expression and phenotypic changes like biofilm formation [289]. While *V. cholerae* appears to use T6 only for eliminating non-kin cells and for pathogenesis in the conditions tested to date, the ecological role in outside of human hosts has never been described. For example, environmental *V. cholerae* always expresses their T6 even though they are surrounded with clones [59]. It is possible that they may also inject effectors or other T6 proteins into the sibling cells for purposes other than killing. To test this hypothesis, future studies using RNA-seq might be used to compare gene expression profiles of *V. cholerae* isolated from a clonal population in the presence or absence of T6 activity. That will provide valuable insights on how sibling cells response to self-T6 attacks.

4.4 Conclusions

The T6 serves many important ecological roles in the bacterial community with contribution to antimicrobial competition, kin discrimination, spacial organization, and pathogenesis [16, 27, 32, 34, 38–40, 60, 111, 112, 131, 290]. With 25% of Gram-negative bacteria encoding T6 genes, the wide distribution of T6 implies the significant of this machinery in bacterial adaptation and interactions with other organisms [36, 37]. Research of the T6 as well as other protein secretion systems is essential to understand the general principles how bacteria interact and respond to the surrounding environment.

The findings discussed in this dissertation have advanced the scientific understanding of processes contributing to bacterial interactions, evolution of T6 regulation in *V. cholerae*, and T6 defense strategies in *E. coli*. In addition, this dissertation serves as a important reminder that reference strains cannot always represent the species. Interstrain variation is common, and the phenotypic differences could be a result of single nucleotide mutations, which could occur in not only coding but also non-coding regions, which are often over-

looked. Because the T6 plays a major role in shaping bacterial community composition, these findings lay a foundation for future studies that will lead to a better understanding of the fundamental question - how bacteria adapt to compete and survive in their natural environments.

Appendices

APPENDIX A

SUPPLEMENTARY INFORMATION FOR CHAPTER 2

Table A.1: **List of strains used in Chapter 2**

Bacterial strain	Genotype and description	Carrying plasmid	Strain Source
BGT41	V. cholerae VC22 O1		"Bernardy et al., 2016"
BGT62	V. cholerae 2512-86 O1		"Bernardy et al., 2016"
BGT65	V. cholerae 2479-86 O1		"Bernardy et al., 2016"
BGT69	V. cholerae 3223-74 O1		"Bernardy et al., 2016"
BH1512	V. cholerae C6706 O1 El Tor	pBB1	This study
BH1514	V. cholerae C6706 O1 El Tor		"Thelin and Taylor, 1996"
BH1546	V. cholerae C6706 ΔhapR	pBB1	This study
BH1659	V. cholerae C6706 ΔluxO	pBB1	This study
CC116	E. coli NRD204 MG1655 ΔaraBAD::cat ΔlacZ::pKAS-sfGFP		"Crisan et al., 2021"
EB282	V. cholerae 2011EL-1141 O1		"Bernardy et al., 2016"
EB286	V. cholerae 2011EL-1938 O1		"Bernardy et al., 2016"
EB290	V. cholerae 2012V-1001 O1		"Bernardy et al., 2016"
JT101	V. cholerae C6706 Ptac-qstR		"Thomas et al., 2017"
JT932	V. cholerae C6706 Ptac-qstR ΔvasK		"Thomas et al., 2017"
PB501	E. coli NRD204 MG1655 ΔaraBAD::cat		"De Lay and Cronan, 2007"
SK10	V. cholerae 2512-86 ΔvasK		This study
SK11	V. cholerae 2479-86 ΔvasK		This study
SK12	V. cholerae VC22 ΔvasK		This study
SK19	V. cholerae V52 O37	pBB1	This study
SK30	V. cholerae 3223-74 ΔlacZ::IGR3223-74vipA-T7RBS-sfGFP		This study
SK31	V. cholerae 3223-74 ΔtfoY ΔlacZ::IGR3223-74vipA-T7RBS-sfGFP		This study
SK32	V. cholerae 3223-74 ΔqstR ΔlacZ::IGR3223-74vipA-T7RBS-sfGFP		This study
SK34	V. cholerae 3223-74 ΔqstR ΔtfoY ΔlacZ::IGR3223-74vipA-T7RBS-sfGFP		This study
SK36	V. cholerae V52 ΔqstR ΔlacZ::IGRV52vipA-T7RBS-sfGFP		This study
SK37	V. cholerae C6706 5'IGR of T6SS large cluster is replaced with the 5'IGR from V52 ΔlacZ::5'IGRV52vipA-T7RBS-sfGFP		This study
SK38	V. cholerae C6706 Ptac-qstR Δtfoy ΔlacZ::IGRC6706vipA-T7RBS-sfGFP		This study
SK39	V. cholerae C6706 5'IGR of T6SS large cluster is replaced with the 5'IGR from 3223-74 ΔlacZ::5'IGR3223-74vipA-T7RBS-sfGFP		This study
SN433	V. cholerae C6706 Ptac-qstR	pKE2	This study
SN436	V. cholerae C6706 ΔqstR	pKE2	This study
SN467	E. coli NRD204 MG1655	pKE2	This study
SN498	V. cholerae 3223-74 ΔtfoY	pSN27	This study
SN511	E. coli NRD204 MG1655	pSN27	This study
SN513	V. cholerae C6706 Ptac-qstR ΔtfoY		This study
SN522	V. cholerae 3223-74 O1	pSN27	This study
SN598	V. cholerae C6706 Ptac-qstR 5'IGR-T7terminator-vipA		This study
SN632	V. cholerae 3223-74 ΔqstR ΔtfoY		This study
SN682	V. cholerae C6706 5'IGR of T6SS large cluster is replaced with the 5'IGR from 3223-74		This study
SN701	V. cholerae 3223-74 O1	pBB1	This study
SN740	V. cholerae 3223-74 ΔhapR	pBB1	This study
SN741	V. cholerae 3223-74 ΔluxO	pBB1	This study
SN796	V. cholerae 3223-74 O1	pSLS3	This study
SN797	V. cholerae C6706 O1 El Tor	pSLS3	This study
SN798	E. coli NRD204 MG1655	pSLS3	This study
SN830	V. cholerae C6706 5'IGR of T6SS large cluster is replaced with the 5'IGR from 3223-74 ΔtfoY		This study
SN842	V. cholerae C6706 5'IGR of T6SS large cluster is replaced with the 5'IGR from V52		This study
SN846	V. cholerae C6706 5'IGR of T6SS large cluster is replaced with the 5'IGR from V52 ΔtfoY		This study
SN849	V. cholerae C6706 5'IGR of T6SS large cluster is replaced with the 5'IGR from V52 ΔqstR		This study
SN869	V. cholerae 3223-74 Δ5'IGRvipA::T-68G		This study
SN870	V. cholerae C6706 ΔtfoY		This study
SN876	V. cholerae V52 ΔqstR		This study
SN877	V. cholerae 3223-74 Δ5'IGRvipA::T-68G Ptac-qstR		This study
SN890	V. cholerae V52 ΔlacZ::IGRV52vipA-T7RBS-sfGFP		This study
SN891	V. cholerae C6706 Ptac-qstR ΔlacZ::IGRC6706vipA-T7RBS-sfGFP		This study
SN892	V. cholerae C6706 ΔlacZ::IGRC6706vipA-T7RBS-sfGFP		This study
SN893	V. cholerae C6706 ΔqstR ΔlacZ::IGRC6706vipA-T7RBS-sfGFP		This study
SN894	V. cholerae V52 ΔtfoY ΔlacZ::IGRV52vipA-T7RBS-sfGFP		This study
SN895	V. cholerae 3223-74 Δ5'IGRvipA::T-68C		This study
SN896	V. cholerae 3223-74 Δ5'IGRvipA::T-68A		This study
SN897	V. cholerae 3223-74 Δ5'IGRvipA::T-68G ΔqstR		This study
SN903	V. cholerae C6706 5'IGR of T6SS large cluster is replaced with the 5'IGR from V52 ΔtfoY ΔlacZ::5'IGRV52vipA-T7RBS-sfGFP		This study
SN904	V. cholerae C6706 5'IGR of T6SS large cluster is replaced with the 5'IGR from 3223-74 ΔtfoY ΔlacZ::5'IGR3223-74vipA-T7RBS-sfGFP		This study
SN905	V. cholerae 3223-74 Δ5'IGRvipA::T-68G ΔlacZ::Δ5'IGRvipA::T-68G-T7RBS-sfGFP		This study
SN906	V. cholerae 3223-74 Δ5'IGRvipA::T-68G ΔlacZ::Δ5'IGRvipA::T-68G-T7RBS-sfGFP Ptac-qstR		This study
SN907	V. cholerae 3223-74 Δ5'IGRvipA::T-68G ΔlacZ::Δ5'IGRvipA::T-68G-T7RBS-sfGFP ΔqstR		This study
SN927	V. cholerae C6706 5'IGR of T6SS large cluster is replaced with the 5'IGR from V52 ΔqstR ΔlacZ::5'IGRV52vipA-T7RBS-sfGFP		This study
SN930	V. cholerae 3223-74 T7terminator-5'IGR-vipA		This study
SN931	V. cholerae C6706 T7terminator-5'IGR-vipA		This study
SW38	V. cholerae 2011EL-1939 O1		"Bernardy et al., 2016"
SW491	V. cholerae V52 O37		"Zinnaka and Carpenter, 1972"
SW75	V. cholerae C6706 ΔqstR		This study
TH51	V. cholerae V52 ΔtfoY		This study
TH59	V. cholerae V52 ΔvasK		This study
TH63	V. cholerae 3223-74 ΔvasK		This study
TH66	V. cholerae 3223-74 ΔtfoY		This study
TH69	V. cholerae VC22 ΔtfoY		This study
TH70	V. cholerae 2512-86 ΔtfoY		This study
TH71	V. cholerae 2479-86 ΔtfoY		This study
TH74	V. cholerae VC22 ΔqstR		This study
TH75	V. cholerae 2512-86 ΔqstR		This study
TH77	V. cholerae 2479-86 ΔqstR		This study
TH79	V. cholerae 3223-74 ΔqstR		This study

Table A.2: **List of plasmids used in Chapter 2**

Plasmid	Description	Cloning Vector	Antibiotic Resistance	Counter selectable marker	Source
pBB1	luxCDABE of V. harveyi on a cosmid	-	Tetracycline	-	"Miller et al., 2002"
pKE2	pSLS3-T6IGRC6706-sfGFP	pSLS3	Chloramphenicol	-	This study
pSLS3	Cloning vector	-	Chloramphenicol	-	"Tu and Bassler, 2007"
pSN27	pSLS3-T6IGR3223-74-sfGFP	pSLS3	Chloramphenicol	-	This study
pRE118	Cloning vector	-	Kanamycin	Sucrose	https://www.addgene.org/43830/
pKAS32-Amp	Cloning vector	-	Ampicillin	Streptomycin	"Skorupski and Taylor, 1996"
pKAS32-Kan	Cloning vector	-	Kanamycin	Streptomycin	"Skorupski and Taylor, 1996"
pJT88	adding Ptac promoter upstream of qstR in C6706	pKAS32-Amp	Ampicillin	Streptomycin	"Thomas et al., 2017"
pJT634	vasK clean deletion in C6706	pKAS32-Amp	Ampicillin	Streptomycin	"Thomas et al., 2017"
pSW55	qstR clean deletion in C6706	pKAS32-Amp	Ampicillin	Streptomycin	"Thomas et al., 2017"
pSN58	hapR clean deletion in 3223-74	pRE118	Kanamycin	Sucrose	This study
pSN40	luxO in-frame deletion in 3223-74	pRE118	Kanamycin	Sucrose	This study
pCC115	Insert pKAS-Kan-Ptac-T7RBS-sfGFP in E. coli MG1655 lacZ	pKAS32-Kan	Kanamycin	N/A - Only used for intergration	"Crisan et al., 2021"
pJT981	vasK clean deletion in environmental isolates and V52	pRE118	Kanamycin	Sucrose	This study
pSN67-C6706	Insert IGRC6706vipA-T7RBS-sfGFP in V. cholerae lacZ	pRE118	Kanamycin	Sucrose	This study
pSN67-V52	Insert IGRV52vipA-T7RBS-sfGFP in V. cholerae lacZ	pRE118	Kanamycin	Sucrose	This study
pSN67-3223-74	Insert IGR3223-74vipA-T7RBS-sfGFP in V. cholerae lacZ	pRE118	Kanamycin	Sucrose	This study
pSK3	Insert IGR3223-74vipA::T-68G-T7RBS-sfGFP in 3223-74 lacZ	pRE118	Kanamycin	Sucrose	This study
pTH25	tfoY deletion in environmental isolates and V52	pRE118	Kanamycin	Sucrose	This study
pTH30	qstR deletion in environmental isolates and V52	pRE118	Kanamycin	Sucrose	This study
pJT85	tfoY clean deletion in C6706	pKAS32-Amp	Ampicillin	Streptomycin	This study
pSN78	V. cholerae C6706 5'IGR of T6SS large cluster is replaced with the 5'IGR from V52	pKAS32-Kan	Kanamycin	Streptomycin	This study
pSN20	V. cholerae C6706 5'IGR of T6SS large cluster is replaced with the 5'IGR from 3223-74	pKAS32-Kan	Kanamycin	Streptomycin	This study
pHN1	Insert T7 terminator before the start codon of vipA in V. cholerae C6706	pKAS32-Kan	Kanamycin	Streptomycin	This study
pSN95	Insert T7 terminator after the coding sequence of vca0106 in V. cholerae C6706	pRE118	Kanamycin	Sucrose	This study
pSN96	Insert T7 terminator after the coding sequence of vca0106 in V. cholerae 3223-74	pRE118	Kanamycin	Sucrose	This study
pSN87	Introducing a SNP at -68 of the 5'IGR of T6SS large cluster in 3223-74	pRE118	Kanamycin	Sucrose	This study

Table A.3: **List of primers used in Chapter 2**

Primers	Description	Sequence (5'-3')
GT2899	Constructing pKE2 - Primer overlapping pSLS vector and 5' IGR of C6706/3223-74 T6SS large cluster	TGCATGCGGCGCCTGATCTGTTCCCTGTTAAGTATTATTTAAGTATGGTTATTGG
GT2900	Constructing pKE2 - Primer overlapping T7RBS-sfGFP and 5' IGR of C6706 T6SS large cluster	ATTATTTCTAGGGCCAAACGTTGTCAATGAAAC
GT2901	Constructing pKE2 - Primer overlapping 5' IGR of C6706 T6SS large cluster and T7RBS-sfGFP	ACAACGTTTGGCCCTAGAAATAATTTTGTTTAACTTTAAGAAGGAG
GT2902	Constructing pKE2 - Primer overlapping pSLS vector and T7RBS-sfGFP	GCTTGCTCAATCAATCACCGTCACTTGTACAGCTCGTCCAT
GT2943	Constructing pSN27 - Primer overlapping T7RBS-sfGFP and 5' IGR of 3223-74 T6SS large cluster	AAATTATTTCTAGGCCAAACGTTGTCAATG
GT2944	Constructing pSN27 - Primer overlapping 5' IGR of 3223-74 T6SS large cluster and T7RBS-sfGFP	ACAACGTTTGGCCTAGAAATAATTTTGTTTAACTTTAAGAAGGAG
GT2745	Confirming the constructs with pSLS3 vector backbone	ATGAAGGGTCTTTTTGCATG
GT2746	Confirming the constructs with pSLS3 vector backbone	TACAAGCATAAAGCTTGCTCAAT
GT2566	Confirming the 5' IGR sequence of the T6SS large cluster	CGCTTGAGTCATGTCTACC
GT2567	Confirming the 5' IGR sequence of the T6SS large cluster	AGTCAGCTTGTTTTTTCACCG
GT3264	Confirming cDNA sample contains vipA transcript - binds to the non-coding region of C6706 vipA	TTTCAAATCCTTAGCCGACTTC
GT3265	5' RACE - for reverse transcription and binds to the coding region of C6706 vipA	TAATGACTGTAAACGCTCACGA
GT3269	5' RACE - for reverse transcription and binds to the coding region of 3223-74 vipA	TAGTGACTGTAAACGCTCACGA
GT3270	Confirming cDNA sample contains vipA transcript - binds to the non-coding region of 3223-74 vipA	GAATGCTGAGCTTCCAGTTGAA
GT3056	5' RACE - for sequencing the 5' IGR of C6706/3223-74 T6SS large cluster	CCACCGCATCAGGAGCGAAG
GT3060	5' RACE - for sequencing the 5' IGR of C6706/3223-74 T6SS large cluster	CAATACCTATGCCAAACGTTGTC
GT3266	Confirming gDNA contamination in RNA samples by amplifying rrsA	ACCTTACCTACTCTTGACATCCA
GT3267	Confirming gDNA contamination in RNA samples by amplifying rrsA	CCCAACATTTCACAACACGAG
Primers for cloning	Description	Sequence (5'-3')
GT3045	Confirming the constructs with pRE118 vector backbone	CATCCAACGCCATTCATGGC
GT3046	Confirming the constructs with pRE118 vector backbone	CTAATCAGAATTGGTTAATTGGTTGTAACACTGG
GT3103	Constructing pSN58 - Primer overlapping pRE118 and 3223-74 1000bp upstream of hapR	CTCGATATCGCATGCGGTACTCGAGGATGGCCGAC
GT3104	Constructing pSN58 - Primer overlapping 3223-74 1000bp downstream and 1000bp upstream of hapR	CTGCCCAAGAAATTTGCTCTAATGATTATTTTGTTATTTGCT
GT3105	Constructing pSN58 - Primer overlapping 3223-74 1000bp upstream and 1000bp downstream of hapR	CATTAGAGCAAATTTCTTGGGCAGCACAAAG
GT3106	Constructing pSN58 - Primer overlapping pRE118 and 3223-74 1000bp downstream of hapR	CGACGGATCCCAAGCTTCTTACATCACACAACGCGC
GT178	hapR deletion check	CTTTCACTTTGTTTAAGGTATTCCCTGTATCG
GT179	hapR deletion check	GCACGCCTCTGATCAGTGATCC
GT3089	Constructing pSN40 - Primer overlapping pRE118 and 3223-74 1000bp upstream of luxO	CATGAATTCCCGGAGAGAGCTGGATCAACTTGCTCCGTG
GT3010	Constructing pSN58 - Primer overlapping 3223-74 1000bp downstream and 1000bp upstream of luxO	GGAATATTACCATAGGTAGAACGATACAGCGC
GT3011	Constructing pSN58 - Primer overlapping 3223-74 1000bp upstream and 1000bp downstream of luxO	TCGTTCTTACCTATGGTAATATTCCTCGCGC
GT3012	Constructing pSN58 - Primer overlapping pRE118 and 3223-74 1000bp downstream of luxO	CGACGGATCCCAAGCTTCTTTCAATCTTATTCGCAACATGCT
GT1412	luxO deletion check	CAAAATGCAATTCCAAATGCAATTATT
GT1413	luxO deletion check	GTTCACCAAGAAAAATGTTGACC
GT1201	Constructing pJT88 - Primer overlapping pKAS-Amp and C6706 500bp upstream of qstR	CGCATGCTAGCTATAGTTCTAGATCACCAGCCACTTCTGCC
GT1202	Constructing pJT88 - Primer overlapping Ptac and C6706 500bp upstream of qstR	CCAGAACCGTTATGATGTCGGATGAATTACAGACTCAGTTAATATG
GT1203	Constructing pJT88 - Primer overlapping C6706 500bp upstream of qstR and Ptac	CATATTAACTGAGTCTGTAATTCATCCGACATCATAACGGTTCTGG
GT1204	Constructing pJT88 - Primer overlapping C6706 500bp downstream of qstR and Ptac	GCATAGTTGGCTCGTTGCATTTAGCTTCCTTAGCTCCTGAA
GT1205	Constructing pJT88 - Primer overlapping Ptac and C6706 500bp downstream of qstR	TTCAGAGCTTAAGGAGCTAAAATGCAACGAGCCAACTATGC
GT1206	Constructing pJT88 - Primer overlapping pKAS-Amp and C6706 500bp downstream of qstR	TTAACGGCTGACATGGGAATTCTGTAAACAGCGCAGGATCTG
GT1062	Constructing pSW55 - Primer overlapping pKAS-Amp and C6706 500bp upstream of qstR	CGCATGCTAGCTATAGTTCTAGATCACCAGCCACTTCTGCCAATTTTC
GT1063	Constructing pSW55 - Primer overlapping C6706 500bp downstream and 500bp upstream of qstR	CCGCTAGGTTGAGCGCCTGATGAATTACAGACTCAG
GT1064	Constructing pSW55 - Primer overlapping C6706 500bp upstream and 500bp upstream of qstR	CTGAGTCTGTAATTCATCAGGCGCTCAACCTAGCGG
GT1065	Constructing pSW55 - Primer overlapping pKAS-Amp and C6706 500bp downstream of qstR	TTAACGGCTGACATGGGAATTGACCCAAGCCTTTCATTTCGC
GT1207	Ptac-qstR or qstR deletion check (for C6706)	CGCCATATTAAGTGCATTATTTC
GT1208	Ptac-qstR or qstR deletion check (for C6706)	GCATTGTTACTACATTTTTCTCC
GT1863	Constructing pJT634 - Primer overlapping pKAS-Amp and C6706 500bp upstream of vasK	CGCATGCTAGCTATAGTTCTAGAGGATGAGTTACACCATTGCC
GT1864	Constructing pJT634 - Primer overlapping C6706 500bp downstream and 500bp upstream of vasK	AAAACTCGCTCTGGCAACCTAGAATTGTGTCCTTGTTTACTCTG
GT1865	Constructing pJT634 - Primer overlapping C6706 500bp upstream and 500bp upstream of vasK	CAGAGTAAACAAGGACACAATTCTAGTTGCCAGAGCGAGTTTT
GT1866	Constructing pJT634 - Primer overlapping pKAS-Amp and C6706 500bp downstream of vasK	TTAACGGCTGACATGGGAATTCCAGCTGATGTAACCGCTCG
GT1867	vasK deletion check	CCGAGTTTAGTGGAACAAATTC
GT1868	vasK deletion check	CAACTTCGTCCTAAAAAGCCAG
GT2911	Constructing pCC115 - Primer overlapping pKAS-Kan and E. coli MG1655 1000bp upstream of lacZ	TTGCGCATGCTAGCTATAGTTCTGTTGACTGTAGCGGCTGAT
GT2912	Constructing pCC115 - Primer overlapping Ptac-T7RBS-sfGFP and E. coli MG1655 1000bp upstream of lacZ	TGTACAAGTGACGTCATAGCGATAACGAGCTC
GT2913	Constructing pCC115 - Primer overlapping E. coli MG1655 1000bp upstream of lacZ and Ptac-T7RBS-sfGFP	CGCTATGACGTCACTTGTACAGCTCGTCCAT
GT2914	Constructing pCC115 - Primer overlapping E. coli MG1655 1000bp downstream of lacZ and Ptac-T7RBS-sfGFP	CGAATACCTGTTCTTGACAATTAATCATCGGCTCGTATAA
GT2915	Constructing pCC115 - Primer overlapping Ptac-T7RBS-sfGFP and E. coli MG1655 1000bp downstream of lacZ	ATTAATTGTCAAGAACAGGTATTCGCTGGTCACT
GT2916	Constructing pCC115 - Primer overlapping pKAS-Kan and E. coli MG1655 1000bp downstream of lacZ	CACTTAACGGCTGACATGGGGGTGGTTGAACTGCACACCG
GT2451	Confirming the constructs with pKAS-Kan/pKAS-Amp vector backbone	TCAGCGCTTTAAATTTGC
GT2452	Confirming the constructs with pKAS-Kan/pKAS-Amp vector backbone	TTTCAGTGACACAGGAACAC
GT2238	Constructing pJT981 - Primer overlapping pKAS-Kan and C6706 1000bp upstream of vasK	GGGAGAGCTCGATATCGCATGCAGCGGATCGCCAAGC
GT2239	Constructing pJT981 - Primer overlapping C6706 1000bp downstream and 1000bp upstream of vasK	TCTGGCAACCTAGAATTGTGTCCTTGTTTACTCTGACG
GT2240	Constructing pJT981 - Primer overlapping C6706 1000bp upstream and 1000bp upstream of vasK	AGGACACAATTCTAGGTTGCCAGAGCGAGTTTT
GT2241	Constructing pJT981 - Primer overlapping pKAS-Kan and C6706 1000bp downstream of vasK	CGACGGATCCCAAGCTTCTTCTAGATGCTGCTGAAGGGCAAAC
GT3151	Constructing pSN67 - Primer overlapping pRE118 and V. cholerae 1000bp upstream of lacZ	CTCGATATCGCATGCGGTACTATTGAGGGGATGACGCTTT
GT3152	Constructing pSN67 and pSK3 - Primer overlapping IGRvipA-T7RBS-sfGFP and V. cholerae 1000bp upstream of lacZ	CTTAACAGGGAATCAATGCAGTCTTATTGTGTCG
GT3153	Constructing pSN67 and pSK3 - Primer overlapping V. cholerae 1000bp upstream of lacZ and IGRvipA-T7RBS-sfGFP	GACTGCAATTGATTCCTGTTAAGTATTATTTAAGTATGGTTATT
GT3154	Constructing pSN67 and pSK3 - Primer overlapping V. cholerae 1000bp downstream of lacZ and IGRvipA-T7RBS-sfGFP	ATGAATACCACCTCACTTGTACAGCTCGTCC
GT3155	Constructing pSN67 and pSK3 - Primer overlapping IGRvipA-T7RBS-sfGFP and V. cholerae 1000bp downstream of lacZ	CTGTACAAGTGAGGTGGTATTCATGCTCTGG
GT3156	Constructing pSN67 and pSK3 - Primer overlapping pRE118 and V. cholerae 1000bp downstream of lacZ	CGACGGATCCCAAGCTTCTTCCAGAACTCGGGCATG
GT313	sfGFP insertion in lacZ check	GCCTTAAGGCTCTCTGGC
GT3143	sfGFP insertion in lacZ check	GGATCTTGAAGTTCACCTTGAT
GT2366	Constructing pTH25 - Primer overlapping pRE118 and 1496-86 1000bp upstream of tfoY	GGGAGAGCTCGATATCGCATGCGACCTGACCCAAGAGCTGCA
GT2367	Constructing pTH25 - Primer overlapping 1496-86 1000bp downstream and 1000bp upstream of tfoY	TCAAAATGAAACTCACATGCTGTTAGTCTCGGAGTATTGTTACA
GT2368	Constructing pTH25 - Primer overlapping 1496-86 1000bp upstream and 1000bp downstream of tfoY	AGACTAACAGCATGTGAGTTTCATTTTGAGTTCATCAACGCCTGTAATCA
GT2369	Constructing pTH25 - Primer overlapping pRE118 and 1496-86 1000bp downstream of tfoY	CGACGGATCCCAAGCTTCTTCTAGATTACTTCACTGGCGATTGAGTGGC
GT2370	tfoY deletion check (for environmental isolates)	ATTATTTTTATCAGGAAAAATGTCACGCACAGG
GT2371	tfoY deletion check (for environmental isolates)	CCGACGTGTCACTCCAAGTCA
GT2373	Constructing pTH30 - Primer overlapping pRE118 and 1496-86 1000bp upstream of qstR	GGGAGAGCTCGATATCGCATGCGTTTTTCTTGTACATGTTTTCGTAG
GT2374	Constructing pTH30 - Primer overlapping 1496-86 1000bp downstream and 1000bp upstream of qstR	TGTAATTCATCATGTAAAGGCGCTCAACCTAGC
GT2375	Constructing pTH30 - Primer overlapping 1496-86 1000bp upstream and 1000bp downstream of qstR	TTGAGCGCCTTTACATGATGAATTACAGACTCAGTTAATATGAAATAAT
GT2376	Constructing pTH30 - Primer overlapping pRE118 and 1496-86 1000bp downstream of qstR	CGACGGATCCCAAGCTTCTTCTAGACGAACGCCACTAACCG
GT2377	qstR deletion check (for environmental isolates)	GATACCCGCTTGAATCGCTTCA
GT2378	qstR deletion check (for environmental isolates)	AGTCGGCAAGGATAACACCG
GT1190	Constructing pJT85 - Primer overlapping pKAS-Amp and C6706 500bp upstream of tfoY	CGCATGCTAGCTATAGTTCTAGACGGAGGCCAAGTTGACCG
GT1191	Constructing pJT85 - Primer overlapping C6706 500bp downstream and 500bp upstream of tfoY	CGTTGATGACTCAAAATGAACGCTGTTAGTCTCGGAGTATTG
GT1192	Constructing pJT85 - Primer overlapping C6706 500bp upstream and 500bp upstream of tfoY	CAATACTCCGAGACTAACAGCGTTTCATTTTGAGTTCATCAACG
GT1193	Constructing pJT85 - Primer overlapping pKAS-Amp and C6706 500bp downstream of tfoY	TTAACGGCTGACATGGGAATTCGCTTGCAGCAAATGGGCATC
GT1199	tfoY deletion check (for C6706)	CGAGTATTATTAGTAGGGCTC
GT1200	tfoY deletion check (for C6706)	AACACAGGATGATTACAGGCG
GT2844	Constructing pSN20 - Primer overlapping pKAS-Kan and 500bp upstream of C6706 5'IGR of T6SS large cluster	TTGCGCATGCTAGCTATAGTTACAGATTGAGCAAGGAGAGG
GT2845	Constructing pSN20 - Primer overlapping 3223-74 5'IGR of T6SS large cluster and 500bp upstream of C6706 5'IGR of T6SS large cluster	GTGTTGTTGTATTTAACCATACTTAAATAATACTTAACAGGGAAC
GT2846	Constructing pSN20 - Primer overlapping 500bp upstream of C6706 5'IGR of T6SS large cluster and 3223-74 5'IGR of T6SS large cluster	TAAGTATGGTTAAATACAACAACACTCTGTGATACG
GT2847	Constructing pSN20 - Primer overlapping 500bp downstream of C6706 5'IGR of T6SS large cluster and 3223-74 5'IGR of T6SS large cluster	CTTCTTAGACATATTACGTCTCCAATACCTATGC
GT2848	Constructing pSN20 - Primer overlapping 3223-74 5'IGR of T6SS large cluster and 500bp downstream of C6706 5'IGR of T6SS large cluster	TGGAGACGTAATATGTCTAAAGAAGGAAGTGTAGCTC
GT2849	Constructing pSN20 - Primer overlapping pKAS-Kan and 500bp downstream of C6706 5'IGR of T6SS large cluster	CACTTAACGGCTGACATGGGTGTGGCTCTTCTTGACCACT
GT2882	Constructing pSN78 - Primer overlapping pKAS-Kan and 500bp upstream of C6706 5'IGR of T6SS large cluster	TTGCGCATGCTAGCTATAGTTAACACCCCGCAGC
GT2883	Constructing pSN78 - Primer overlapping V52 5'IGR of T6SS large cluster and 500bp upstream of C6706 5'IGR of T6SS large cluster	ACTTAACAGGGAACTAATTATCCCAGTAAGCATCATGG
GT2884	Constructing pSN78 - Primer overlapping 500bp upstream of C6706 5'IGR of T6SS large cluster and V52 5'IGR of T6SS large cluster	TGGGATAATTAGTTCCCTGTTAAGTATTATTTAAGTATGGTTATTGG
GT2885	Constructing pSN78 - Primer overlapping 500bp downstream of C6706 5'IGR of T6SS large cluster and V52 5'IGR of T6SS large cluster	CTTCTTTAGACATATTACGTCTCCAATACCTATGC
GT2886	Constructing pSN78 - Primer overlapping V52 5'IGR of T6SS large cluster and 500bp downstream of C6706 5'IGR of T6SS large cluster	TGGAGACGTAATATGTCTAAAGAAGGAAGTGTAGCTC
GT2887	Constructing pSN78 - Primer overlapping pKAS-Kan and 500bp downstream of C6706 5'IGR of T6SS large cluster	CACTTAACGGCTGACATGGGTGTGGCTCTTCTTGACCACT
GT3220	Constructing pSN87 - Primer overlapping pRE118 and 500bp upstream of the -68 of T6SS large cluster 5'IGR in 3223-74	CTCGATATCGCATGCGGTACTATCCCATGCCTGGTAGCC
GT3221 (-68 T-to-G)	Constructing pSN87 - Primer overlapping the -68 of T6SS large cluster 5'IGR and 500bp upstream of the -68 of T6SS large cluster 5'IGR in 3223-74	ACCCCAAATATATCCAATAACCATACT
GT3221 (-68 T-to-G)	Constructing pSN87 - Primer overlapping 500bp upstream of the -68 of T6SS large cluster 5'IGR and the -68 of T6SS large cluster 5'IGR in 3223-74	TGGTTATTGGATATATTTTGGGGTAAAAGAT
GT3223	Constructing pSN87 - Primer overlapping 500bp downstream of the -68 of T6SS large cluster 5'IGR and the -68 of T6SS large cluster 5'IGR in 3223-74	CTTCTTTAGACATATTACGTCTCCAATACCTATGC
GT3224	Constructing pSN87 - Primer overlapping the -68 of T6SS large cluster 5'IGR and 500bp downstream of the -68 of T6SS large cluster 5'IGR in 3223-74	TGGAGACGTAATATGTCTAAAGAAGGAAGTGTAGC
GT3225	Constructing pSN87 - Primer overlapping pRE118 and 500bp downstream of the -68 of T6SS large cluster 5'IGR in 3223-74	CGACGGATCCCAAGCTTCTTTGTGGCTCTTCTTGACCAC
GT3226 (-68 T-to-A)	Constructing pSN87 - Primer overlapping the -68 of T6SS large cluster 5'IGR and 500bp upstream of the -68 of T6SS large cluster 5'IGR in 3223-74	TGGTTATTGGATATATTTTAGGGTAAAAGAT
GT3227 (-68 T-to-A)	Constructing pSN87 - Primer overlapping 500bp upstream of the -68 of T6SS large cluster 5'IGR and the -68 of T6SS large cluster 5'IGR in 3223-74	ACCCTAAAATATATCCAATAACCATACT
GT3228 (-68 T-to-C)	Constructing pSN87 - Primer overlapping the -68 of T6SS large cluster 5'IGR and 500bp upstream of the -68 of T6SS large cluster 5'IGR in 3223-74	TGGTTATTGGATATATTTTCGGGTAAAAGAT
GT3229 (-68 T-to-C)	Constructing pSN87 - Primer overlapping 500bp upstream of the -68 of T6SS large cluster 5'IGR and the -68 of T6SS large cluster 5'IGR in 3223-74	ACCCGAAAATATATCCAATAACCATACT
GT2557	Constructing pHN1 - Primer overlapping pKAS and 500bp upstream of vipA	aaattgCGCATGCTAGCTATAGTTGCCAAGGCTTACTTCAATC
GT2558	Constructing pHN1 - Primer overlapping T7 terminator and 500bp upstream of vipA	gctttgttagcagTCAATCACTTCCGGTGACAC
GT2559	Constructing pHN1 - Primer overlapping 500bp upstream of vipA and T7 terminator	ggaagtgattgactgctaatcaaagcccgaa
GT2560	Constructing pHN1 - Primer overlapping 500bp downstream of vipA and T7 terminator	ctctttagacatatccggatatagttcctcctt
GT2561	Constructing pHN1 - Primer overlapping T7 terminator and 500bp downstream of vipA	ctatatccggatatgtctaaagaaggaagtgtagc
GT2562	Constructing pHN1 - Primer overlapping pKAS and 500bp downstream of vipA	aggaacacTTAACGGCTGACATGGGTGTGGCTCTTCTTGACC
GT3306	Constructing pSN95 - Primer overlapping pRE118 and 500bp upstream of 5'IGR and vipA	ctcgatatcgcatgcggtacaacaccctgcagctc
GT3307	Constructing pSN95/96 - Primer overlapping T7 terminator and 500bp upstream of 5'IGR and vipA	gctttgttagcagctaattatcccagtaagcatcatgg
GT3308	Constructing pSN95/96 - Primer overlapping 500bp upstream of 5'IGR and vipA and T7 terminator	tgggataaattagctgctaacaaagcccga
GT3309	Constructing pSN95/96 - Primer overlapping 500bp downstream of vipA and T7 terminator	acttaacagggaatcccggatatagttcctcctt
GT3310	Constructing pSN95/96 - Primer overlapping T7 terminator and 500bp downstream of vipA	ctatatccggattccctgttaagtattatttaagtatggttatt
GT3311	Constructing pSN95 - Primer overlapping pRE118 and 500bp downstream of vipA	CGACGGATCCcaagcttcttcctgtgcatccccg
GT3312	Constructing pSN96 - Primer overlapping pRE118 and 500bp upstream of 5'IGR and vipA	ctcgatatcgcatgcggtacaacaccccgcagctc
GT3313	Constructing pSN96 - Primer overlapping pRE118 and 500bp downstream of vipA	CGACGGATCCcaagcttcttgctcaacctcagcctg
GT2566	5'IGR of T6SS large cluster check	CGCTTGAGTCATGTCTACC
GT2567	5'IGR of T6SS large cluster check	AGTCAGCTTGTTTTTCACCG

Table A.4: **List of genomes used in Chapter 2 with strain details**

Organism	Lab stock #	Strain	Clincal/Environmental	Serogroup	Assembly accession	T6SS activity	Base at -68 site
Vibrio cholerae	BGT11	MZO-2	Clinical	O14	GCA_001729155.1	Constitutive	T
Vibrio cholerae	BGT5	NCTC 8457	Clinical	O1 El Tor	GCA_000153945.1	Constitutive	T
Vibrio cholerae	SW31	2010EL-1749	Clinical	O1 El Tor	GCA_000237505.2	Constitutive	G
Vibrio cholerae	BGT6	MAK 757	Clinical	O1 El Tor	GCA_000153865.1	Constitutive	T
Vibrio cholerae	BH1514	C6706	Clinical	O1 El Tor	GCA_001857435.1	Inducible	G
Vibrio cholerae	EB293	3546-06	Clinical	O1 El Tor	GCA_000237705.2	Inducible	G
Vibrio cholerae	SW39	3554-08	Clinical	O1 El Tor	GCA_000237725.2	Inducible	G
Vibrio cholerae	SW29	2009V-1096	Clinical	O1 El Tor	GCA_000237445.2	Inducible	G
Vibrio cholerae	EB291	3500-05	Clinical	O1 El Tor	GCA_000237685.2	Inducible	G
Vibrio cholerae	EB287	2010V-1014	Clinical	O1 El Tor	GCA_000237585.2	Inducible	G
Vibrio cholerae	EA810	2010EL-1786	Clinical	O1 El Tor	GCA_000166455.2	Inducible	G
Vibrio cholerae	EB283	2011EL-1137	Clinical	O1 El Tor	GCA_000237645.2	Inducible	G
Vibrio cholerae	BGT10	MO10	Clinical	O139 El Tor	GCA_017948345.1	Inducible	G
Vibrio cholerae	SW491	V52	Clinical	O37	GCA_001857545.1	Constitutive	T
Vibrio cholerae	BGT70	3225-74	Environmental	O1	GCA_001857365.1	Constitutive	T
Vibrio cholerae	BGT69	3223-74	Environmental	O1	GCA_001743085.1	Constitutive	T
Vibrio cholerae	BGT65	2479-86	Environmental	O1	GCA_001857305.1	Constitutive	T
Vibrio cholerae	BGT41	VC22	Environmental	O1	GCA_001729195.1	Constitutive	T
Vibrio cholerae	BGT62	2512-86	Environmental	O1	GCA_001857245.1	Constitutive	T
Vibrio cholerae	BGT7	857	Environmental	O1	GCA_001729125.1	Constitutive	T
Vibrio cholerae	BGT64	692-79	Environmental	O1	GCA_001857285.1	Constitutive	T
Vibrio cholerae	Colwell #10	HE46	Environmental	NAg	GCA_001857515.1	Constitutive	T
Vibrio cholerae	BGT61	2631-78	Environmental	O1	GCA_001857225.1	Constitutive	T
Vibrio cholerae	EB649	3568-07	Environmental	O141	GCA_001857505.1	Constitutive	T
Vibrio cholerae	BGT71	1074-78	Environmental	O1	GCA_001857405.1	Constitutive	T
Vibrio cholerae	BGT8	2740-80	Environmental	O1	GCA_001729185.1	Constitutive	T
Vibrio cholerae	BH2680	SIO	Environmental	NAg	GCA_001857455.1	Constitutive	T
Vibrio cholerae	BGT60	2559-78	Environmental	O1	GCA_001857145.1	Constitutive	T
Vibrio cholerae	BGT67	2497-86	Environmental	O1	GCA_001857355.1	Constitutive	T
Vibrio cholerae	BGT49	VC56	Environmental	O1	GCA_001857175.1	Constitutive	T
Vibrio cholerae	BGT46	VC53	Environmental	NAg	GCA_001857155.1	Constitutive	T
Vibrio cholerae	BGT72	2633-78	Environmental	O1	GCA_001857425.1	Constitutive	T
Vibrio cholerae	BGT63	3272-78	Environmental	O1	GCA_001857265.1	Constitutive	T
Vibrio cholerae	BH2681	TP	Environmental	NAg	GCA_001857485.1	Constitutive	T
Vibrio cholerae	BGT42	VC48	Environmental	NAg	GCA_001857165.1	Constitutive	T
Vibrio cholerae	BGT66	1496-86	Environmental	O1	GCA_001857325.1	Inducible	T

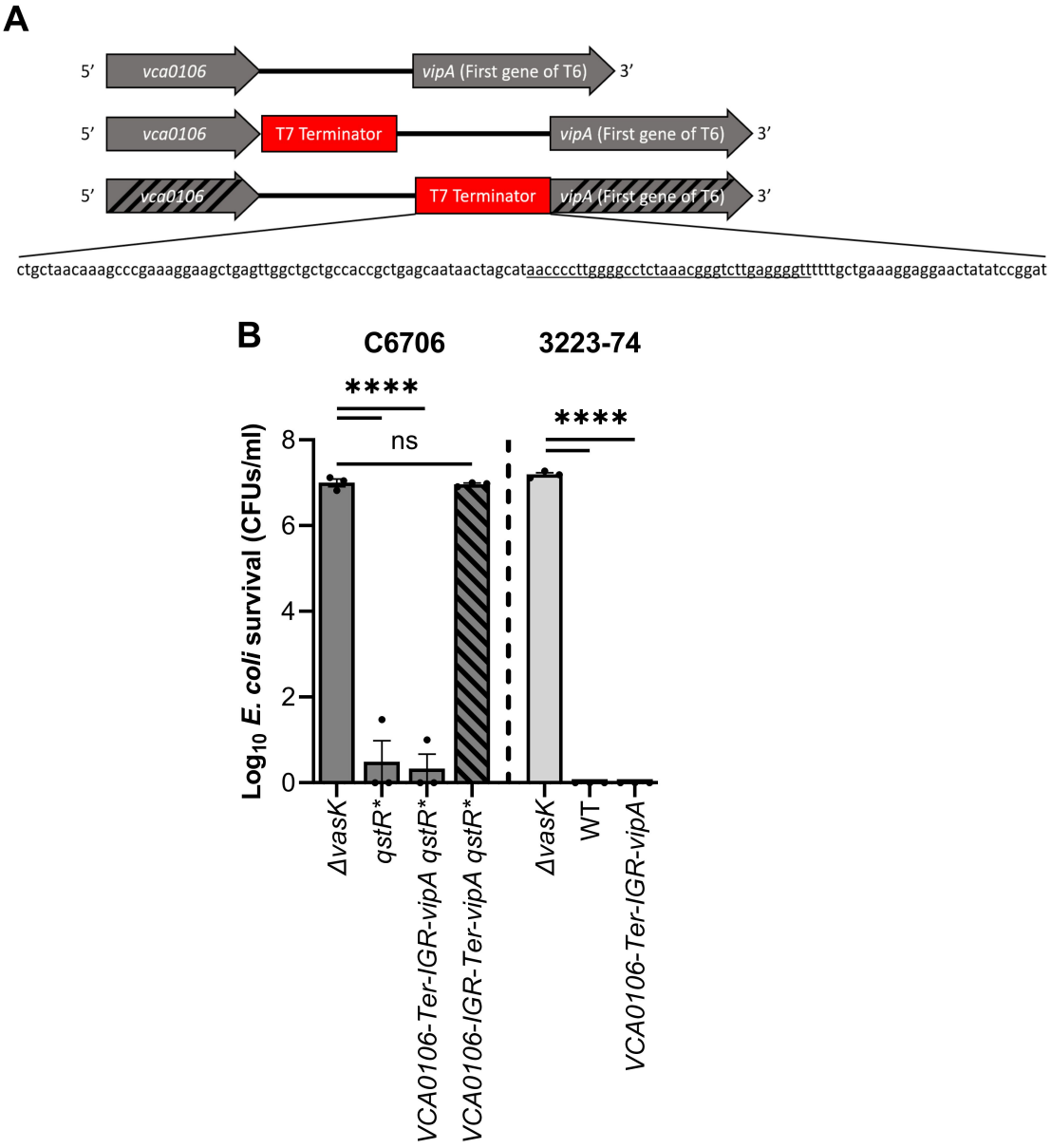

Figure A.1: **Activity of the major T6 gene cluster is not controlled by transcriptional read-through.** (A) Schematic shows the WT T6 5' IGR. The T7 terminator DNA sequence [156] encoding an RNA hairpin (underlined) is indicted, as well as the location the terminator was inserted before and after the T6 5' IGR. (B) Competition assays were conducted by coculturing *V. cholerae* and chloramphenicol (Cm) resistant *E. coli* target followed by determination of *E. coli* survival by counting of CFUs on LB agar with Cm. The *V. cholerae* Δ*vasK* mutant served as a T6- negative control. Data shown are mean values ± S.E. from three independent biological replicates. A one-way ANOVA with Dunnett post-hoc test was conducted to determine the significance. ns, not significant; ****, $P \leq 0.0001$.

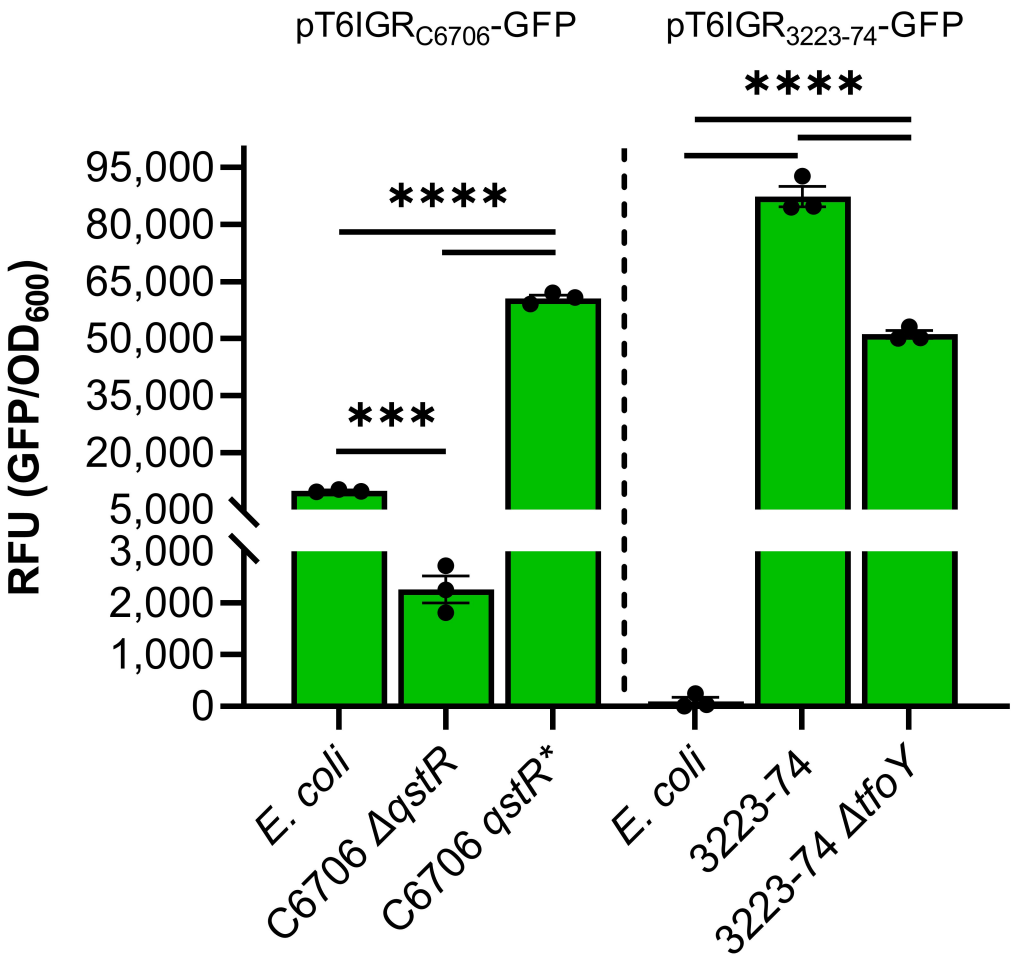

Figure A.2: **The major *V. cholerae* T6 promoter is not constitutively expressed in *E. coli*.** *V. cholerae* or *E. coli* carrying a plasmid-encoded *gfp* gene driven by either the C6706 or 3223-74 5' T6 IGR was grown in liquid LB with Cm. *gfp* is represented as relative fluorescent units per OD_{600} (RFU). Data shown are mean values ± S.E. from 3 independent biological replicates. A one-way ANOVA with Tukey post-hoc test was conducted to determine the significance: ****, $P \leq 0.0001$; ***, $P \leq 0.001$.

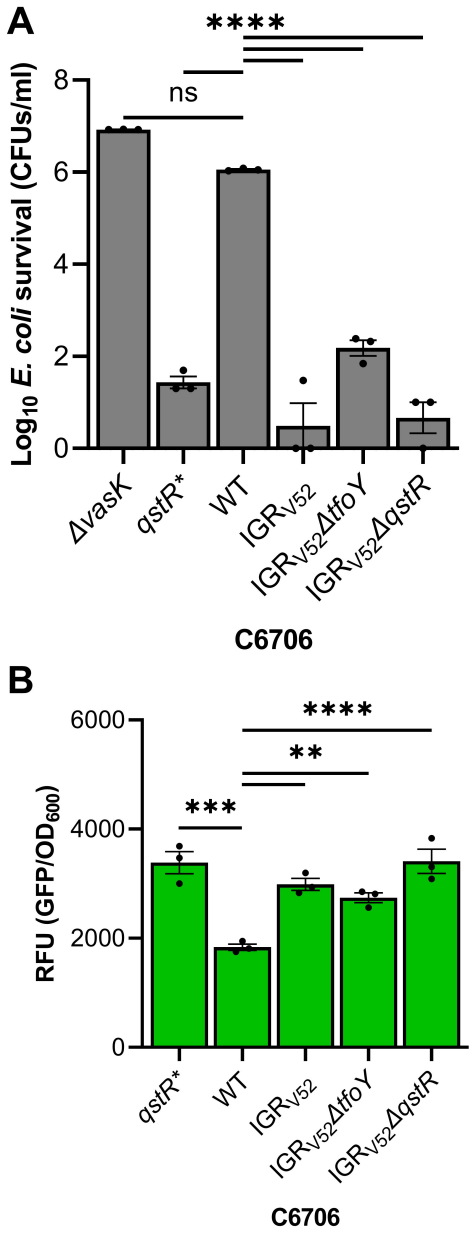

Figure A.3: **C6706 T6 is no longer activated by QstR after acquiring the G-68T mutation.** (A) Competition assays were conducted by coculturing *V. cholerae* and Cm^R *E. coli* target cells followed by determination of *E. coli* survival by counting of CFUs on LB agar with Cm. The *V. cholerae* Δ*vasK* mutant served as a T6- negative control. (B) Fluorescence levels are from reporters with *gfp* fused to the IGR 5' of *vipA* derived from the strains shown. Data shown are mean values ± S.E. from three independent biological replicates. A one-way ANOVA with Dunnett post-hoc test was conducted to determine the significance. ns, not significant; ****, $P \leq 0.0001$; ***, $P \leq 0.001$; **, $P \leq 0.01$.

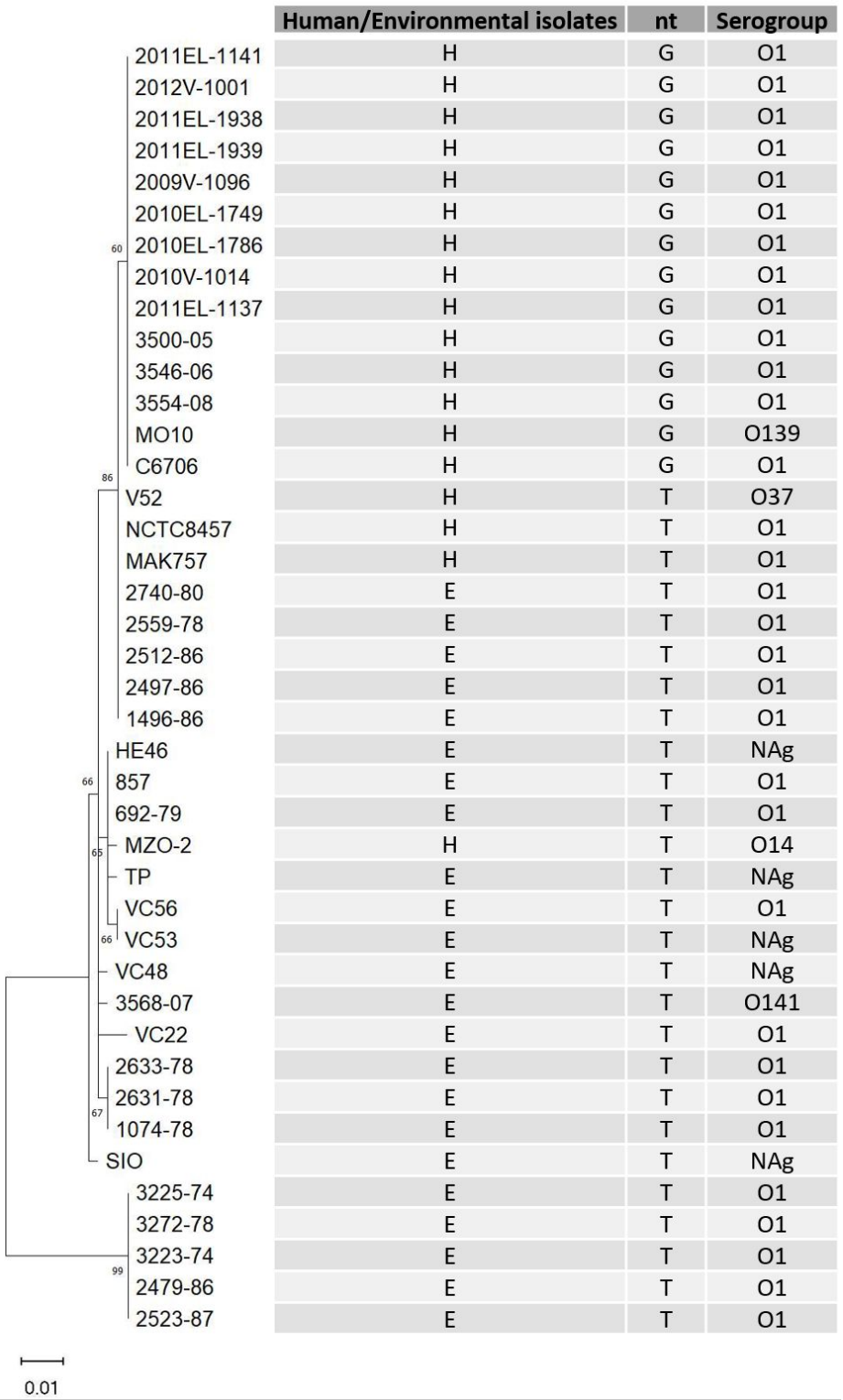

Human/Environmental isolates	nt	Serogroup
2011EL-1141	H	G	O1
2012V-1001	H	G	O1
2011EL-1938	H	G	O1
2011EL-1939	H	G	O1
2009V-1096	H	G	O1
2010EL-1749	H	G	O1
2010EL-1786	H	G	O1
2010V-1014	H	G	O1
2011EL-1137	H	G	O1
3500-05	H	G	O1
3546-06	H	G	O1
3554-08	H	G	O1
MO10	H	G	O139
C6706	H	G	O1
V52	H	T	O37
NCTC8457	H	T	O1
MAK757	H	T	O1
2740-80	E	T	O1
2559-78	E	T	O1
2512-86	E	T	O1
2497-86	E	T	O1
1496-86	E	T	O1
HE46	E	T	NAg
857	E	T	O1
692-79	E	T	O1
MZO-2	H	T	O14
TP	E	T	NAg
VC56	E	T	O1
VC53	E	T	NAg
VC48	E	T	NAg
3568-07	E	T	O141
VC22	E	T	O1
2633-78	E	T	O1
2631-78	E	T	O1
1074-78	E	T	O1
SIO	E	T	NAg
3225-74	E	T	O1
3272-78	E	T	O1
3223-74	E	T	O1
2479-86	E	T	O1
2523-87	E	T	O1

Figure A.4: **Most human isolates are in a clade distinct from environmental isolates.** The 5' IGR sequences of the *V. cholerae* strains described in [59] were used to conduct the maximum likelihood phylogenetic analysis with MEGA. Nag, nonagglutinating; H, human isolates; E, environmental isolates.

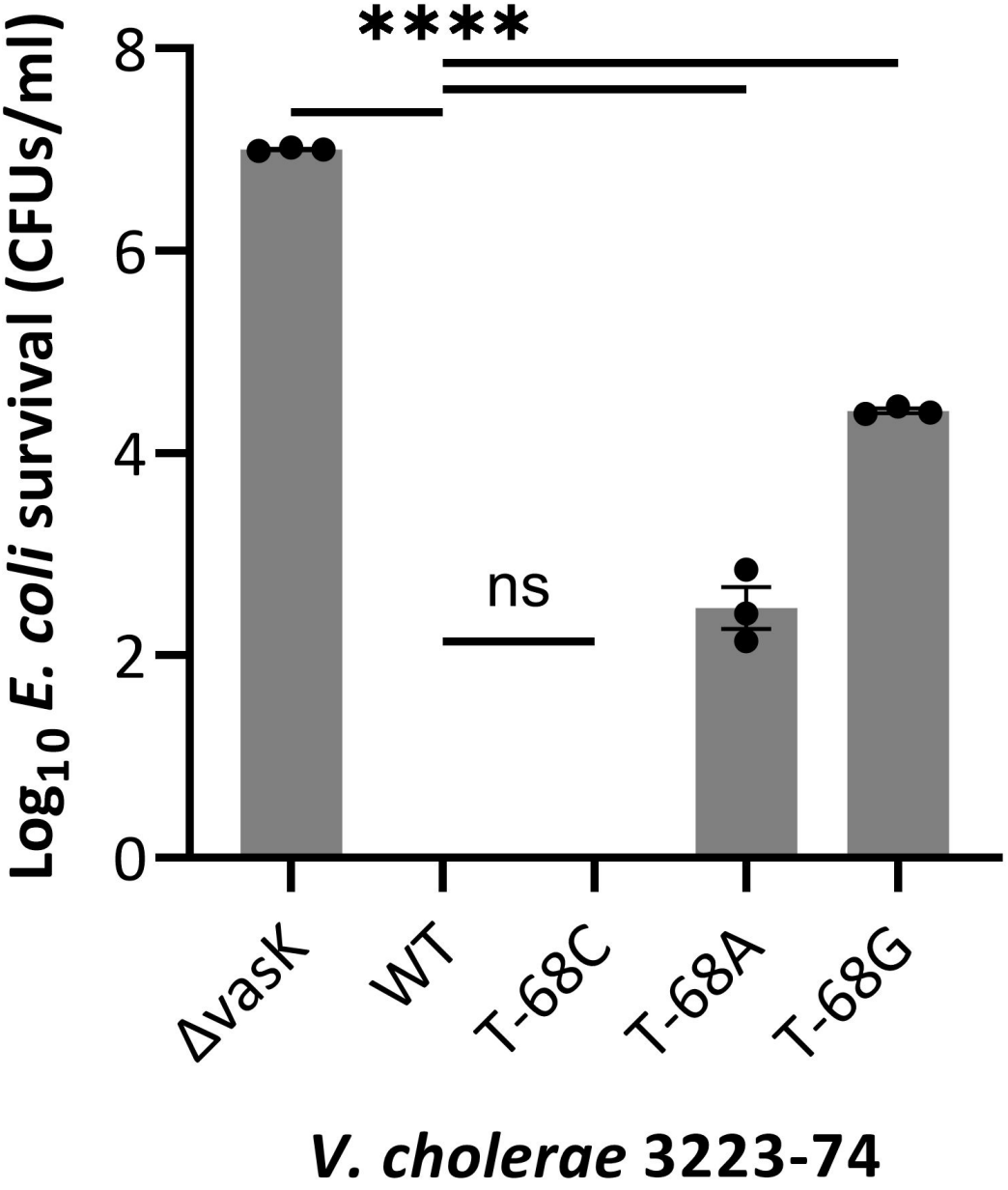

Figure A.5: **Transversions at -68 alter T6 control.** Transversion mutations (T-68A, T-68G) but not a transition mutation (T-68C) introduced into the 3223-74 IGR change T6 control. Competition assays were conducted by coculturing *V. cholerae* with Cm^R *E. coli* at a ratio of 1:10 for 3 h on LB agar plates. Survival *E. coli* was selected by Cm and determined by counts of CFUs. Δ*vasK* in *V. cholerae* prevents assembly of T6 and was served as a T6- negative control. Data shown are the mean ± S.E. from three independent biological replicates. A one-way ANOVA with Dunnett post-hoc test was conducted to determine the significance. ns, not significant; ****, $P \leq 0.0001$.

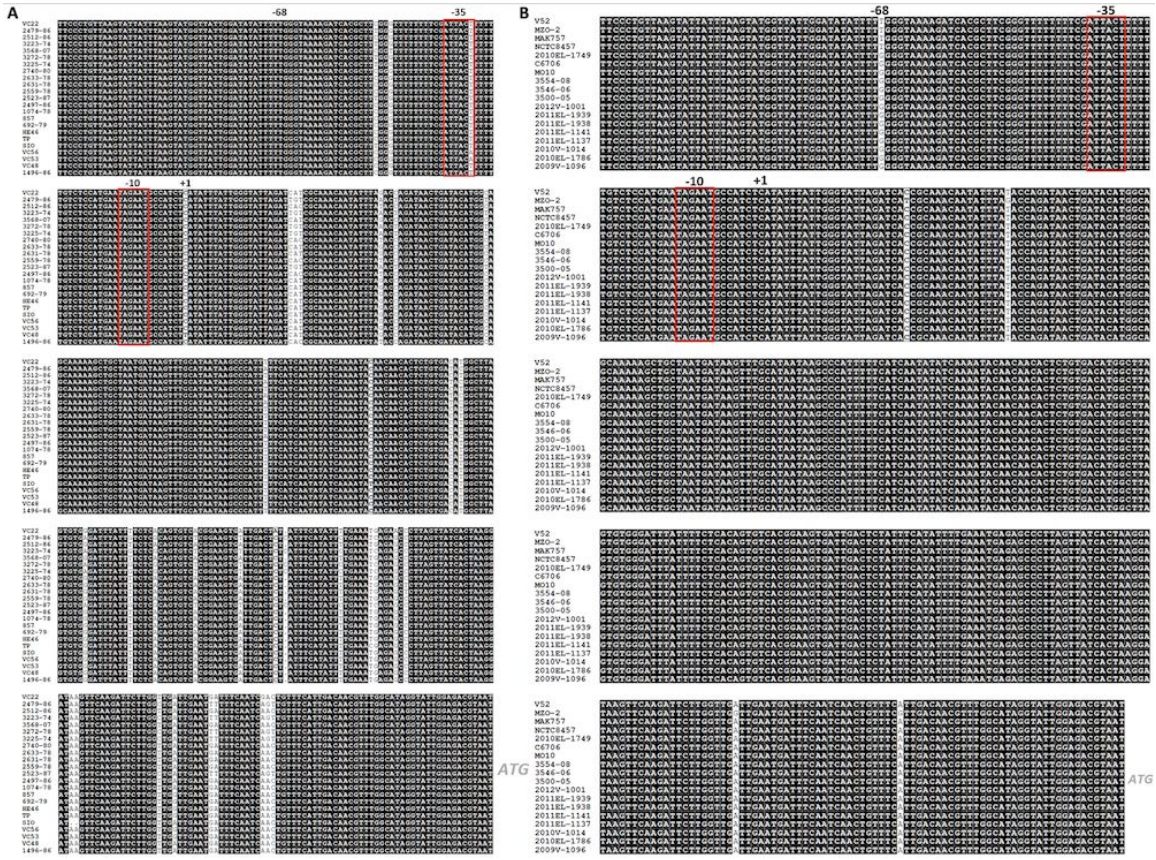

Figure A.6: **Alignment of T6 IGR of environmental and human-derived isolates.** (A) Sequences of the *V. cholerae* environmental strains described in [59] were collected from NCBI database (Table S4). The T6 5' IGR sequences were aligned using MUSCLE and generated using ESPript. Conserved bases are highlighted in black, the putative promoter is boxed, and the start codon of *vipA* is in gray. (B) Sequences the *V. cholerae* human-derived strains described in [59] were collected from NCBI database (Table S4), except 2012V-1001, 2011EL-1939, 2011EL-1938, and 2011EL-1141 that were generated by Sanger sequencing. The T6 5' IGR sequences were aligned using MUSCLE and generated using ESPript. Conserved bases are highlighted in black, the putative promoter is boxed, and the start codon of *vipA* is in grey.

APPENDIX B

SUPPLEMENTARY INFORMATION FOR CHAPTER 3

Table B.1: **List of strains and plasmids used in Chapter 3**

Strain or plasmid	Description	Source or reference
E. coli strains		
RLG717/BGT134	MG1655 DaraBAD::cat DapaH::tetA	This study
RLG718/BGT135	MG1655 DaraBAD::cat zei-722::Tn10	This study
RLG719/BGT136	MG1655 DaraBAD::cat zei-722::Tn10 yejM427N	This study
RLG720/BGT137	MG1655 DaraBAD::cat zei-722::Tn10 yejM1694	This study
RLG792/BGT151	MG1655 DaraBAD::cat DyjeI::ampR	This study
RLG793/BGT152	MG1655 DaraBAD::cat DyjeI::ampR yjePI724T	This study
RLG795/BGT154	MG1655 DaraBAD::cat DyjeI::ampR zei-722::Tn10	This study
RLG796/BGT155	MG1655 DaraBAD::cat DyjeI::ampR zei-722::Tn10 yjePI724T	This study
RLG797/BGT156	MG1655 DaraBAD::cat DyjeI::ampR zei-722::Tn10 yejM1694	This study
RLG798/BGT157	MG1655 DaraBAD::cat DyjeI::ampR zei-722::Tn10 yejM427N	This study
RLG799/BGT158	MG1655 DaraBAD::cat DyjeI::ampR zei-722::Tn10 yjePI724T yejM1694	This study
RLG800/BGT159	MG1655 DaraBAD::cat DyjeI::ampR zei-722::Tn10 yjePI724T yejM427N	This study
RLG803/BGT166	MG1655 DaraBAD::cat DyjeP::tetA	This study
RLG845/BGT165	MG1655 DaraBAD::cat DapaH::tetA attTn7::apaH-W	This study
RLG860/BGT168	MG1655 DaraBAD::cat DyjeP::tetA attTn7::yjeP-W	This study
RLG861/BGT169	MG1655 DaraBAD::cat DyjeI::ampR attTn7::yjeP-W	This study
RLG862/BGT170	MG1655 DaraBAD::cat DyjeI::ampR yjePI724T attTn7::yjeP-W	This study
RLG910/BGT171	MG1655 DaraBAD::cat DrlmE::tetA	This study
RLG1040/BGT177	MG1655 DaraBAD::cat purE79::Tn10 ybdG1671T	This study
RLG1039/BGT176	MG1655 DaraBAD::cat purE79::Tn10	This study
RLG1038/BGT175	MG1655 DaraBAD::cat DybdG::tetA	This study
DY378	W3110 λcI857 D(cro-bioA)	"Thomason et al., 2007"
CAG12098	MG1655 zei-722::Tn10	"Singer et al., 1989; Nicols et al., 1998"
CAG12171	MG1655 purE79::Tn10	"Singer et al., 1989; Nicols et al., 1998"
JW0048	BW25113 DapaH::kan	"Baba et al., 2006"
JW4120	BW25113 DyjeP::kan	"Baba et al., 2006"
JW0566	BW2513 DybdG::kan	"Baba et al., 2006"
PB501	MG1655 DaraBAD::cat	"De Lay et al., 2007"
SSW12	MG1655 DaraBAD::cat Dcrp::kanR	This study
KM1	MG1655 DaraBAD::cat carrying pEVS143	This study
C1	Clonal isolate from control population #1 – Evolved KM1 in experimental evolution without T6 killing	This study
C2	Clonal isolate from control population #2 – Evolved KM1 in experimental evolution without T6 killing	This study
C3	Clonal isolate from control population #3 – Evolved KM1 in experimental evolution without T6 killing	This study
C4	Clonal isolate from control population #4 – Evolved KM1 in experimental evolution without T6 killing	This study
E1	Clonal isolate from experimental population #1 – Evolved KM1 in experimental evolution with T6 killing	This study
E2	Clonal isolate from experimental population #2 – Evolved KM1 in experimental evolution with T6 killing	This study
E3	Clonal isolate from experimental population #3 – Evolved KM1 in experimental evolution with T6 killing	This study
E4	Clonal isolate from experimental population #4 – Evolved KM1 in experimental evolution with T6 killing	This study
E5	Clonal isolate from experimental population #5 – Evolved KM1 in experimental evolution with T6 killing	This study
E6	Clonal isolate from experimental population #6 – Evolved KM1 in experimental evolution with T6 killing	This study
E7	Clonal isolate from experimental population #7 – Evolved KM1 in experimental evolution with T6 killing	This study
E8	Clonal isolate from experimental population #8 – Evolved KM1 in experimental evolution with T6 killing	This study
V. cholerae strains		
JT101	C6706 Ptac-qstR	"Thomas et al., 2017"
JT932	C6706 Ptac-qstR ΔvasK	"Thomas et al., 2017"
BGT41/VC22	Environmental isolate – WT	"Bernardy et al., 2016"
Plasmids		
pUC19	Cloning vector carrying ampR; ampR	"Norrander et al., 1983"
pCRISPR	Empty crRNA expression vector; kanR	"Jiang et al., 2013"
pCRISPR-ybdG493	ybdG targeting crRNA expression vector; kanR	This study
pCas9	Vector carrying Cas9, the tracrRNA, and crRNA guide; camR	"Jiang et al., 2013"
pZS21	Empty expression vector containing the PLtetO-1 promoter; kanR	"Lutz et al., 1997"
pZS21-apaH	Vector expressing apaH from the J23119 promoter kanR	This study
pZS21-yjeP	Vector expressing yjeP from the J23119 promoter; kanR	This study
pGRG25-ModularBamA-Kan	Temperature sensitive plasmid that expresses IrnABCD from an arabinose inducible promoter and contains bamA and a kanamycin resistance cassette flanked by transposase recognition sites.	"Hart et al., 2019"
pHP45W	Vector carrying the W streptomycin/spectinomycin resistance cassette.	"Prentki et al., 1984"
pGRG25-apaH-W	Derivative of pGRG25-ModularBamA-Kan in which DNA driving expression of apaH from the J23119 promoter followed by the rrnB1 transcription terminator and the W streptomycin/spectinomycin resistance cassette is flanked by transposase recognition sites.	This study
pGRG25-yjeP-W	Derivative of pGRG25-ModularBamA-Kan in which DNA driving expression of yjeP from the J23119 promoter followed by the rrnB1 transcription terminator and the W streptomycin/spectinomycin resistance cassette is flanked by transposase recognition sites.	This study
pEVS143	Vector carrying the kanamycin resistance cassette.	"Dunn et al., 2006"

Table B.2: **List of primers used in Chapter 3**

Name	DNA sequence (5'-3')	Description
apaH.Fwd	GAGTACCAGTACACCAGCGG	130bp upstream of apaH start codon.
apaH.Rev	TAACGTGGGTGAAGTCGGTG	323bp downstream of apaH stop codon.
apaHHindIII.Rev	TTTTAAGCTTCCTTCCTATATCAGGCTGTG	Clone apaH into pZS21
apaHXhoI.Fwd	TTTTCTCGAGTTGACAGCTAGCTCAGTCCTAGGTATAATACTAGTGAATTCATTAAAGAAAGGTACCCTCATTCATTAAAAGAATATGGCG	Clone apaH into pZS21
KOyjeJBla.Fwd	AAATTAAAATTAATTATTTAATTGAGAAATGGTTAGGGAGAACCTACATGCATTCAAATATGTATCCGCTC	yjeJ deletion primer
KOyjeJBla.Rev	GCTCCAGCCTCGCATTAGCAAAGATGAGATTATTTCGCCTGTGGTGCAGTAGAGTTGGTAGCTCTTGATC	yjeJ deletion primer
mscM.Fwd	CTGTTTGCACCGGGTAAAGT	196bp upstream of yjeP start codon.
mscM.Rev	TGGCTATTTTCGGCTACTGG	67bp downstream of yjeP stop codon
mscMHindIII.Rev	TTTTAAGCTTATCAGTTTTGTTTGTGAGCCG	Clone yjeP into pZS21
mscMInt.Fwd	GCTGCTGTGGGTAGTGATGA	yjeP internal sequencing primer
mscMInt.Rev	GGAATGGATTTCTGACCACAGC	yjeP internal sequencing primer
mscMXhoI.Fwd	TTTTCTCGAGTTGACAGCTAGCTCAGTCCTAGGTATAATACTAGTGAATTCATTAAAGAAAGGTACCCCATCAAAGGAAACGCTGAC	Clone yjeP into pZS21
pGRG25GA.Fwd	CTAGTAAGCCACGTTTTAATTAAGAAACCATTATTATCATGAC	Clone promoter, gene, and transcription terminator of pZS21 into pGRG25-modularBamA-kan
pGRG25GA.Rev	ATAGGAACTTCAAAAGGGCCCGGCGGATTTGTCCTACTCAG	Clone promoter, gene, and transcription terminator of pZS21 into pGRG25-modularBamA-kan
pGRG25SpcGA.Fwd	GGGCCCTTTTGAAGTTCCTATCACCGTGGAAACGGATGAAGG	Clone W streptomycin/spectinomycin resistance cassette into pGRG25-modularBamA-kan
pGRG25SpcGA.Rev	CTCCTAGGTGCTCGAGTGGCAGGGCTTATTATGCACGCTTAA	Clone W streptomycin/spectinomycin resistance cassette into pGRG25-modularBamA-kan
pKD13TetA.Fwd	AGAGCGCTTTTGAAGCTCACGCTGCCGCAAGCACTCAGGGCGCAAGGGCTTTCCTAATTTTTGTTGACACTCTA	Replace kanamycin resistance cassette with tetA
pKD13TetA.Rev	GAATAGGAACTTCAAGATCCCCTTATTAGAAGAACTCGTCAAGAAGGCGACAAGAGGGTCATTATATTTCG	Replace kanamycin resistance cassette with tetA
rlmE.Fwd	CAGAACAACTGGCTTGAGCG	174bp upstream of rlmE start codon
rlmE.Rev	ACATCAGCACAACGGCAATG	128bp downstream of rlmE stop codon.
rrnJTET.Fwd	AAATTTACGCAATTGGTTACGATGAGTTATCCCCATGGGAAAGTTAAATGTCCTAATTTTTGTTGACACTCTA	rlmE deletion primer
rrnJTET.Rev	CTTTCAAACTTTCGTCTGAAATCTCCCGGTTAGGGTTTACGCCCGGTCGCCAAGAGGGTCATTATATTTCG	rlmE deletion primer
ybdG.Fwd	CTCGTCTGCCGCAAAACATC	125bp upstream of ybdG start codon
ybdG.Rev	AATCAACTATCTGCTGCCGC	367cp downstreak of ybdG stop codon
ybdG493.CRISPR	FORWARD: AAACCATTGCACCAAGACCGCTGATCAGAATCGCG	ybdG duplexed DNA to clone into pCRISPR. Contains 5' and 3' overhangs corresponding to BsaI cut sites in pCRISPR.
	REVERSE: AAAACGCGATTCTGATCAGCGGTCTTGGTGCAATG	
ybdGI167T.MAGE	T*A*CCAACATCAGCACGGCAGCCATTGCACCAAGACCGCTGATCAGGGTCGCTGGCGACTGACCAATCAGCAGCGAGATCATCAAAATG*C*C	Repair oligonucleotide for creating the ybdGI167T mutation. * indicates location of phosphorothioate bonds.
yejM.Fwd	AACATAAGGCTCCGACCGAC	154bp upstream of yejM start codon
yejM.Rev	CGGCACGAGAGGATTTGAAC	127bp downstream of yejM stop codon
yjeJ.Fwd	GGCAAGAGCAACAAACGCAA	246bp upstream of yjeJ start codon
yjeJ.Rev	GCCCGAACTGATGTGATCCA	193bp downstream of yjeJ stop codon
GT1201	CGCATGCTAGCTATAGTTCTAGATCACCAGCCACTTCTGCC	Constructing pJT88 - Primer overlapping pKAS-Amp and C6706 500bp upstream of qstR
GT1202	CCAGAACCGTTATGATGTCGGATGAATTACAGACTCAGTTAATATG	Constructing pJT88 - Primer overlapping Ptac and C6706 500bp upstream of qstR
GT1203	CATATTAACTGAGTCTGTAATTCATCCGACATCATAACGGTTCTGG	Constructing pJT88 - Primer overlapping C6706 500bp upstream of qstR and Ptac
GT1204	GCATAGTTGGCTCGTTGCATTTTAGCTTCCTTAGCTCCTGAA	Constructing pJT88 - Primer overlapping C6706 500bp downstream of qstR and Ptac
GT1205	TTCAGGAGCTAAGGAAGCTAAAATGCAACGAGCCCAACTATGC	Constructing pJT88 - Primer overlapping Ptac and C6706 500bp downstream of qstR
GT1206	TTAACGGCTGACATGGGAATTCTGTAAACAGCGCAGGATCTG	Constructing pJT88 - Primer overlapping pKAS-Amp and C6706 500bp downstream of qstR
GT1207	CGCCATATTAAGTGCATTATTTC	Ptac-qstR check (for C6706)
GT1208	GCATTGTTACTACATTTTTCTCC	Ptac-qstR check (for C6706)
GT1863	CGCATGCTAGCTATAGTTCTAGAGGATGAGTTACACCATTGCC	Constructing pJT634 - Primer overlapping pKAS-Amp and C6706 500bp upstream of vasK
GT1864	AAAACTCGCTCTGGCAACCTAGAATTGTGTCCTTGTTTACTCTG	Constructing pJT634 - Primer overlapping C6706 500bp downstream and 500bp upstream of vasK
GT1865	CAGAGTAAACAAGGACACAATTCTAGGTTGCCAGAGCGAGTTTT	Constructing pJT634 - Primer overlapping C6706 500bp upstream and 500bp upstream of vasK
GT1866	TTAACGGCTGACATGGGAATTCCAGCTGATGTAACCGCTCG	Constructing pJT634 - Primer overlapping pKAS-Amp and C6706 500bp downstream of vasK
GT1867	CCGAGTTTAGTGGAACAAATTC	vasK deletion check
GT1868	CAACTTCGTCCTAAAAAGCCAG	vasK deletion check
GT1863	CGCATGCTAGCTATAGTTCTAGAGGATGAGTTACACCATTGCC	Constructing pJT634 - Primer overlapping pKAS-Amp and C6706 500bp upstream of vasK

Predicted mutations

position	mutation	C1-ref	C2-ref	C3-ref	C4_ref	E1-ref	E2-ref	E3-ref	E4-ref	E5-ref	E6-ref	E7-ref	E8-ref	anc-ref	annotation	gene	description
50,476	C→T												100%		W249* (TGG→TGA)	*apaH* ←	diadenosine tetraphosphatase
50,609	Δ13 bp						100%								coding (602-614/843 nt)	*apaH* ←	diadenosine tetraphosphatase
50,864	Δ1 bp								100%						coding (359/843 nt)	*apaH* ←	diadenosine tetraphosphatase
51,095	Δ4 bp											100%			coding (125-128/843 nt)	*apaH* ←	diadenosine tetraphosphatase
51,102	Δ1 bp					100%									coding (121/843 nt)	*apaH* ←	diadenosine tetraphosphatase
51,114	C→T										100%				D37N (GAT→AAT)	*apaH* ←	diadenosine tetraphosphatase
134,935	IS*1* (–) +9 bp					100%									coding (640-648/795 nt)	*speD* ←	S-adenosylmethionine decarboxylase proenzyme
257,908	Δ776 bp	100%	100%	100%	100%	100%	100%	100%	100%	100%	100%	100%	100%	100%		*insB9–[crl]*	*insB9*, *insA9*, *[crl]*
366,351	2 bp→TT	100%	100%				100%						100%		intergenic (-46/+76)	*lacZ* ← / ← *lacI*	beta-galactosidase/DNA-binding transcriptional repressor LacI
367,573	G→A	100%	100%	100%	100%	100%	100%	100%	100%	100%	100%	100%	100%	100%	intergenic (-63/+14)	*lacI* ← / ← *mhpR*	DNA-binding transcriptional repressor LacI/DNA-binding transcriptional activator MhpR

position	mutation	C1-ref	C2-ref	C3-ref	C4_ref	E1-ref	E2-ref	E3-ref	E4-ref	E5-ref	E6-ref	E7-ref	E8-ref	anc-ref	annotation	gene	description
967,549	G→T					100%									R310L (CGC→CTC)	*msbA* →	ATP-binding lipopolysaccharide transport protein
1,074,056	G→T				100%										intergenic (-45/-186)	*rutA* ← / → *rutR*	pyrimidine oxygenase/DNA-binding transcriptional dual regulator RutR
1,212,337	A→G		100%												intergenic (-33/+203)	*ymgK* ← / ← *ymgL*	protein YmgK/protein YmgL
1,261,524	A→C										100%				S118A (TCC→GCC)	*prs* ←	ribose-phosphate diphosphokinase
1,267,961	T→A										100%				D214E (GAT→GAA)	*ychA* →	transglutaminase-like/TPR repeat-containing protein
1,299,499	Δ1,199 bp	?	?	?	?	?	?	100%	?	?	?	100%	?	?		*insH21*	insH21
1,637,786	IS*1* (+) +9 bp		100%												intergenic (-4/+160)	*gnsB* ← / ← *ynfN*	Qin prophage; protein GnsB/Qin prophage; protein YnfN
1,705,932	G→A								100%						A56T (GCC→ACC)	*rsxA* →	SoxR [2Fe-2S] reducing system protein RsxA
1,978,503	Δ776 bp	100%	100%	100%	100%	100%	100%	100%	100%	100%	100%	100%	100%	100%		*insB-5–insA-5*	*insB-5*, *insA-5*
2,173,363	Δ2 bp	100%	100%	100%	100%	100%	100%	100%	100%	100%	100%	100%	100%	100%	pseudogene (915-916/1358 nt)	*gatC* ←	galactitol-specific PTS enzyme IIC component

position	mutation	C1-ref	C2-ref	C3-ref	C4_ref	E1-ref	E2-ref	E3-ref	E4-ref	E5-ref	E6-ref	E7-ref	E8-ref	anc-ref	annotation	gene	description
2,285,655	T→A									100%					I427N (ATC→AAC)	*yejM* →	putative cardiolipin transport protein
2,286,069	$(GTGAAAGA)_{2\to3}$							100%							coding (1694/1761 nt)	*yejM* →	putative cardiolipin transport protein
2,521,007	Δ120 bp		100%	100%	100%	100%	100%	100%	100%			100%	100%			*[valX]*	*[valX]*
2,561,053	C→T										100%				intergenic (+155/-315)	*yffL* → / → *yffM*	CPZ-55 prophage; uncharacterized protein YffL/CPZ-55 prophage; uncharacterized protein YffM
2,912,166	A→G		100%												F496L (TTC→CTC)	*relA* ←	GDP/GTP pyrophosphokinase
3,560,455	+G	100%	100%	100%	100%	100%	100%	100%	100%	100%	100%	100%	100%	100%	pseudogene (151/758 nt)	*glpR* ←	DNA-binding transcriptional repressor GlpR
3,913,505	A→T												100%		L55Q (CTG→CAG)	*glmS* ←	L-glutamine--D-fructose-6-phosphate aminotransferase
4,051,187	IS*2* (+) +5 bp											100%			noncoding (152-156/245 nt)	*csrC* →	small regulatory RNA CsrC
4,213,066	C→A											100%			noncoding (27/120 nt)	*rrfE* →	5S ribosomal RNA
4,296,381	+GC	100%	100%	100%	100%	100%	100%	100%	100%	100%	100%	100%	100%	100%	intergenic (+587/+55)	*gltP* → / ← *yjcO*	glutamate/aspartate : H(+) symporter GltP/Sel1 repeat-containing protein YjcO

position	mutation	C1-ref	C2-ref	C3-ref	C4_ref	E1-ref	E2-ref	E3-ref	E4-ref	E5-ref	E6-ref	E7-ref	E8-ref	anc-ref	annotation	gene	description
4,353,486	IS*2* (+) +5 bp						100%								coding (1228-1232/1518 nt)	*lysU* ←	lysine--tRNA ligase/Ap4A synthetase/Ap3A synthetase
4,353,655	IS*5* (+) +4 bp											100%			coding (1060-1063/1518 nt)	*lysU* ←	lysine--tRNA ligase/Ap4A synthetase/Ap3A synthetase
4,358,274	IS*5* (+) +4 bp	100%													coding (341-344/2148 nt)	*cadA* ←	lysine decarboxylase 1
4,387,200	A→G							100%		100%					I724T (ATC→ACC)	*mscM* ←	miniconductance mechanosensitive channel MscM
4,388,769	T→A										100%				Q201L (CAG→CTG)	*mscM* ←	miniconductance mechanosensitive channel MscM

Figure B.1: Breseq result summary. Genome sequences were compared against *E. coli* MG1655 reference genome (accession U00096) using Breseq. "100%" indicates there are significant differences at the specific position between the compared genomes. "?" indicates where the coverage at the specific position was too low to call that a mutation. Description shows the annotated function or feature of the genes based on the reference genome.

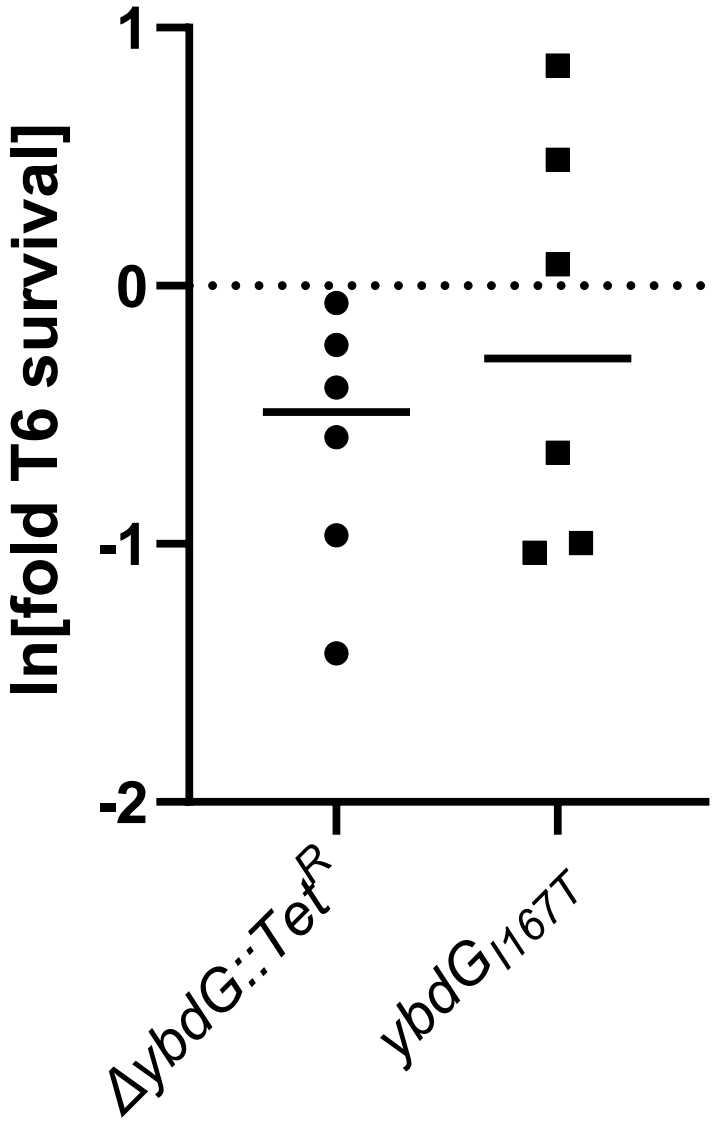

Figure B.2: Gain of Function Mutation in YjeP homolog YbdG does not affect T6 survival in *E. coli*. Data shows no significant difference in T6 survival when comparing the *ybdG* mutants to the WT *E. coli*. Linked markers used to construct the mutants are not indicated in the figure.

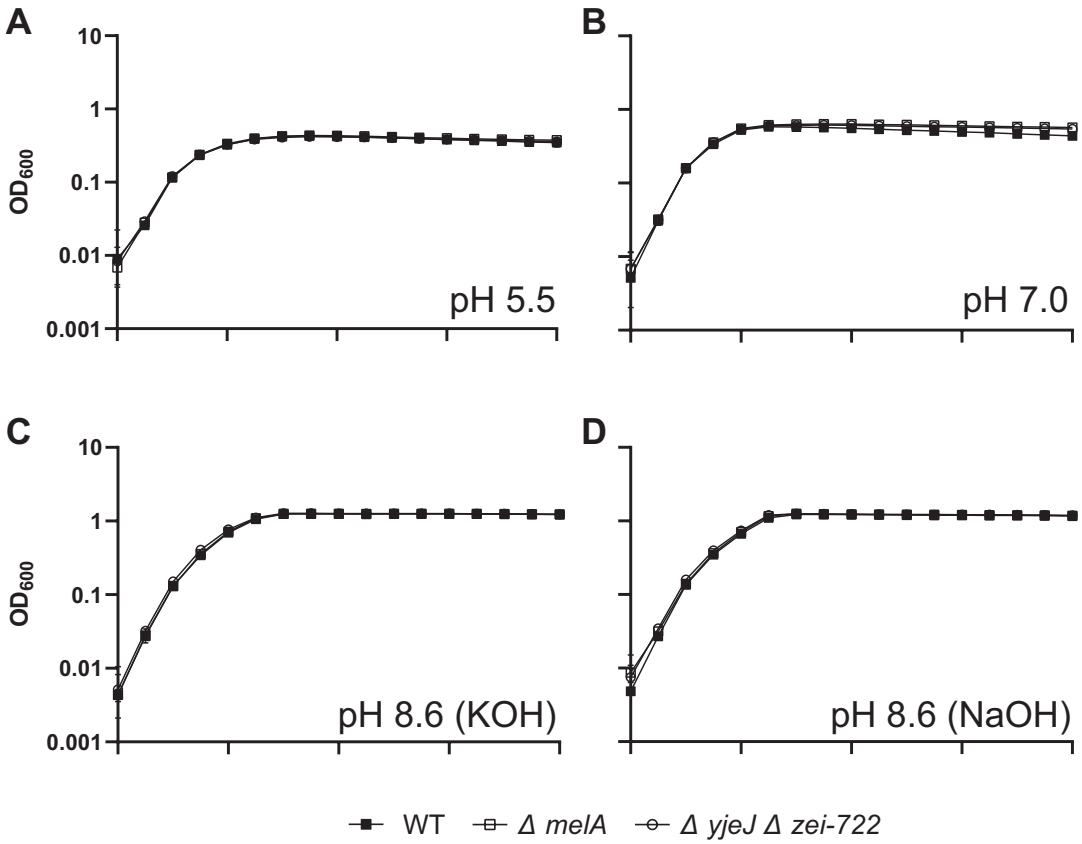

Figure B.3: Linked markers used to introduce mutations in *E. coli* do not affect the growth in tested conditions. Linkers introduced into *E. coli* did not have significant growth differences in the tested pH concentrations.

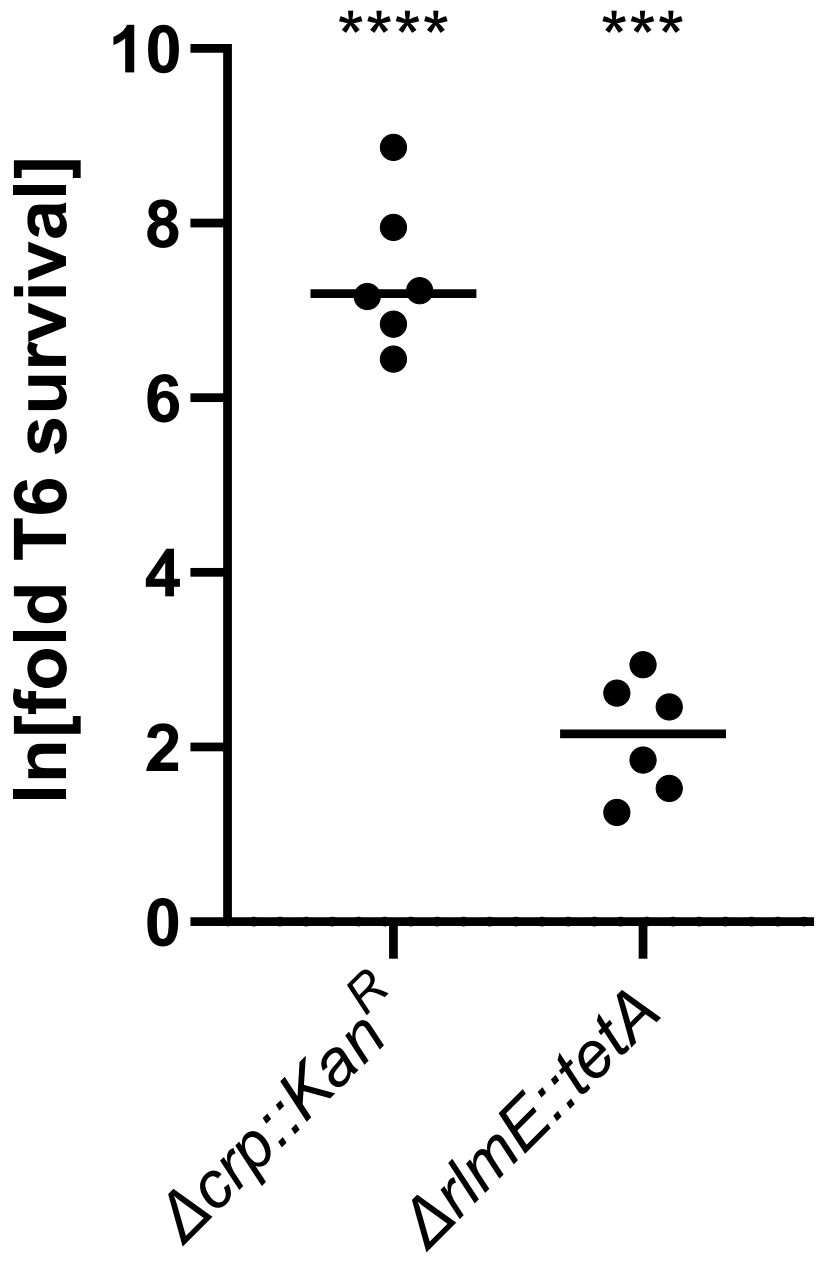

Figure B.4: T6 survival of slow growing *E. coli*. A *crp* null mutant survives T6 attack over 2,000-fold better than the ancestor, while an *rmlE* mutant only survives 10-fold better.

REFERENCES

[1] C. De Duve, "The beginnings of life on earth," *American Scientist*, vol. 83, no. 5, pp. 428–437, 1995.

[2] T. Mattila-Sandholm and G. Wirtanen, "Biofilm formation in the industry: A review," *Food reviews international*, vol. 8, no. 4, pp. 573–603, 1992.

[3] D. Lindsay and A. Von Holy, "Bacterial biofilms within the clinical setting: What healthcare professionals should know," *Journal of Hospital Infection*, vol. 64, no. 4, pp. 313–325, 2006.

[4] L. Hall-Stoodley, J. W. Costerton, and P. Stoodley, "Bacterial biofilms: From the natural environment to infectious diseases," *Nature reviews microbiology*, vol. 2, no. 2, pp. 95–108, 2004.

[5] M. B. Miller, B. L. Bassler, *et al.*, "Quorum sensing in bacteria," *Annual review of microbiology*, vol. 55, no. 1, pp. 165–199, 2001.

[6] J. Antunes, P. Leão, and V. Vasconcelos, "Marine biofilms: Diversity of communities and of chemical cues," *Environmental microbiology reports*, vol. 11, no. 3, pp. 287–305, 2019.

[7] C. Pruzzo, L. Vezzulli, and R. R. Colwell, "Global impact of vibrio cholerae interactions with chitin," *Environmental microbiology*, vol. 10, no. 6, pp. 1400–1410, 2008.

[8] G. Reguera and R. Kolter, "Virulence and the environment: A novel role for vibrio cholerae toxin-coregulated pili in biofilm formation on chitin," *Journal of bacteriology*, vol. 187, no. 10, pp. 3551–3555, 2005.

[9] J. D. Palmer and K. R. Foster, "Bacterial species rarely work together," *Science*, vol. 376, no. 6593, pp. 581–582, 2022.

[10] S. B. Peterson, S. K. Bertolli, and J. D. Mougous, "The central role of interbacterial antagonism in bacterial life," *Current Biology*, vol. 30, no. 19, R1203–R1214, 2020.

[11] S. Hall *et al.*, "Cellular effects of pyocyanin, a secreted virulence factor of pseudomonas aeruginosa," *Toxins*, vol. 8, no. 8, p. 236, 2016.

[12] M. Michalska and P. Wolf, "Pseudomonas exotoxin a: Optimized by evolution for effective killing," *Frontiers in microbiology*, vol. 6, p. 963, 2015.

[13] S. D. Rabin and A. R. Hauser, "Pseudomonas aeruginosa exou, a toxin transported by the type iii secretion system, kills saccharomyces cerevisiae," *Infection and immunity*, vol. 71, no. 7, pp. 4144–4150, 2003.

[14] R. E. de Lima Procópio, I. R. da Silva, M. K. Martins, J. L. de Azevedo, and J. M. de Araújo, "Antibiotics produced by streptomyces," *The Brazilian Journal of infectious diseases*, vol. 16, no. 5, pp. 466–471, 2012.

[15] A. Hasani, A. Kariminik, and K. Issazadeh, "Streptomycetes: Characteristics and their antimicrobial activities," 2014.

[16] S. Pukatzki *et al.*, "Identification of a conserved bacterial protein secretion system in vibrio cholerae using the dictyostelium host model system," *Proceedings of the National Academy of Sciences*, vol. 103, no. 5, pp. 1528–1533, 2006.

[17] M. Halpern and I. Izhaki, "Fish as hosts of vibrio cholerae," *Frontiers in microbiology*, vol. 8, p. 282, 2017.

[18] Y. Senderovich, I. Izhaki, and M. Halpern, "Fish as reservoirs and vectors of vibrio cholerae," *PloS one*, vol. 5, no. 1, e8607, 2010.

[19] R. M. Twedt *et al.*, "Characterization of vibrio cholerae isolated from oysters," *Applied and environmental microbiology*, vol. 41, no. 6, pp. 1475–1478, 1981.

[20] L. Vezzulli, C. Pruzzo, A. Huq, and R. R. Colwell, "Environmental reservoirs of vibrio cholerae and their role in cholera," *Environmental microbiology reports*, vol. 2, no. 1, pp. 27–33, 2010.

[21] S. Almagro-Moreno and R. K. Taylor, "Cholera: Environmental reservoirs and impact on disease transmission," *Microbiology spectrum*, vol. 1, no. 2, pp. 1–2, 2013.

[22] J. Reidl and K. E. Klose, "Vibrio cholerae and cholera: Out of the water and into the host," *FEMS microbiology reviews*, vol. 26, no. 2, pp. 125–139, 2002.

[23] J. K. Teschler *et al.*, "Living in the matrix: Assembly and control of vibrio cholerae biofilms," *Nature Reviews Microbiology*, vol. 13, no. 5, pp. 255–268, 2015.

[24] F. Le Roux and M. Blokesch, "Eco-evolutionary dynamics linked to horizontal gene transfer in vibrios," *Annual review of microbiology*, vol. 72, pp. 89–110, 2018.

[25] A. J. Silva and J. A. Benitez, "Vibrio cholerae biofilms and cholera pathogenesis," *PLoS neglected tropical diseases*, vol. 10, no. 2, e0004330, 2016.

[26] J. Zheng, O. S. Shin, D. E. Cameron, and J. J. Mekalanos, "Quorum sensing and a global regulator tsra control expression of type vi secretion and virulence in vib-

rio cholerae," *Proceedings of the National Academy of Sciences*, vol. 107, no. 49, pp. 21 128–21 133, 2010.

[27] S. T. Miyata, M. Kitaoka, T. M. Brooks, S. B. McAuley, and S. Pukatzki, "Vibrio cholerae requires the type vi secretion system virulence factor vasx to kill dictyostelium discoideum," *Infection and immunity*, vol. 79, no. 7, pp. 2941–2949, 2011.

[28] J. G. Conner, J. K. Teschler, C. J. Jones, and F. H. Yildiz, "Staying alive: Vibrio cholerae's cycle of environmental survival, transmission, and dissemination," *Microbiology spectrum*, vol. 4, no. 2, pp. 4–2, 2016.

[29] E. R. Green and J. Mecsas, "Bacterial secretion systems: An overview," *Microbiology spectrum*, vol. 4, no. 1, pp. 4–1, 2016.

[30] D. L. MacIntyre, S. T. Miyata, M. Kitaoka, and S. Pukatzki, "The vibrio cholerae type vi secretion system displays antimicrobial properties," *Proceedings of the National Academy of Sciences*, vol. 107, no. 45, pp. 19 520–19 524, 2010.

[31] T. G. Dong, B. T. Ho, D. R. Yoder-Himes, and J. J. Mekalanos, "Identification of t6ss-dependent effector and immunity proteins by tn-seq in vibrio cholerae," *Proceedings of the National Academy of Sciences*, vol. 110, no. 7, pp. 2623–2628, 2013.

[32] Y. Fu, M. K. Waldor, and J. J. Mekalanos, "Tn-seq analysis of vibrio cholerae intestinal colonization reveals a role for t6ss-mediated antibacterial activity in the host," *Cell host & microbe*, vol. 14, no. 6, pp. 652–663, 2013.

[33] á. Basler, á. Pilhofer, G. Henderson, G. Jensen, and J. Mekalanos, "Type vi secretion requires a dynamic contractile phage tail-like structure," *Nature*, vol. 483, no. 7388, pp. 182–186, 2012.

[34] M. Basler, B. Ho, and J. Mekalanos, "Tit-for-tat: Type vi secretion system counterattack during bacterial cell-cell interactions," *Cell*, vol. 152, no. 4, pp. 884–894, 2013.

[35] á. Basler and J. Mekalanos, "Type 6 secretion dynamics within and between bacterial cells," *Science*, vol. 337, no. 6096, pp. 815–815, 2012.

[36] L. E. Bingle, C. M. Bailey, and M. J. Pallen, "Type vi secretion: A beginner's guide," *Current opinion in microbiology*, vol. 11, no. 1, pp. 3–8, 2008.

[37] F. Boyer, G. Fichant, J. Berthod, Y. Vandenbrouck, and I. Attree, "Dissecting the bacterial type vi secretion system by a genome wide in silico analysis: What can

be learned from available microbial genomic resources?" *BMC genomics*, vol. 10, no. 1, pp. 1–14, 2009.

[38] D. DeShazer, "A novel contact-independent t6ss that maintains redox homeostasis via zn2+ and mn2+ acquisition is conserved in the burkholderia pseudomallei complex," *Microbiological research*, vol. 226, pp. 48–54, 2019.

[39] M. Si *et al.*, "Manganese scavenging and oxidative stress response mediated by type vi secretion system in burkholderia thailandensis," *Proceedings of the National Academy of Sciences*, vol. 114, no. 11, E2233–E2242, 2017.

[40] C. C. Saak and K. A. Gibbs, "The self-identity protein idsd is communicated between cells in swarming proteus mirabilis colonies," *Journal of bacteriology*, vol. 198, no. 24, pp. 3278–3286, 2016.

[41] C. V. Crisan and B. K. Hammer, "The vibrio cholerae type vi secretion system: Toxins, regulators and consequences," *Environmental Microbiology*, vol. 22, no. 10, pp. 4112–4122, 2020.

[42] L. Chen, Y. Zou, P. She, and Y. Wu, "Composition, function, and regulation of t6ss in pseudomonas aeruginosa," *Microbiological research*, vol. 172, pp. 19–25, 2015.

[43] J. Wang *et al.*, "Cryo-em structure of the extended type vi secretion system sheath–tube complex," *Nature microbiology*, vol. 2, no. 11, pp. 1507–1512, 2017.

[44] M. S. Stietz, X. Liang, H. Li, X. Zhang, and T. G. Dong, "Tssa–tssm–taga interaction modulates type vi secretion system sheath-tube assembly in vibrio cholerae," *Nature communications*, vol. 11, no. 1, pp. 1–11, 2020.

[45] Y. G. Santin, T. Doan, R. Lebrun, L. Espinosa, L. Journet, and E. Cascales, "In vivo tssa proximity labelling during type vi secretion biogenesis reveals taga as a protein that stops and holds the sheath," *Nature microbiology*, vol. 3, no. 11, pp. 1304–1313, 2018.

[46] S. Kube, N. Kapitein, T. Zimniak, F. Herzog, A. Mogk, and P. Wendler, "Structure of the vipa/b type vi secretion complex suggests a contraction-state-specific recycling mechanism," *Cell reports*, vol. 8, no. 1, pp. 20–30, 2014.

[47] N. Kapitein *et al.*, "Clpv recycles vipa/vipb tubules and prevents non-productive tubule formation to ensure efficient type vi protein secretion," *Molecular microbiology*, vol. 87, no. 5, pp. 1013–1028, 2013.

[48] A. Vettiger and M. Basler, "Type vi secretion system substrates are transferred and reused among sister cells," *Cell*, vol. 167, no. 1, pp. 99–110, 2016.

[49] P. G. Leiman *et al.*, "Type vi secretion apparatus and phage tail-associated protein complexes share a common evolutionary origin," *Proceedings of the National Academy of Sciences*, vol. 106, no. 11, pp. 4154–4159, 2009.

[50] A. Joshi, B. Kostiuk, A. Rogers, J. Teschler, S. Pukatzki, and F. H. Yildiz, "Rules of engagement: The type vi secretion system in vibrio cholerae," *Trends in microbiology*, vol. 25, no. 4, pp. 267–279, 2017.

[51] C. V. Crisan *et al.*, "Analysis of vibrio cholerae genomes identifies new type vi secretion system gene clusters," *Genome biology*, vol. 20, no. 1, pp. 1–14, 2019.

[52] M. Kitaoka, S. T. Miyata, T. M. Brooks, D. Unterweger, and S. Pukatzki, "Vash is a transcriptional regulator of the type vi secretion system functional in endemic and pandemic vibrio cholerae," *Journal of bacteriology*, vol. 193, no. 23, pp. 6471–6482, 2011.

[53] N. C. Drebes Doerr and M. Blokesch, "Interbacterial competition and anti-predatory behaviour of environmental vibrio cholerae strains," *Environmental microbiology*, vol. 22, no. 10, pp. 4485–4504, 2020.

[54] L. Journet and E. Cascales, "The type vi secretion system in escherichia coli and related species," *EcoSal Plus*, vol. 7, no. 1, 2016.

[55] Y. R. Brunet, C. S. Bernard, M. Gavioli, R. Lloubès, and E. Cascales, "An epigenetic switch involving overlapping fur and dna methylation optimizes expression of a type vi secretion gene cluster," *PLoS genetics*, vol. 7, no. 7, e1002205, 2011.

[56] E. G. Dudley, N. R. Thomson, J. Parkhill, N. P. Morin, and J. P. Nataro, "Proteomic and microarray characterization of the aggr regulon identifies a pheu pathogenicity island in enteroaggregative escherichia coli," *Molecular microbiology*, vol. 61, no. 5, pp. 1267–1282, 2006.

[57] á. Lesic, á. Starkey, J. He, R. Hazan, and L. Rahme, "Quorum sensing differentially regulates pseudomonas aeruginosa type vi secretion locus i and homologous loci ii and iii, which are required for pathogenesis," *Microbiology*, vol. 155, no. Pt 9, p. 2845, 2009.

[58] E. E. Smith *et al.*, "Genetic adaptation by pseudomonas aeruginosa to the airways of cystic fibrosis patients," *Proceedings of the National Academy of Sciences*, vol. 103, no. 22, pp. 8487–8492, 2006.

[59] E. E. Bernardy, M. A. Turnsek, S. K. Wilson, C. L. Tarr, and B. K. Hammer, "Diversity of clinical and environmental isolates of vibrio cholerae in natural transformation and contact-dependent bacterial killing indicative of type vi secretion system

activity," *Applied and environmental microbiology*, vol. 82, no. 9, pp. 2833–2842, 2016.

[60] N. A. Hussain, P. C. Kirchberger, R. J. Case, and Y. F. Boucher, "Modular molecular weaponry plays a key role in competition within an environmental vibrio cholerae population," *Frontiers in microbiology*, vol. 12, 2021.

[61] S. L. Ng, S. Kammann, G. Steinbach, T. Hoffmann, P. J. Yunker, and B. K. Hammer, "Evolution of a cis-acting snp that controls type vi secretion in vibrio cholerae," *mBio*, e00422–22, 2022.

[62] N. C. Drebes Dörr, A. Proutière, M. Jaskólska, S. Stutzmann, L. Bader, and M. Blokesch, "Single nucleotide polymorphism determines constitutive versus inducible type vi secretion in vibrio cholerae," *The ISME Journal*, pp. 1–5, 2022.

[63] D. Unterweger *et al.*, "Constitutive type vi secretion system expression gives vibrio cholerae intra-and interspecific competitive advantages," *PloS one*, vol. 7, no. 10, e48320, 2012.

[64] K. H. Thelin and R. K. Taylor, "Toxin-coregulated pilus, but not mannose-sensitive hemagglutinin, is required for colonization by vibrio cholerae o1 el tor biotype and o139 strains," *Infection and immunity*, vol. 64, no. 7, pp. 2853–2856, 1996.

[65] M. Jaskólska, S. Stutzmann, C. Stoudmann, and M. Blokesch, "Qstr-dependent regulation of natural competence and type vi secretion in vibrio cholerae," *Nucleic acids research*, vol. 46, no. 20, pp. 10 619–10 634, 2018.

[66] S. S. Watve, J. Thomas, and B. K. Hammer, "Cytr is a global positive regulator of competence, type vi secretion, and chitinases in vibrio cholerae," *PloS one*, vol. 10, no. 9, e0138834, 2015.

[67] L. C. Metzger, S. Stutzmann, T. Scrignari, C. Van der Henst, N. Matthey, and M. Blokesch, "Independent regulation of type vi secretion in vibrio cholerae by tfox and tfoy," *Cell reports*, vol. 15, no. 5, pp. 951–958, 2016.

[68] E. S. Antonova and B. K. Hammer, "Genetics of natural competence in vibrio cholerae and other vibrios," *Microbiology spectrum*, vol. 3, no. 3, pp. 3–3, 2015.

[69] M. N. R. Kumar, "A review of chitin and chitosan applications," *Reactive and functional polymers*, vol. 46, no. 1, pp. 1–27, 2000.

[70] C. P. Souza, B. C. Almeida, R. R. Colwell, and I. N. Rivera, "The importance of chitin in the marine environment," *Marine biotechnology*, vol. 13, no. 5, pp. 823–830, 2011.

[71] K. L. Meibom, M. Blokesch, N. A. Dolganov, C.-Y. Wu, and G. K. Schoolnik, "Chitin induces natural competence in vibrio cholerae," *Science*, vol. 310, no. 5755, pp. 1824–1827, 2005.

[72] A. M. Baty III, C. C. Eastburn, Z. Diwu, S. Techkarnjanaruk, A. E. Goodman, and G. G. Geesey, "Differentiation of chitinase-active and non-chitinase-active subpopulations of a marine bacterium during chitin degradation," *Applied and Environmental Microbiology*, vol. 66, no. 8, pp. 3566–3573, 2000.

[73] A. B. Dalia, D. W. Lazinski, and A. Camilli, "Identification of a membrane-bound transcriptional regulator that links chitin and natural competence in vibrio cholerae," *MBio*, vol. 5, no. 1, e01028–13, 2014.

[74] S. Yamamoto *et al.*, "Regulation of natural competence by the orphan two-component system sensor kinase chis involves a non-canonical transmembrane regulator in v ibrio cholerae," *Molecular microbiology*, vol. 91, no. 2, pp. 326–347, 2014.

[75] S. Yamamoto *et al.*, "Identification of a chitin-induced small rna that regulates translation of the tfox gene, encoding a positive regulator of natural competence in vibrio cholerae," *Journal of bacteriology*, vol. 193, no. 8, pp. 1953–1965, 2011.

[76] R. Wu, M. Zhao, J. Li, H. Gao, B. Kan, and W. Liang, "Direct regulation of the natural competence regulator gene tfox by cyclic amp (camp) and camp receptor protein (crp) in vibrios," *Scientific Reports*, vol. 5, no. 1, pp. 1–15, 2015.

[77] S. S. Watve, "Genetics of type vi secretion and natural transformation in vibrio cholerae," Ph.D. dissertation, Georgia Institute of Technology, 2017.

[78] T. Gumpenberger *et al.*, "Nucleoside uptake in v ibrio cholerae and its role in the transition fitness from host to environment," *Molecular microbiology*, vol. 99, no. 3, pp. 470–483, 2016.

[79] E. S. Antonova, E. E. Bernardy, and B. K. Hammer, "Natural competence in v ibrio cholerae is controlled by a nucleoside scavenging response that requires cytr-dependent anti-activation," *Molecular microbiology*, vol. 86, no. 5, pp. 1215–1231, 2012.

[80] P. Valentin-Hansen, L. Søgaard-Andersen, and H. Pedersen, "A flexible partnership: The cytr anti-activator and the camp–crp activator protein, comrades in transcription control," *Molecular microbiology*, vol. 20, no. 3, pp. 461–466, 1996.

[81] A. J. Haugo and P. I. Watnick, "Vibrio cholerae cytr is a repressor of biofilm development," *Molecular microbiology*, vol. 45, no. 2, pp. 471–483, 2002.

[82] D. A. Higgins, M. E. Pomianek, C. M. Kraml, R. K. Taylor, M. F. Semmelhack, and B. L. Bassler, "The major vibrio cholerae autoinducer and its role in virulence factor production," *Nature*, vol. 450, no. 7171, pp. 883–886, 2007.

[83] J. M. Henke and B. L. Bassler, "Three parallel quorum-sensing systems regulate gene expression in vibrio harveyi," *Journal of bacteriology*, vol. 186, no. 20, pp. 6902–6914, 2004.

[84] K. B. Xavier and B. L. Bassler, "Luxs quorum sensing: More than just a numbers game," *Current opinion in microbiology*, vol. 6, no. 2, pp. 191–197, 2003.

[85] S. A. Jung, L. A. Hawver, and W.-L. Ng, "Parallel quorum sensing signaling pathways in vibrio cholerae," *Current genetics*, vol. 62, no. 2, pp. 255–260, 2016.

[86] M. G. Jobling and R. K. Holmes, "Characterization of hapr, a positive regulator of the vibrio cholerae ha/protease gene hap, and its identification as a functional homologue of the vibrio harveyi luxr gene," *Molecular microbiology*, vol. 26, no. 5, pp. 1023–1034, 1997.

[87] J. Zhu, M. B. Miller, R. E. Vance, M. Dziejman, B. L. Bassler, and J. J. Mekalanos, "Quorum-sensing regulators control virulence gene expression in vibrio cholerae," *Proceedings of the National Academy of Sciences*, vol. 99, no. 5, pp. 3129–3134, 2002.

[88] M. Lo Scrudato and M. Blokesch, "A transcriptional regulator linking quorum sensing and chitin induction to render vibrio cholerae naturally transformable," *Nucleic acids research*, vol. 41, no. 6, pp. 3644–3658, 2013.

[89] J. Zhu and J. J. Mekalanos, "Quorum sensing-dependent biofilms enhance colonization in vibrio cholerae," *Developmental cell*, vol. 5, no. 4, pp. 647–656, 2003.

[90] M. Haring, S. Offermann, T. Danker, I. Horst, C. Peterhansel, and M. Stam, "Chromatin immunoprecipitation: Optimization, quantitative analysis and data normalization," *Plant methods*, vol. 3, no. 1, pp. 1–16, 2007.

[91] L. Baranello, F. Kouzine, S. Sanford, and D. Levens, "Chip bias as a function of cross-linking time," *Chromosome Research*, vol. 24, no. 2, pp. 175–181, 2016.

[92] M. Dziejman, E. Balon, D. Boyd, C. M. Fraser, J. F. Heidelberg, and J. J. Mekalanos, "Comparative genomic analysis of vibrio cholerae: Genes that correlate with cholera endemic and pandemic disease," *Proceedings of the National Academy of Sciences*, vol. 99, no. 3, pp. 1556–1561, 2002.

[93] A. Pollack-Berti, M. S. Wollenberg, and E. G. Ruby, "Natural transformation of vibrio fischeri requires tfox and tfoyemi_2250," 2010.

[94] B. R. Pursley, M. M. Maiden, M.-L. Hsieh, N. L. Fernandez, G. B. Severin, and C. M. Waters, "Cyclic di-gmp regulates tfoy in vibrio cholerae to control motility by both transcriptional and posttranscriptional mechanisms," *Journal of bacteriology*, vol. 200, no. 7, e00578–17, 2018.

[95] N. Ausmees *et al.*, "Genetic data indicate that proteins containing the ggdef domain possess diguanylate cyclase activity," *FEMS microbiology letters*, vol. 204, no. 1, pp. 163–167, 2001.

[96] D. A. Ryjenkov, M. Tarutina, O. V. Moskvin, and M. Gomelsky, "Cyclic diguanylate is a ubiquitous signaling molecule in bacteria: Insights into biochemistry of the ggdef protein domain," *Journal of bacteriology*, vol. 187, no. 5, pp. 1792–1798, 2005.

[97] A. J. Schmidt, D. A. Ryjenkov, and M. Gomelsky, "The ubiquitous protein domain eal is a cyclic diguanylate-specific phosphodiesterase: Enzymatically active and inactive eal domains," *Journal of bacteriology*, vol. 187, no. 14, pp. 4774–4781, 2005.

[98] R. P. Ryan *et al.*, "Cell–cell signaling in xanthomonas campestris involves an hd-gyp domain protein that functions in cyclic di-gmp turnover," *Proceedings of the National Academy of Sciences*, vol. 103, no. 17, pp. 6712–6717, 2006.

[99] M. S. Islam, B. S. Drasar, and R. B. Sack, "The aquatic environment as a reservoir of vibrio cholerae: A review," *Journal of diarrhoeal diseases research*, pp. 197–206, 1993.

[100] E. V. Sokurenko, D. L. Hasty, and D. E. Dykhuizen, "Pathoadaptive mutations: Gene loss and variation in bacterial pathogens," *Trends in microbiology*, vol. 7, no. 5, pp. 191–195, 1999.

[101] T. Ishikawa *et al.*, "Pathoadaptive conditional regulation of the type vi secretion system in vibrio cholerae o1 strains," *Infection and immunity*, vol. 80, no. 2, pp. 575–584, 2012.

[102] T. M. Brooks, D. Unterweger, V. Bachmann, B. Kostiuk, and S. Pukatzki, "Lytic activity of the vibrio cholerae type vi secretion toxin vgrg-3 is inhibited by the antitoxin tsab," *Journal of Biological Chemistry*, vol. 288, no. 11, pp. 7618–7625, 2013.

[103] X. Liang, F. Kamal, T.-T. Pei, P. Xu, J. J. Mekalanos, and T. G. Dong, "An onboard checking mechanism ensures effector delivery of the type vi secretion system in vibrio cholerae," *Proceedings of the National Academy of Sciences*, vol. 116, no. 46, pp. 23 292–23 298, 2019.

[104] D. D. Bondage, J.-S. Lin, L.-S. Ma, C.-H. Kuo, and E.-M. Lai, "Vgrg c terminus confers the type vi effector transport specificity and is required for binding with paar and adaptor–effector complex," *Proceedings of the National Academy of Sciences*, vol. 113, no. 27, E3931–E3940, 2016.

[105] D. Unterweger, B. Kostiuk, R. Ötjengerdes, A. Wilton, L. Diaz-Satizabal, and S. Pukatzki, "Chimeric adaptor proteins translocate diverse type vi secretion system effectors in vibrio cholerae," *The EMBO journal*, vol. 34, no. 16, pp. 2198–2210, 2015.

[106] S. T. Miyata, D. Unterweger, S. P. Rudko, and S. Pukatzki, "Dual expression profile of type vi secretion system immunity genes protects pandemic vibrio cholerae," *PLoS pathogens*, vol. 9, no. 12, e1003752, 2013.

[107] X. Liang *et al.*, "Vgrg-dependent effectors and chaperones modulate the assembly of the type vi secretion system," *PLoS pathogens*, vol. 17, no. 12, e1010116, 2021.

[108] E. Altindis, T. Dong, C. Catalano, and J. Mekalanos, "Secretome analysis of vibrio cholerae type vi secretion system reveals a new effector-immunity pair," *MBio*, vol. 6, no. 2, e00075–15, 2015.

[109] E. Durand *et al.*, "Crystal structure of the vgrg1 actin cross-linking domain of the vibrio cholerae type vi secretion system," *Journal of Biological Chemistry*, vol. 287, no. 45, pp. 38 190–38 199, 2012.

[110] A. T. Ma, S. McAuley, S. Pukatzki, and J. J. Mekalanos, "Translocation of a vibrio cholerae type vi secretion effector requires bacterial endocytosis by host cells," *Cell host & microbe*, vol. 5, no. 3, pp. 234–243, 2009.

[111] A. T. Ma and J. J. Mekalanos, "In vivo actin cross-linking induced by vibrio cholerae type vi secretion system is associated with intestinal inflammation," *Proceedings of the National Academy of Sciences*, vol. 107, no. 9, pp. 4365–4370, 2010.

[112] S. L. Logan *et al.*, "The vibrio cholerae type vi secretion system can modulate host intestinal mechanics to displace gut bacterial symbionts," *Proceedings of the National Academy of Sciences*, vol. 115, no. 16, E3779–E3787, 2018.

[113] C. V. Crisan *et al.*, "A new contact killing toxin permeabilizes cells and belongs to a broadly distributed protein family," *Msphere*, vol. 6, no. 4, e00318–21, 2021.

[114] J. Thomas, S. S. Watve, W. C. Ratcliff, and B. K. Hammer, "Horizontal gene transfer of functional type vi killing genes by natural transformation," *MBio*, vol. 8, no. 4, e00654–17, 2017.

[115] P. S. Stewart and J. W. Costerton, "Antibiotic resistance of bacteria in biofilms," *The lancet*, vol. 358, no. 9276, pp. 135–138, 2001.

[116] X. Yang, M. Long, and X. Shen, "Effector–immunity pairs provide the t6ss nanomachine its offensive and defensive capabilities," *Molecules*, vol. 23, no. 5, p. 1009, 2018.

[117] X. Yang *et al.*, "Molecular mechanism for self-protection against the type vi secretion system in vibrio cholerae," *Acta Crystallographica Section D: Biological Crystallography*, vol. 70, no. 4, pp. 1094–1103, 2014.

[118] T. G. Sana, K. A. Lugo, and D. M. Monack, "T6ss: The bacterial" fight club" in the host gut," *PLoS pathogens*, vol. 13, no. 6, e1006325, 2017.

[119] M. J. Coyne and L. E. Comstock, "Type vi secretion systems and the gut microbiota," *Microbiology spectrum*, vol. 7, no. 2, pp. 7–2, 2019.

[120] B. D. Ross *et al.*, "Human gut bacteria contain acquired interbacterial defence systems," *Nature*, vol. 575, no. 7781, pp. 224–228, 2019.

[121] A. G. Wexler *et al.*, "Human symbionts inject and neutralize antibacterial toxins to persist in the gut," *Proceedings of the National Academy of Sciences*, vol. 113, no. 13, pp. 3639–3644, 2016.

[122] P. C. Kirchberger, D. Unterweger, D. Provenzano, S. Pukatzki, and Y. Boucher, "Sequential displacement of type vi secretion system effector genes leads to evolution of diverse immunity gene arrays in vibrio cholerae," *Scientific reports*, vol. 7, no. 1, pp. 1–12, 2017.

[123] V. Stockwell and B. Duffy, "Use of antibiotics in plant agriculture," *Revue Scientifique Et Technique-Office International Des Epizooties*, vol. 31, no. 1, 2012.

[124] M. I. Hutchings, A. W. Truman, and B. Wilkinson, "Antibiotics: Past, present and future," *Current opinion in microbiology*, vol. 51, pp. 72–80, 2019.

[125] C. De la Fuente-Núñez, F. Reffuveille, L. Fernández, and R. E. Hancock, "Bacterial biofilm development as a multicellular adaptation: Antibiotic resistance and new therapeutic strategies," *Current opinion in microbiology*, vol. 16, no. 5, pp. 580–589, 2013.

[126] D. de Beer, P. Stoodley, and Z. Lewandowski, "Measurement of local diffusion coefficients in biofilms by microinjection and confocal microscopy," *Biotechnology and bioengineering*, vol. 53, no. 2, pp. 151–158, 1997.

[127] T.-F. C. Mah and G. A. O'Toole, "Mechanisms of biofilm resistance to antimicrobial agents," *Trends in microbiology*, vol. 9, no. 1, pp. 34–39, 2001.

[128] J. Toska, B. T. Ho, and J. J. Mekalanos, "Exopolysaccharide protects vibrio cholerae from exogenous attacks by the type 6 secretion system," *Proceedings of the National Academy of Sciences*, vol. 115, no. 31, pp. 7997–8002, 2018.

[129] G. Steinbach, C. Crisan, S. L. Ng, B. K. Hammer, and P. J. Yunker, "Accumulation of dead cells from contact killing facilitates coexistence in bacterial biofilms," *Journal of the Royal Society Interface*, vol. 17, no. 173, p. 20 200 486, 2020.

[130] P. Ghosh, J. Mondal, E. Ben-Jacob, and H. Levine, "Mechanically-driven phase separation in a growing bacterial colony," *Proceedings of the National Academy of Sciences*, vol. 112, no. 17, E2166–E2173, 2015.

[131] L. McNally *et al.*, "Killing by type vi secretion drives genetic phase separation and correlates with increased cooperation," *Nature communications*, vol. 8, no. 1, pp. 1–11, 2017.

[132] M. J. Wong *et al.*, "Microbial herd protection mediated by antagonistic interaction in polymicrobial communities," *Applied and environmental microbiology*, vol. 82, no. 23, pp. 6881–6888, 2016.

[133] A. B. Russell, S. B. Peterson, and J. D. Mougous, "Type vi secretion system effectors: Poisons with a purpose," *Nature reviews microbiology*, vol. 12, no. 2, pp. 137–148, 2014.

[134] V. B. Borisov, S. A. Siletsky, M. R. Nastasi, and E. Forte, "Ros defense systems and terminal oxidases in bacteria," *Antioxidants*, vol. 10, no. 6, p. 839, 2021.

[135] E. Cabiscol Català, J. Tamarit Sumalla, and J. Ros Salvador, "Oxidative stress in bacteria and protein damage by reactive oxygen species," *International Microbiology, 2000, vol. 3, núm. 1, p. 3-8*, 2000.

[136] S. M. Chiang and H. E. Schellhorn, "Regulators of oxidative stress response genes in escherichia coli and their functional conservation in bacteria," *Archives of biochemistry and biophysics*, vol. 525, no. 2, pp. 161–169, 2012.

[137] K.-W. Yu, P. Xue, Y. Fu, and L. Yang, "T6ss mediated stress responses for bacterial environmental survival and host adaptation," *International Journal of Molecular Sciences*, vol. 22, no. 2, p. 478, 2021.

[138] S. J. Hersch *et al.*, "Envelope stress responses defend against type six secretion system attacks independently of immunity proteins," *Nature microbiology*, vol. 5, no. 5, pp. 706–714, 2020.

[139] V. Stout, A. Torres-Cabassa, M. Maurizi, D. Gutnick, and S. Gottesman, "Rcsa, an unstable positive regulator of capsular polysaccharide synthesis," *Journal of bacteriology*, vol. 173, no. 5, pp. 1738–1747, 1991.

[140] C. V. Crisan, H. L. Nichols, S. Wiesenfeld, G. Steinbach, P. J. Yunker, and B. K. Hammer, "Glucose confers protection to escherichia coli against contact killing by vibrio cholerae," *Scientific reports*, vol. 11, no. 1, pp. 1–11, 2021.

[141] S. L. Ng, S. Kammann, G. Steinbach, T. Hoffmann, P. J. Yunker, and B. K. Hammer, "Evolution of a *cis*-Acting SNP That Controls Type VI Secretion in Vibrio cholerae," *mBio*, vol. 0, no. 0, e00422–22, 2022. eprint: https://journals.asm.org/doi/pdf/10.1128/mbio.00422-22.

[142] G. A. Wray, "The evolutionary significance of cis-regulatory mutations," *Nature Reviews Genetics*, vol. 8, no. 3, pp. 206–216, 2007.

[143] D. L. Stern and V. Orgogozo, "The loci of evolution: How predictable is genetic evolution?" *Evolution: International Journal of Organic Evolution*, vol. 62, no. 9, pp. 2155–2177, 2008.

[144] P. J. Wittkopp and G. Kalay, "Cis-regulatory elements: Molecular mechanisms and evolutionary processes underlying divergence," *Nature Reviews Genetics*, vol. 13, no. 1, pp. 59–69, 2012.

[145] A. N. Norsworthy and K. L. Visick, "Signaling between two interacting sensor kinases promotes biofilms and colonization by a bacterial symbiont," *Molecular microbiology*, vol. 96, no. 2, pp. 233–248, 2015.

[146] M. J. Mandel, M. S. Wollenberg, E. V. Stabb, K. L. Visick, and E. G. Ruby, "A single regulatory gene is sufficient to alter bacterial host range," *Nature*, vol. 458, no. 7235, pp. 215–218, 2009.

[147] J. C. Perez and E. A. Groisman, "Evolution of transcriptional regulatory circuits in bacteria," *Cell*, vol. 138, no. 2, pp. 233–244, 2009.

[148] S. M. Faruque, M. J. Albert, and J. J. Mekalanos, "Epidemiology, genetics, and ecology of toxigenic vibrio cholerae," *Microbiology and molecular biology reviews*, vol. 62, no. 4, pp. 1301–1314, 1998.

[149] D. K. Karaolis, J. A. Johnson, C. C. Bailey, E. C. Boedeker, J. B. Kaper, and P. R. Reeves, "A vibrio cholerae pathogenicity island associated with epidemic and pandemic strains," *Proceedings of the National Academy of Sciences*, vol. 95, no. 6, pp. 3134–3139, 1998.

[150] R. Gallegos-Monterrosa and S. J. Coulthurst, "The ecological impact of a bacterial weapon: Microbial interactions and the type vi secretion system," *FEMS Microbiology Reviews*, vol. 45, no. 6, fuab033, 2021.

[151] F. J. Santoriello and S. Pukatzki, "When the pandemic opts for the lockdown: Secretion system evolution in the cholera bacterium," *Microbial Cell*, vol. 8, no. 3, p. 69, 2021.

[152] D. Unterweger *et al.*, "The vibrio cholerae type vi secretion system employs diverse effector modules for intraspecific competition," *Nature communications*, vol. 5, no. 1, pp. 1–9, 2014.

[153] B. Kostiuk *et al.*, "Type vi secretion system mutations reduced competitive fitness of classical vibrio cholerae biotype," *Nature communications*, vol. 12, no. 1, pp. 1–11, 2021.

[154] A. Joshi *et al.*, "C-di-gmp inhibits lona-dependent proteolysis of tfoy in vibrio cholerae," *PLoS genetics*, vol. 16, no. 6, e1008897, 2020.

[155] A. M. Tsou, T. Cai, Z. Liu, J. Zhu, and R. V. Kulkarni, "Regulatory targets of quorum sensing in vibrio cholerae: Evidence for two distinct hapr-binding motifs," *Nucleic acids research*, vol. 37, no. 8, pp. 2747–2756, 2009.

[156] J. J. Dunn, F. W. Studier, and M. Gottesman, "Complete nucleotide sequence of bacteriophage t7 dna and the locations of t7 genetic elements," *Journal of molecular biology*, vol. 166, no. 4, pp. 477–535, 1983.

[157] C. A. Schneider, W. S. Rasband, and K. W. Eliceiri, "Nih image to imagej: 25 years of image analysis," *Nature methods*, vol. 9, no. 7, pp. 671–675, 2012.

[158] A. Joelsson, Z. Liu, and J. Zhu, "Genetic and phenotypic diversity of quorum-sensing systems in clinical and environmental isolates of vibrio cholerae," *Infection and immunity*, vol. 74, no. 2, pp. 1141–1147, 2006.

[159] J. Hołówka and J. Zakrzewska-Czerwińska, "Nucleoid associated proteins: The small organizers that help to cope with stress," *Frontiers in Microbiology*, vol. 11, p. 590, 2020.

[160] J. C. Ayala, A. J. Silva, and J. A. Benitez, "H-ns: An overarching regulator of the vibrio cholerae life cycle," *Research in microbiology*, vol. 168, no. 1, pp. 16–25, 2017.

[161] R. R. Chaparian, S. G. Olney, C. M. Hustmyer, D. A. Rowe-Magnus, and J. C. van Kessel, "Integration host factor and luxr synergistically bind dna to coactivate

quorum-sensing genes in vibrio harveyi," *Molecular microbiology*, vol. 101, no. 5, pp. 823–840, 2016.

[162] K. Papenfort, K. U. Förstner, J.-P. Cong, C. M. Sharma, and B. L. Bassler, "Differential rna-seq of vibrio cholerae identifies the vqmr small rna as a regulator of biofilm formation," *Proceedings of the National Academy of Sciences*, vol. 112, no. 7, E766–E775, 2015.

[163] Y. Shao and B. L. Bassler, "Quorum regulatory small rnas repress type vi secretion in v ibrio cholerae," *Molecular microbiology*, vol. 92, no. 5, pp. 921–930, 2014.

[164] R. L. Gourse, W. Ross, and T. Gaal, "Ups and downs in bacterial transcription initiation: The role of the alpha subunit of rna polymerase in promoter recognition," *Molecular microbiology*, vol. 37, no. 4, pp. 687–695, 2000.

[165] C. Guo *et al.*, "Transversions have larger regulatory effects than transitions," *BMC genomics*, vol. 18, no. 1, pp. 1–9, 2017.

[166] M. Slattery, T. Zhou, L. Yang, A. C. D. Machado, R. Gordân, and R. Rohs, "Absence of a simple code: How transcription factors read the genome," *Trends in biochemical sciences*, vol. 39, no. 9, pp. 381–399, 2014.

[167] K. D. MacKenzie *et al.*, "Parallel evolution leading to impaired biofilm formation in invasive salmonella strains," *PLoS genetics*, vol. 15, no. 6, e1008233, 2019.

[168] S. E. Osborne *et al.*, "Pathogenic adaptation of intracellular bacteria by rewiring a cis-regulatory input function," *Proceedings of the National Academy of Sciences*, vol. 106, no. 10, pp. 3982–3987, 2009.

[169] W. Zhao, F. Caro, W. Robins, and J. J. Mekalanos, "Antagonism toward the intestinal microbiota and its effect on vibrio cholerae virulence," *Science*, vol. 359, no. 6372, pp. 210–213, 2018.

[170] S. Seal, G. Dharmarajan, and I. Khan, "Evolution of pathogen tolerance and emerging infections: A missing experimental paradigm," *Elife*, vol. 10, e68874, 2021.

[171] J. E. San *et al.*, "Current affairs of microbial genome-wide association studies: Approaches, bottlenecks and analytical pitfalls," *Frontiers in microbiology*, vol. 10, p. 3119, 2020.

[172] K. Skorupski and R. K. Taylor, "Positive selection vectors for allelic exchange," *Gene*, vol. 169, no. 1, pp. 47–52, 1996.

[173] S. S. Watve, E. E. Bernardy, and B. K. Hammer, "Vibrio cholerae: Measuring natural transformation frequency," *Current protocols in microbiology*, vol. 35, no. 1, 6A–4, 2014.

[174] M. B. Miller, K. Skorupski, D. H. Lenz, R. K. Taylor, and B. L. Bassler, "Parallel quorum sensing systems converge to regulate virulence in vibrio cholerae," *Cell*, vol. 110, no. 3, pp. 303–314, 2002.

[175] J. S. Matson, "Preparation of vibrio cholerae samples for rna-seq analysis," in *Vibrio Cholerae*, Springer, 2018, pp. 29–38.

[176] K. Manera *et al.*, "Sensing of intracellular hcp levels controls t6ss expression in vibrio cholerae," *Proceedings of the National Academy of Sciences*, vol. 118, no. 25, 2021.

[177] E. W. Sayers *et al.*, "Database resources of the national center for biotechnology information," *Nucleic acids research*, vol. 47, no. Database issue, p. D23, 2019.

[178] C. Camacho *et al.*, "Blast+: Architecture and applications," *BMC bioinformatics*, vol. 10, no. 1, pp. 1–9, 2009.

[179] R. C. Edgar, "Muscle: Multiple sequence alignment with high accuracy and high throughput," *Nucleic acids research*, vol. 32, no. 5, pp. 1792–1797, 2004.

[180] F. Madeira *et al.*, "The embl-ebi search and sequence analysis tools apis in 2019," *Nucleic acids research*, vol. 47, no. W1, W636–W641, 2019.

[181] X. Robert and P. Gouet, "Deciphering key features in protein structures with the new endscript server," *Nucleic acids research*, vol. 42, no. W1, W320–W324, 2014.

[182] J. Felsenstein, "Evolutionary trees from dna sequences: A maximum likelihood approach," *Journal of molecular evolution*, vol. 17, no. 6, pp. 368–376, 1981.

[183] K. Tamura, G. Stecher, and S. Kumar, "MEGA11: Molecular Evolutionary Genetics Analysis Version 11," *Molecular Biology and Evolution*, vol. 38, no. 7, pp. 3022–3027, Apr. 2021. eprint: https://academic.oup.com/mbe/article-pdf/38/7/3022/38827102/msab120.pdf.

[184] R. I. Aminov, "The role of antibiotics and antibiotic resistance in nature," *Environmental microbiology*, vol. 11, no. 12, pp. 2970–2988, 2009.

[185] S. Borgeaud, L. C. Metzger, T. Scrignari, and M. Blokesch, "The type vi secretion system of vibrio cholerae fosters horizontal gene transfer," *Science*, vol. 347, no. 6217, pp. 63–67, 2015.

[186] M. LeRoux *et al.*, "Kin cell lysis is a danger signal that activates antibacterial pathways of pseudomonas aeruginosa," *Elife*, vol. 4, e05701, 2015.

[187] N. Flaugnatti *et al.*, "Human commensal gut proteobacteria withstand type vi secretion attacks through immunity protein-independent mechanisms," *Nature communications*, vol. 12, no. 1, pp. 1–13, 2021.

[188] F. Kamal *et al.*, "Differential cellular response to translocated toxic effectors and physical penetration by the type vi secretion system," *Cell reports*, vol. 31, no. 11, p. 107 766, 2020.

[189] T. Van Opijnen, K. L. Bodi, and A. Camilli, "Tn-seq: High-throughput parallel sequencing for fitness and genetic interaction studies in microorganisms," *Nature methods*, vol. 6, no. 10, pp. 767–772, 2009.

[190] S. J. Hersch, R. T. Sejuty, K. Manera, and T. G. Dong, "High throughput identification of genes conferring resistance or sensitivity to toxic effectors delivered by the type vi secretion system," *bioRxiv*, 2021.

[191] T. J. Kawecki, R. E. Lenski, D. Ebert, B. Hollis, I. Olivieri, and M. C. Whitlock, "Experimental evolution," *Trends in ecology & evolution*, vol. 27, no. 10, pp. 547–560, 2012.

[192] S. F. Levy, J. R. Blundell, S. Venkataram, D. A. Petrov, D. S. Fisher, and G. Sherlock, "Quantitative evolutionary dynamics using high-resolution lineage tracking," *Nature*, vol. 519, no. 7542, pp. 181–186, 2015.

[193] A. H. Melnyk, A. Wong, and R. Kassen, "The fitness costs of antibiotic resistance mutations," *Evolutionary applications*, vol. 8, no. 3, pp. 273–283, 2015.

[194] D. J. Luciano, R. Levenson-Palmer, and J. G. Belasco, "Stresses that raise np4a levels induce protective nucleoside tetraphosphate capping of bacterial rna," *Molecular cell*, vol. 75, no. 5, pp. 957–966, 2019.

[195] M. D. Edwards *et al.*, "Characterization of three novel mechanosensitive channel activities in escherichia coli," *Channels*, vol. 6, no. 4, pp. 272–281, 2012.

[196] U. Gabale, P. A. Peña Palomino, H. Kim, W. Chen, and S. Ressl, "The essential inner membrane protein yejm is a metalloenzyme," *Scientific reports*, vol. 10, no. 1, pp. 1–14, 2020.

[197] E. M. Fivenson and T. G. Bernhardt, "An essential membrane protein modulates the proteolysis of lpxc to control lipopolysaccharide synthesis in escherichia coli," *MBio*, vol. 11, no. 3, e00939–20, 2020.

[198] R. L. Guest, D. Samé Guerra, M. Wissler, J. Grimm, and T. J. Silhavy, "Yejm modulates activity of the ycim/ftsh protease complex to prevent lethal accumulation of lipopolysaccharide," *MBio*, vol. 11, no. 2, e00598–20, 2020.

[199] S. Amemiya *et al.*, "The mechanosensitive channel ybdg from escherichia coli has a role in adaptation to osmotic up-shock," *Journal of Biological Chemistry*, vol. 294, no. 33, pp. 12 281–12 292, 2019.

[200] T. Ferenci, "Trade-off mechanisms shaping the diversity of bacteria," *Trends in microbiology*, vol. 24, no. 3, pp. 209–223, 2016.

[201] S. Uppal, S. R. Maurya, R. S. Hire, and N. Jawali, "Cyclic amp receptor protein regulates cspe, an early cold-inducible gene, in escherichia coli," *Journal of bacteriology*, vol. 193, no. 22, pp. 6142–6151, 2011.

[202] O. Lamrabet, J. Plumbridge, M. Martin, R. E. Lenski, D. Schneider, and T. Hindré, "Plasticity of promoter-core sequences allows bacteria to compensate for the loss of a key global regulatory gene," *Molecular biology and evolution*, vol. 36, no. 6, pp. 1121–1133, 2019.

[203] X. Ji *et al.*, "Alarmone ap4a is elevated by aminoglycoside antibiotics and enhances their bactericidal activity," *Proceedings of the National Academy of Sciences*, vol. 116, no. 19, pp. 9578–9585, 2019.

[204] M. J. Behe, "Experimental evolution, loss-of-function mutations, and "the first rule of adaptive evolution"," *The Quarterly Review of Biology*, vol. 85, no. 4, pp. 419–445, 2010.

[205] T. G. Dong, S. Dong, C. Catalano, R. Moore, X. Liang, and J. J. Mekalanos, "Generation of reactive oxygen species by lethal attacks from competing microbes," *Proceedings of the National Academy of Sciences*, vol. 112, no. 7, pp. 2181–2186, 2015.

[206] S. L. Myint *et al.*, "Ecotin and lamb in escherichia coli influence the susceptibility to type vi secretion-mediated interbacterial competition and killing by vibrio cholerae," *Biochimica et Biophysica Acta (BBA)-General Subjects*, vol. 1865, no. 7, p. 129 912, 2021.

[207] H.-H. Lin, M. Yu, M. K. Sriramoju, S.-T. D. Hsu, C.-T. Liu, and E.-M. Lai, "A high-throughput interbacterial competition screen identifies clpap in enhancing recipient susceptibility to type vi secretion system-mediated attack by agrobacterium tumefaciens," *Frontiers in microbiology*, vol. 10, p. 3077, 2020.

[208] J. Jee *et al.*, "Rates and mechanisms of bacterial mutagenesis from maximum-depth sequencing," *Nature*, vol. 534, no. 7609, pp. 693–696, 2016.

[209] J. Blair, M. A. Webber, A. J. Baylay, D. O. Ogbolu, and L. J. Piddock, "Molecular mechanisms of antibiotic resistance," *Nature reviews microbiology*, vol. 13, no. 1, pp. 42–51, 2015.

[210] M. F. Schenk and J. A. G. de Visser, "Predicting the evolution of antibiotic resistance," *BMC biology*, vol. 11, no. 1, pp. 1–3, 2013.

[211] G. G. Perron, A. Gonzalez, and A. Buckling, "Source–sink dynamics shape the evolution of antibiotic resistance and its pleiotropic fitness cost," *Proceedings of the Royal Society B: Biological Sciences*, vol. 274, no. 1623, pp. 2351–2356, 2007.

[212] B. Van den Bergh *et al.*, "Frequency of antibiotic application drives rapid evolutionary adaptation of escherichia coli persistence," *Nature microbiology*, vol. 1, no. 5, pp. 1–7, 2016.

[213] C. M. Herren and M. Baym, "Decreased thermal niche breadth as a trade-off of antibiotic resistance," *The ISME Journal*, pp. 1–10, 2022.

[214] D. I. Andersson, S. M. Patin, A. I. Nilsson, and E. Kugelberg, "The biological cost of antibiotic resistance," *Enzyme-Mediated Resistance to Antibiotics: Mechanisms, Dissemination, and Prospects for Inhibition*, pp. 339–348, 2007.

[215] E. C. Böttger, B. Springer, M. Pletschette, and P. Sander, "Fitness of antibiotic-resistant microorganisms and compensatory mutations," *Nature medicine*, vol. 4, no. 12, pp. 1343–1344, 1998.

[216] J. Bjorkman, I. Nagaev, O. Berg, D. Hughes, and D. I. Andersson, "Effects of environment on compensatory mutations to ameliorate costs of antibiotic resistance," *Science*, vol. 287, no. 5457, pp. 1479–1482, 2000.

[217] B. R. Levin, V. Perrot, and N. Walker, "Compensatory mutations, antibiotic resistance and the population genetics of adaptive evolution in bacteria," *Genetics*, vol. 154, no. 3, pp. 985–997, 2000.

[218] C. Winter, T. Bouvier, M. G. Weinbauer, and T. F. Thingstad, "Trade-offs between competition and defense specialists among unicellular planktonic organisms: The "killing the winner" hypothesis revisited," *Microbiology and Molecular Biology Reviews*, vol. 74, no. 1, pp. 42–57, 2010.

[219] M. Doebeli, Y. Ispolatov, and B. Simon, "Point of view: Towards a mechanistic foundation of evolutionary theory," *Elife*, vol. 6, e23804, 2017.

[220] J. Alcoforado Diniz, Y.-C. Liu, and S. J. Coulthurst, "Molecular weaponry: Diverse effectors delivered by the type vi secretion system," *Cellular microbiology*, vol. 17, no. 12, pp. 1742–1751, 2015.

[221] S. Kim, T. D. Lieberman, and R. Kishony, "Alternating antibiotic treatments constrain evolutionary paths to multidrug resistance," *Proceedings of the National Academy of Sciences*, vol. 111, no. 40, pp. 14 494–14 499, 2014.

[222] T. Latrille, L. Duret, and N. Lartillot, "The red queen model of recombination hot-spot evolution: A theoretical investigation," *Philosophical Transactions of the Royal Society B: Biological Sciences*, vol. 372, no. 1736, p. 20 160 463, 2017.

[223] S. Blanford, M. B. Thomas, C. Pugh, and J. K. Pell, "Temperature checks the red queen? resistance and virulence in a fluctuating environment," *Ecology Letters*, vol. 6, no. 1, pp. 2–5, 2003.

[224] A. J. Robson, "Complex evolutionary systems and the red queen," *The Economic Journal*, vol. 115, no. 504, F211–F224, 2005.

[225] Y.-H. Li and X.-L. Tian, "Quorum sensing and bacterial social interactions in biofilms: Bacterial cooperation and competition," *Stress and environmental regulation of gene expression and adaptation in bacteria*, pp. 1195–1205, 2016.

[226] J. S. Madsen, S. J. Sørensen, and M. Burmølle, "Bacterial social interactions and the emergence of community-intrinsic properties," *Current opinion in microbiology*, vol. 42, pp. 104–109, 2018.

[227] T. J. Silhavy, M. L. Berman, and L. W. Enquist, *Experiments with gene fusions*. Cold Spring Harbor Laboratory, 1984.

[228] L. C. Thomason, J. A. Sawitzke, X. Li, N. Costantino, and D. L. Court, "Recombineering: Genetic engineering in bacteria using homologous recombination," *Current protocols in molecular biology*, vol. 106, no. 1, pp. 1–16, 2014.

[229] T. Baba *et al.*, "Construction of escherichia coli k-12 in-frame, single-gene knockout mutants: The keio collection," *Molecular systems biology*, vol. 2, no. 1, pp. 2006–0008, 2006.

[230] W. Jiang, D. Bikard, D. Cox, F. Zhang, and L. A. Marraffini, "Rna-guided editing of bacterial genomes using crispr-cas systems," *Nature biotechnology*, vol. 31, no. 3, pp. 233–239, 2013.

[231] G. J. McKenzie and N. L. Craig, "Fast, easy and efficient: Site-specific insertion of transgenes into enterobacterial chromosomes using tn7 without need for selection of the insertion event," *BMC microbiology*, vol. 6, no. 1, pp. 1–7, 2006.

[232] E. M. Hart, M. Gupta, M. Wühr, and T. J. Silhavy, "The synthetic phenotype of Δ bamb Δ bame double mutants results from a lethal jamming of the bam complex by the lipoprotein rcsf," *MBio*, vol. 10, no. 3, e00662–19, 2019.

[233] S. Chen, Y. Zhou, Y. Chen, and J. Gu, "Fastp: An ultra-fast all-in-one fastq preprocessor," *Bioinformatics*, vol. 34, no. 17, pp. i884–i890, 2018.

[234] D. E. Deatherage and J. E. Barrick, "Identification of mutations in laboratory-evolved microbes from next-generation sequencing data using breseq," in *Engineering and analyzing multicellular systems*, Springer, 2014, pp. 165–188.

[235] B. Langmead and S. L. Salzberg, "Fast gapped-read alignment with bowtie 2," *Nature methods*, vol. 9, no. 4, pp. 357–359, 2012.

[236] J. B. Stock, A. M. Stock, and J. M. Mottonen, "Signal transduction in bacteria," *Nature*, vol. 344, no. 6265, pp. 395–400, 1990.

[237] M. Y. Galperin, "Bacterial signal transduction network in a genomic perspective," *Environmental microbiology*, vol. 6, no. 6, pp. 552–567, 2004.

[238] A. Alonso, F. Rojo, and J. L. Martınez, "Environmental and clinical isolates of pseudomonas aeruginosa show pathogenic and biodegradative properties irrespective of their origin," *Environmental microbiology*, vol. 1, no. 5, pp. 421–430, 1999.

[239] T. G. Sana *et al.*, "The second type vi secretion system of pseudomonas aeruginosa strain pao1 is regulated by quorum sensing and fur and modulates internalization in epithelial cells," *Journal of Biological Chemistry*, vol. 287, no. 32, pp. 27 095–27 105, 2012.

[240] J. A. Moscoso, H. Mikkelsen, S. Heeb, P. Williams, and A. Filloux, "The pseudomonas aeruginosa sensor rets switches type iii and type vi secretion via c-di-gmp signalling," *Environmental microbiology*, vol. 13, no. 12, pp. 3128–3138, 2011.

[241] Y. Han *et al.*, "A pseudomonas aeruginosa type vi secretion system regulated by cuer facilitates copper acquisition," *PLoS pathogens*, vol. 15, no. 12, e1008198, 2019.

[242] D. L. Runft *et al.*, "Zebrafish as a natural host model for vibrio cholerae colonization and transmission," *Applied and environmental microbiology*, vol. 80, no. 5, pp. 1710–1717, 2014.

[243] J. E. Ogg, R. A. Ryder, and H. L. Smith Jr, "Isolation of vibrio cholerae from aquatic birds in colorado and utah," *Applied and environmental microbiology*, vol. 55, no. 1, pp. 95–99, 1989.

[244] K. C. Klontz and S. R. Rippey, "Epidemiology of molluscan-borne illnesses," *Molluscan shellfish depuration*, pp. 47–58, 2018.

[245] A. Huq, E. B. Small, P. A. West, M. I. Huq, R. Rahman, and R. R. Colwell, "Ecological relationships between vibrio cholerae and planktonic crustacean copepods," *Applied and environmental microbiology*, vol. 45, no. 1, pp. 275–283, 1983.

[246] S. Sawasvirojwong, P. Srimanote, V. Chatsudthipong, and C. Muanprasat, "An adult mouse model of vibrio cholerae-induced diarrhea for studying pathogenesis and potential therapy of cholera," *PLoS Neglected Tropical Diseases*, vol. 7, no. 6, e2293, 2013.

[247] K. E. Klose, "The suckling mouse model of cholera," *Trends in microbiology*, vol. 8, no. 4, pp. 189–191, 2000.

[248] B. Sit, B. Fakoya, and M. K. Waldor, "Animal models for dissecting vibrio cholerae intestinal pathogenesis and immunity," *Current Opinion in Microbiology*, vol. 65, pp. 1–7, 2022.

[249] J. M. Ritchie, H. Rui, R. T. Bronson, and M. K. Waldor, "Back to the future: Studying cholera pathogenesis using infant rabbits," *MBio*, vol. 1, no. 1, e00047–10, 2010.

[250] G. W. Takle, I. K. Toth, and M. B. Brurberg, "Evaluation of reference genes for real-time rt-pcr expression studies in the plant pathogen pectobacterium atrosepticum," *BMC plant biology*, vol. 7, no. 1, pp. 1–9, 2007.

[251] C. Li, T. Jiang, M. Li, Y. Zou, and Y. Yan, "Fine-tuning gene expression for improved biosynthesis of natural products: From transcriptional to post-translational regulation," *Biotechnology advances*, p. 107 853, 2021.

[252] E. F. Ruff, M. T. Record Jr, and I. Artsimovitch, "Initial events in bacterial transcription initiation," *Biomolecules*, vol. 5, no. 2, pp. 1035–1062, 2015.

[253] I. Cases, V. De Lorenzo, and C. A. Ouzounis, "Transcription regulation and environmental adaptation in bacteria," *Trends in microbiology*, vol. 11, no. 6, pp. 248–253, 2003.

[254] W.-G. Deng, Y. Zhu, A. Montero, and K. K. Wu, "Quantitative analysis of binding of transcription factor complex to biotinylated dna probe by a streptavidin–agarose pulldown assay," *Analytical biochemistry*, vol. 323, no. 1, pp. 12–18, 2003.

[255] M. Madan Babu and S. A. Teichmann, "Evolution of transcription factors and the gene regulatory network in escherichia coli," *Nucleic acids research*, vol. 31, no. 4, pp. 1234–1244, 2003.

[256] D. Zheng, C. Constantinidou, J. L. Hobman, and S. D. Minchin, "Identification of the crp regulon using in vitro and in vivo transcriptional profiling," *Nucleic acids research*, vol. 32, no. 19, pp. 5874–5893, 2004.

[257] T. P. Malan, A. Kolb, H. Buc, and W. R. McClure, "Mechanism of crp-camp activation of lac operon transcription initiation activation of the p1 promoter," *Journal of molecular biology*, vol. 180, no. 4, pp. 881–909, 1984.

[258] P. Valentin-Hansen, B. Holst, J. Josephsen, K. Hammer, and B. Albrechtsen, "Crp/camp- and cytr-regulated promoters in escherichia coli k12: The cdd promoter," *Molecular microbiology*, vol. 3, no. 10, pp. 1385–1390, 1989.

[259] L. Søgaard-Andersen, H. Pedersen, B. Hoist, and P. Valentin-Hansen, "A novel function of the camp-crp complex in escherichia coli: Camp-crp functions as an adaptor for the cytr repressor in the deo operon," *Molecular microbiology*, vol. 5, no. 4, pp. 969–975, 1991.

[260] S. Zeb, S. M. Gulfam, and H. Bokhari, "Comparative core/pan genome analysis of vibrio cholerae isolates from pakistan," *Infection, Genetics and Evolution*, vol. 82, p. 104 316, 2020.

[261] L. Zheng *et al.*, "Pan-genome analysis of vibrio cholerae and vibrio metschnikovii strains isolated from migratory birds at dali nouer lake in chifeng, china," *Frontiers in Veterinary Science*, vol. 8, p. 638 820, 2021.

[262] A. Pant *et al.*, "Molecular insights into the genome dynamics and interactions between core and acquired genomes of vibrio cholerae," *Proceedings of the National Academy of Sciences*, vol. 117, no. 38, pp. 23 762–23 773, 2020.

[263] Z. Weinberg *et al.*, "Identification of 22 candidate structured rnas in bacteria using the cmfinder comparative genomics pipeline," *Nucleic acids research*, vol. 35, no. 14, pp. 4809–4819, 2007.

[264] J. Jumper *et al.*, "Highly accurate protein structure prediction with alphafold," *Nature*, vol. 596, no. 7873, pp. 583–589, 2021.

[265] C. A. Orengo, A. E. Todd, and J. M. Thornton, "From protein structure to function," *Current opinion in structural biology*, vol. 9, no. 3, pp. 374–382, 1999.

[266] L. C. Metzger, N. Matthey, C. Stoudmann, E. J. Collas, and M. Blokesch, "Ecological implications of gene regulation by tfox and tfoy among diverse vibrio species," *Environmental microbiology*, vol. 21, no. 7, pp. 2231–2247, 2019.

[267] B. R. Pursley, N. L. Fernandez, G. B. Severin, and C. M. Waters, "The vc2 cyclic di-gmp-dependent riboswitch of vibrio cholerae regulates expression of an upstream

putative small rna by controlling rna stability," *Journal of bacteriology*, vol. 201, no. 21, e00293–19, 2019.

[268] M. Grognot, A. Mittal, M. Mah'moud, and K. M. Taute, "Vibrio cholerae motility in aquatic and mucus-mimicking environments," *Applied and Environmental Microbiology*, vol. 87, no. 20, e01293–21, 2021.

[269] M. Guentzel and L. Berry, "Motility as a virulence factor for vibrio cholerae," *Infection and immunity*, vol. 11, no. 5, pp. 890–897, 1975.

[270] C. J. Jones *et al.*, "C-di-gmp regulates motile to sessile transition by modulating msha pili biogenesis and near-surface motility behavior in vibrio cholerae," *PLoS pathogens*, vol. 11, no. 10, e1005068, 2015.

[271] E. N. K. Lim, C. Sasseville, M.-C. Carrier, and E. Massé, "Keeping up with rna-based regulation in bacteria: New roles for rna binding proteins," *Trends in Genetics*, vol. 37, no. 1, pp. 86–97, 2021.

[272] E. Van Assche, S. Van Puyvelde, J. Vanderleyden, and H. P. Steenackers, "Rna-binding proteins involved in post-transcriptional regulation in bacteria," *Frontiers in microbiology*, vol. 6, p. 141, 2015.

[273] Y. Shao and B. L. Bassler, "Quorum-sensing non-coding small rnas use unique pairing regions to differentially control mrna targets," *Molecular microbiology*, vol. 83, no. 3, pp. 599–611, 2012.

[274] C. Chiaruttini and M. Guillier, "On the role of mrna secondary structure in bacterial translation," *Wiley Interdisciplinary Reviews: RNA*, vol. 11, no. 3, e1579, 2020.

[275] D. Kim *et al.*, "Comparative analysis of regulatory elements between escherichia coli and klebsiella pneumoniae by genome-wide transcription start site profiling," 2012.

[276] N. R. Markham and M. Zuker, "Unafold," in *Bioinformatics*, Springer, 2008, pp. 3–31.

[277] D. L. Clemens, P. Ge, B.-Y. Lee, M. A. Horwitz, and Z. H. Zhou, "Atomic structure of t6ss reveals interlaced array essential to function," *Cell*, vol. 160, no. 5, pp. 940–951, 2015.

[278] B. Wan *et al.*, "Type vi secretion system contributes to enterohemorrhagic escherichia coli virulence by secreting catalase against host reactive oxygen species (ros)," *PLoS pathogens*, vol. 13, no. 3, e1006246, 2017.

[279] N. Händel, J. M. Schuurmans, S. Brul, and B. H. ter Kuile, "Compensation of the metabolic costs of antibiotic resistance by physiological adaptation in escherichia coli," *Antimicrobial agents and chemotherapy*, vol. 57, no. 8, pp. 3752–3762, 2013.

[280] J. M. Joshi, "Tuberculosis chemotherapy in the 21st century: Back to the basics," *Lung India: Official Organ of Indian Chest Society*, vol. 28, no. 3, p. 193, 2011.

[281] R. Levenson-Palmer, D. J. Luciano, N. Vasilyev, A. Nuthanakanti, A. Serganov, and J. G. Belasco, "A distinct rna recognition mechanism governs np4 decapping by rpph," *Proceedings of the National Academy of Sciences*, vol. 119, no. 6, e2117318119, 2022.

[282] I. R. Booth, "Bacterial mechanosensitive channels: Progress towards an understanding of their roles in cell physiology," *Current Opinion in Microbiology*, vol. 18, pp. 16–22, 2014.

[283] M. Punta, L. R. Forrest, H. Bigelow, A. Kernytsky, J. Liu, and B. Rost, "Membrane protein prediction methods," *Methods*, vol. 41, no. 4, pp. 460–474, 2007.

[284] N. R. De Lay and J. E. Cronan, "Genetic interaction between the escherichia coli acpt phosphopantetheinyl transferase and the yejm inner membrane protein," *Genetics*, vol. 178, no. 3, pp. 1327–1337, 2008.

[285] R. D. Süssmuth, "Vancomycin resistance: Small molecule approaches targeting the bacterial cell wall biosynthesis," *ChemBioChem*, vol. 3, no. 4, pp. 295–298, 2002.

[286] H. J. Cordell, "Epistasis: What it means, what it doesn't mean, and statistical methods to detect it in humans," *Human molecular genetics*, vol. 11, no. 20, pp. 2463–2468, 2002.

[287] P. Durão, R. Balbontın, and I. Gordo, "Evolutionary mechanisms shaping the maintenance of antibiotic resistance," *Trends in microbiology*, vol. 26, no. 8, pp. 677–691, 2018.

[288] J. Lennings, T. E. West, and S. Schwarz, "The burkholderia type vi secretion system 5: Composition, regulation and role in virulence," *Frontiers in microbiology*, vol. 9, p. 3339, 2019.

[289] E. C. Garcia, A. I. Perault, S. A. Marlatt, and P. A. Cotter, "Interbacterial signaling via burkholderia contact-dependent growth inhibition system proteins," *Proceedings of the National Academy of Sciences*, vol. 113, no. 29, pp. 8296–8301, 2016.

[290] B. Zong *et al.*, "Characterization of multiple type-vi secretion system (t6ss) vgrg proteins in the pathogenicity and antibacterial activity of porcine extra-intestinal pathogenic escherichia coli," *Virulence*, vol. 10, no. 1, pp. 118–132, 2019.